Aus dem Max von Pettenkofer-Institut für Hygiene und Medizinische Mikrobiologie
der Ludwig-Maximilians-Universität München

Lehrstuhl Bakteriologie
Leitung: Prof. Dr. Rainer Haas

Analysing the role of the GEF Rom2 in cell wall integrity and significance of functional septa for echinocandin tolerance in the opportunistic pathogenic mold *Aspergillus fumigatus*.

Dissertation
zum Erwerb des Doktorgrades der Naturwissenschaften
an der Medizinischen Fakultät
der Ludwig-Maximilians-Universität München

vorgelegt von

Sweta Samantaray

aus Burla, India

2014

Mit Genehmigung der Medizinischen Fakultät

der Ludwig-Maximilians-Universität München

Betreuer:	Prof. Dr. rer. nat. Frank Ebel
Zweitgutachter:	Priv. Doz. Dr. Gottfried Wilharm
Mitbetreuung durch den promovierten Mitarbeiter:	Dr. med. Johannes Wagener
Dekan:	Prof. Dr. med. Dr. h.c. M. Reiser, FACR, FRCR
Tag der mündlichen Prüfung:	21.11.2014

Eidesstattliche Versicherung:

(Name, Vorname)

Ich erkläre hiermit an Eides statt,

dass ich die vorliegende Dissertation mit dem Thema:

„Analysing the role of the GEF Rom2 in cell wall integrity and significance of functional septa for echinocandin tolerance in the opportunistic pathogenic mold *Aspergillus fumigatus*."

selbständig verfasst, mich außer der angegebenen keiner weiteren Hilfsmittel bedient und alle Erkenntnisse, die aus dem Schrifttum ganz oder annähernd übernommen sind, als solche kenntlich gemacht und nach ihrer Herkunft unter Bezeichnung der Fundstelle einzeln nachgewiesen habe.

Ich erkläre des Weiteren, dass die hier vorgelegte Dissertation nicht in gleicher oder in ähnlicher Form bei einer anderen Stelle zur Erlangung eines akademischen Grades eingereicht wurde.

Ort, Datum

Unterschrift Doktorandin/Doktorand

Declaration:

I hereby declare that all the present work embodied in this thesis was carried out by me from 04/2011 to 04/2014 at Max von Pettenkofer-Institut für Hygiene und Medizinische Mikrobiologie under Ludwig-Maximilians-Universität München. This dissertation topic has not been submitted to any other institute or university for the award of any academic degree or diploma.

Part of the work was done by others, as mentioned below:

- Christoph Helmschrott, medical student at the Max von Pettenkofer-Institut designed and isolated the $rho1^{G14V}_{tetOn}$ plasmid vector for Rom2 characterization.
- Michael Neubauer, medical student at the Max von Pettenkofer-Institut has performed the Co-IP assay for Rom2 characterization.
- Dr. med. Karl Dichtl, post-doctoral fellow at the Max von Pettenkofer-Institut has performed the *in vitro* studies to analyse the cell wall composition and role of septa in echinocandin tolerance for Fks1characterization.

Date: Signature: .....

Place: Munich, Germany (Sweta Samantaray)

Publications:

Parts of the work have been published or submitted for publication:

- **Samantaray S**, Neubauer M, Helmschrott C, Wagener J. Role of the guanine nucleotide exchange factor Rom2 in cell wall integrity maintenance of *Aspergillus fumigatus*. *Eukaryot. Cell* 2013 Feb.; 12(2):288-98.

- Helmschrott C, Sasse A., **Samantaray S**, Krappmann S, Wagener J. Upgrading fungal gene expression on demand: improved systems for doxycycline-dependent silencing in *Aspergillus fumigatus*. *Appl. Environ. Microbiol.* 2013 Mar; 79(5):1751-4.

- Karl Dichtl*, **Sweta Samantaray***, Vishukumar Aimanianda, Zhaojun Zhu, Marie-Christine Prévost, Jean-Paul Latgé, Frank Ebel, Johannes Wagener. *Aspergillus fumigatus* devoid of c ell wall β-1,3-glucan is viable, massively sheds galactomannan and is killed by septum formation inhibitors. *Mol Microbiol.* 2014 Nov (Accepted)
  ***Equal contribution.**

Dedicated to my mother

“I owe all my endeavours and success to my mother, my creator”

Table of Contents:

Zusammenfassung

Aspergillus fumigatus ist ein opportunistischer Schimmelpilz und als Erreger des Krankheitsbildes der invasiven Aspergillose (IA) von großer medizinischer Bedeutung. Diese systemische Infektion trifft vor allem abwehrgeschwächte Patienten und weist dabei eine hohe Letalität auf. Die *Aspergillus*-Zellen werden durch eine feste, doch zugleich hochdynamische Zellwand vor schädigenden Umwelteinflüssen geschützt. Deshalb stellt diese essentielle und pilzspezifische Struktur einen idealen Angriffspunkt für die antimykotische Therapie dar: Alle derzeit zur Behandlung von systemischen Pilzinfektionen eingesetzten Medikamente wirken auf Zellwand oder Zellmembran. Da auch unter maximaler Therapie ein großer Teil der Infektionen tödlich verläuft, wurde in den letzten Jahren nach neuen antimykotischen Wirkmechanismen gesucht, woraufhin der CWI (*cell wall integrity*) Signalweg als ein möglicher neuer Ansatzpunkt identifiziert wurde. Diese MAPK (*mitogen-activated protein kinase)*-Kaskade dient der Überwachung und Regulierung der funktionellen Integrität der Zellwand und ihres stressbedingten Umbaus. Dazu werden Stressoren detektiert, diese Informationen verarbeitet und in den Zellkern weitergeleitet, wo durch eine veränderte Genexpression dem Zellwandstress entgegengewirkt werden kann. In dieser Arbeit wurde die zentrale Rolle des *guanine nucleotide exchange factor* (GEF) Rom2 im Rahmen der Zellwandstress-Antwort und der Antimykotika-Resistenz untersucht. Es zeigte sich, dass die GEF-Funktion essentiell für das Überleben des Pilzes ist. Mit Hilfe einer konditionellen *rom2*-Mutante konnte das Zusammenspiel mit den kürzlich entdeckten CWI-Sensoren Wsc1, Wsc3 und MidA untersucht werden. Unter repremierter Genexpression weist die Mutante schwere Wachstumsdefekte auf: Wie die Δ*midA*-Mutante ist sie deutlich empfindlicher gegen Hitze, Calcofluor-Weiß und Kongo Rot. Die verminderte Resistenz gegen die klinisch bedeutsamen Echinocandin-Antimykotika, wie z.B. Caspofungin, die die β-1,3-Glucan-Synthese inhibieren, ähnelt dem Phänotyp der Δ*wsc1*-Mutante. Wie auch die GTPase Rho1, mit der eine direkte Interaktion nachgewiesen werden konnte, ist Rom2 in den Hyphenspitzen zu lokalisieren. Auf Basis dieser Erkenntnisse konnte Rom2 als wichtige Schaltstelle zwischen den Oberflächensensoren und Rho1 einerseits sowie dem *downstream* gelegenen MAPK-Modul identifiziert werden.

Weiterhin konnte eine neue Methode zur Verstärkung der Echinocandin-Wirkung auf den Pilz identifiziert werden. In dieser Arbeit wurden die zwei möglichen Erklärungen für den fungistatischen Effekt der Echinocandine gegen den Schimmelpilz untersucht: Das Überleben von *A. fumigatus* beruht entweder auf einer nur unvollständigen Inhibition der β-1,3-Glucan-

Synthese oder auf der Verzichtbarkeit des β-1,3-Glucans für den Aufbau der Zellwand. Zur Untersuchung der Bedeutung der β-1,3-Glucan-Synthase-Untereinheit Fks1 für Überleben, Wachstum und Antimykotika-Wirksamkeit wurde eine konditionelle *fks1*-Mutante generiert. Unterdrückte Expression von *fks1* führt zu einem Phänotyp, den auch Echinocandine im Wildtypstamm hervorrufen. Dies geht mit einer signifikanten Abnahme des β-1,3-Glucans auf der Zelloberfläche, einer Abgabe von Galactomannan an die Umgebung und einem kompensatorischen Anstieg des Chitin-Gehalts der Zellwand einher. Es konnte gezeigt werden, dass Wachstum der konditionellen *fks1*-Mutante durch Echinocandine nicht komplett unterdrückt wird und dass auch eine *fks1*-Deletionsmutante lebensfähig ist. Diese Ergebnisse legen nahe, dass β-1,3-Glucan für *A. fumigatus* nicht essentiell ist, und erklärt somit die eingeschränkte Wirksamkeit der β-1,3-Glucan-Synthase-Inhibitoren. Darüber hinaus wurde die Bedeutung von Septen für die Resistenz gegen Echinocandine untersucht. Substanzen, die die Bildung von Septen unterbinden, weisen einen signifikanten Synergismus mit dem Echinocandin Caspofungin auf. Aus den Erkenntnissen dieser Arbeit folgt, dass die Inhibition der Septierung die fungistatische Wirkweise der Echinocandine in eine fungizide überführen kann und somit eine vielversprechende Strategie zur Verbesserung der heutigen antimykotischen Therapie ist darstellt.

Summary

Aspergillus fumigatus is a major opportunistic, filamentous fungal pathogen causing invasive aspergillosis (IA), a fatal systemic infection in immunocompromised patients with significant mortality rate. The fungal cell is protected by a rigid but highly dynamic cellular structure, the cell wall that forms the first level of defence against environmental stress. The cell wall being an essential and unique structure of the fungus has always been an ideal drug target. The major antifungal drugs used currently either target the fungal cell membrane or cell wall. However, due to the poor efficacy of current antifungal therapy, the CWI (cell wall integrity) pathway has emerged as the focus of research in recent years to discover potential molecular drug targets for designing antifungal therapy with novel mode of action. This signaling cascade is dedicated to monitoring and maintaining functional integrity of the cell wall, remodelling its structure in response to cell surface stress. This MAPK (mitogen activated protein kinase) cascade is highly coordinated to transduce the stress signals to the nucleus and consequently trigger necessary gene expression to counteract the stress. In this study, we explored the pivotal role of guanine nucleotide exchange factor (GEF), Rom2 in cell wall stress response and antifungal drug susceptibility. The findings of this work reveal that the Rom2 GEF is essential for viability of the pathogen. Additionally, characterization of a conditional *rom2* mutant functionally links it to the previously identified CWI sensors, namely, Wsc1, Wsc3 and MidA in *A. fumigatus*. The conditional mutant shows severe growth defects under repressive conditions such as hyper-susceptibility to heat, Calcofluor white and Congo red, similar to the Δ*midA* mutant. Additionally, similar to the Δ*wsc1*, the *rom2* mutant cultured under repressive conditions is increasingly susceptible to the actively used antifungal and inhibitor of cell wall β-1,3-glucan synthesis, echinocandin such as caspofungin. Furthermore, the Rom2 shows a sub-cellular localization similar to the Rho1 GTPase to hyphal tips and also physically interacts with the GTPase. Thus, these relevant findings establish the integral role of Rom2 as an intermediate relay molecule acting between the cell surface sensors and Rho1 GTPase as well as the downstream MAPK module.

This study also reports a novel mechanism imparting echinocandin tolerance to the pathogen. This work explores two possibilities that may explain the fungistatic nature of echinocandins against *Aspergillus*: one either owing to incomplete inhibiton of β-1,3-glucan synthesis or that the cell wall β-1,3-glucan is not essential for *A. fumigatus* viability. In order to evaluate the role of the β-1,3-glucan synthase subunit, Fks1 in viability, growth and antifungal response of the mold, a conditional *fks1* mutant was generated. Downregulation of *fks1*

expression results in characteristic growth behaviour which phenocopies the effect of wild type treated with echinocandins. The mutant cultured under repressive growth conditions also displays significant decrease in cell surface β-1,3-glucan and enhanced galactomannan shedding, marked with a compensatory increase in chitin content. Importantly, the growth of the conditional *fks1* mutant is not completely abolished in presence of echinocandin and an *fks1* deletion mutant is surprisingly viable. These results strongly reflect that β-1,3-glucan is not essential in *A. fumigatus*, and thereby justifies the limited activity of β-1,3-glucan synthesis inhibitor echinocandin on the mold. The novel findings of the work also suggest that presence of septa is an essential means of survival for *A. fumigatus* upon echinocandin treatment. Compounds inhibiting septum formation exhibit significant synergism with the echinocandin caspofungin. Thus, the present study identifies and proposes that septum inhibition is a promising strategy for enhancing echinocandin fungicidal potency and improving existing antifungal therapy.

1. Introduction

1.1. *Aspergillus* spp.

The genus *Aspergillus* represents a diverse group of filamentous 'spore-bearing' fungi comprising more than 250 species (Geiser *et al*., 2007, Sampson and Varga, 2009). *Aspergillus* species are predominantly saprophytic in nature, often inhabiting terrestrial habitats. They are commonly found in soil and organic compost, degrading and utilizing it for nutrients. They share the following taxonomy:

Kingdom- Fungi

Division- Ascomycota

Class- Eurotiomycetes

Order- Eurotiales

Family- Trichocomaceae

Genus- *Aspergillus*

The *Aspergillus* spp. also have a diverse range of clinical, industrial and agricultural relevance and challenges. For instance, *A. niger* is widely used for fermentation processes, particularly for production of citric acid and regarded as industrial 'cell factory' (Pel *et al*., 2007); *A. oryzae* and *A. sojae* are mainly used in the production of sake, miso, vinegar and soy sauce (Machida *et al*., 2008) or *A. nidulans* that represents an important model organism for studying fungal genetics and biology (Galagan *et al*., 2005). On the other hand, some *Aspergillus* species are known for their pathogenicity and regarded as a threat for plant, animal and human life. Some of the common pathogenic species are exemplified by *A. fumigatus*, an opportunist human pathogen causing broad spectrum of infections (Latgé 1999); *A. flavus* and *A. parasiticus*, the potent hepatocarcinogen aflatoxin-producing species which primarily affect crops and also act as opportunist pathogens for both animal and humans (Klich 2007; Horn *et al*., 2009) or *A. sydowii*, the pathogen mainly affecting corals and a major threat to coral ecosystems (Rypien *et al*., 2008; Gibbons and Rokas, 2013).

.

1.2. *Aspergillus fumigatus*

1.2.1. Morphology and life-cycle

Aspergillus fumigatus is a spore-bearing fungus fungus characterized by green echinate conidia (2.5 to 3 micrometer in diameter) produced in chains basipetally from greenish phialides (6 to 8 by 2 to 3 micrometer in size). Colonies of *Aspergillus fumigatus* are dark blue-green to grey green on the surface (Figure 1 A and B). Due to the resemblance of its microscopic asexual spore-bearing structure to the *aspergillum*, a liturgical device used to sprinkle holywater in Roman Catholic Church, Italian priest and botanist Pier Antonio Micheli named these structures '*Aspergillus*' (Bennett 2010).

A. B.

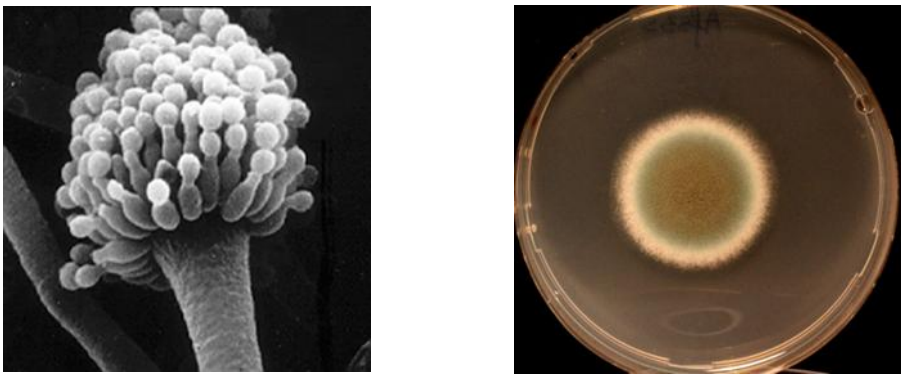

Figure 1. Morphology of *A. fumigatus* (A) Electron micropgraph picture of *A. fumigatus* (http://www.cosmosbiomedical.com/education/mycology/mycology2.shtml) (B) Morphology of *A. fumigatus* colony surface on AMM agar plate after 3 days incubation at 37ºC.

A. fumigatus is an aerobic filamentous fungus and an ascomycete, capable of reproducing both sexually and asexually. In contrast to previous reports, it was recently shown that *A. fumigatus* retains a fully functional sexual reproductive cycle and is able to engage in sexual reproduction successfully (O' Gorman *et al*., 2009). In the asexual phase, the haploid hyphae form foot cells, the tip of which swells to form elongated stalk called conidiophore. The conidiophores have conical-shaped terminal vesicles which bear numerous single rows of phialides terminating in a chain of haploid spores called conidia formed through a series of mitosis (Figure 2 A). These spores disperse and germinate to produce a haploid mycelium (Bennett, 1992). On the other hand, the sexual cycle involves fusion of two haploid hyphae by a process called plasmogamy to form an elongated sac-like structure, ascus which then leads

to fusion of nuclei by a process termed as karyogamy. The diploid ascus then divides meiotically followed by mitotic divisions to produce four haploid ascospores (n). These ascospores are released from the ascocarp, which then grow into haploid mycelia and the cycle is repeated (Figure 2 B).

A. B.

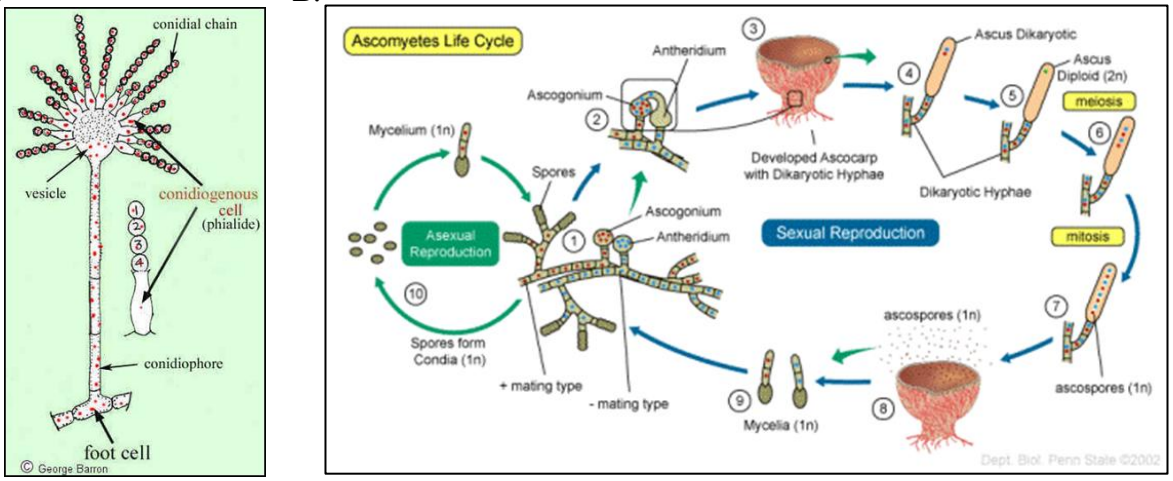

Figure 2. Conidiophore structure and life cycle of *A. fumigatus* (A) Asexual strucuture and life cycle of *Aspergillus* conidiophore (Source: Mycoalbum CD by George Barron (http://www.uoguelph.ca/)) (B) Schematic presentation of life cycle of ascomycetes representing *Aspergillus* (image from Penn State Universitity).

1.2.2. Pathogenicity and clinical significance

Aspergillus fumigatus is known to be the opportunist fungal pathogen with the biggest impact on human health, responsible for the the second highest number of fungal infections after *Candida albicans* and highest number of deaths due to fungal infections (Latgé, 1999). This pathogenic mold is capable of causing a wide range of ailments depending on the immune status of the host, causing asthma and allergies in immunocompetent people to semi-invasive and fatal invasive infections in severely immunocompromised patients (Barnes 2006). In immunocompromised hosts, *A. fumigatus* represents a major cause of morbidity and mortality causing the life-threatening systemic infection known as invasive aspergillosis (IA). In the recent years, this etiologic agent has evolved as the most prevalent cause of mortality in the immunocompromised patient population in developed countries. Due to the increasing incidence of immunosuppressive therapies and diseases such as the HIV/AIDS, there has been a substantial increase in the high risk group patients and the mortality rate due to IA exceeds 50% in such patients (Hohl and Feldmesser, 2007).

Pathogenicity of *A. fumigatus* is multifactorial, depending upon a combination of traits unique to the fungus and the immune status of the host. The virulence of the pathogen largely attributes to the small size and hydrophobicity of its conidia which are ideal for infiltrating the human pulmonary alveoli and escaping mucociliary clearance in the upper respiratory tract. The success of *Aspergillus* spp. is also well explained by their ability to tolerate harsh, abiotic growth conditions including wide range of temperatures (6-55º) and pH (2-12) (Krijgsheld *et al*., 2012). *A. fumigatus* particularly is quite thermo-tolerant and able to withstand temperatures above 50ºC. Several other factors such as its high growth rate and nutritional adaptability are other fundamental characteristics that support the intracellular survival and virulence of this pathogen (Abad *et al*. 2010).

The mode of infection by *A. fumigatus* is via inhalation of air-borne asexual conidia (spores) into the lung alveoli. In a healthy individual, conidia are usually removed by mucociliary clearance by lung epithelial cells. The conidia escaping the initial clearance are further attacked by the innate immune system consisting of alveolar macrophages and neutrophils (Figure 3). However, when such immune responses are compromised as in the case of neutropenic patients, conidia germinate and colonize the pulmonary environment. Hyphal fragments then disseminate through the bloodstream causing invasive infections in severely immunocompromised individuals.

A. B.

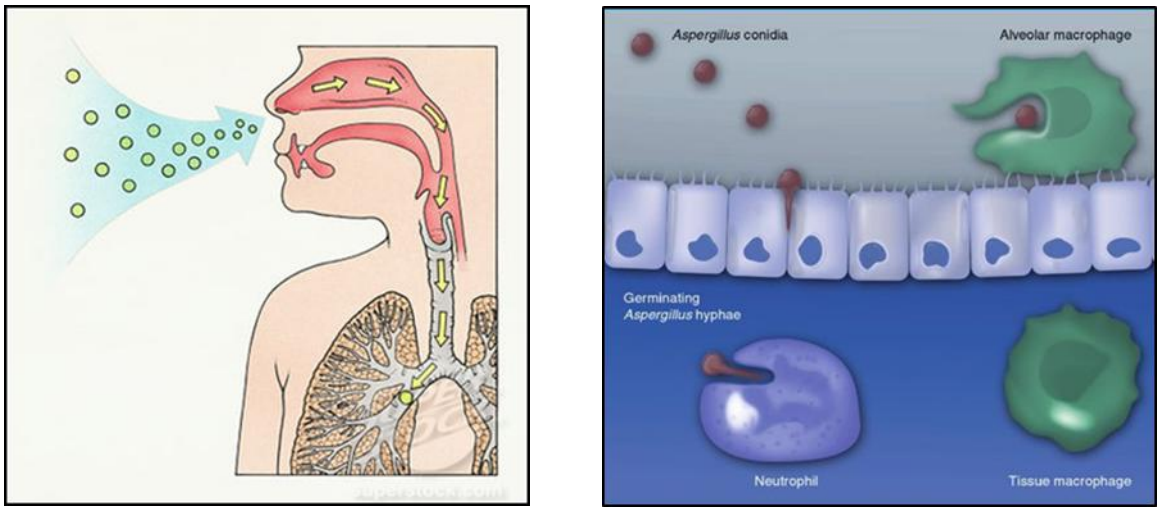

Figure 3. Mode of infection by *A. fumigatus*. (A) Inhalation of air-borne conidia into human lungs, that subsequently reaches alveoli (Source: http://wwwdelivery.superstock.com/WI/223/4268/PreviewComp/SuperStock_4268R-13922.jpg). (B) Alveolar macrophages phagocytose conidia, while germinating hyphae are attacked by infiltrating neutrophils (Chai *et al*., 2011).

The clinical isolate Af293 harbors a 29.4 Mb genome consisting of eight chromosomes containing 9,926 predicted genes. The genome analysis has revealed the presence of about 700 *A. fumigatus* specific genes, which are reportedly lacking or evolutionarily divergent in the closely related species *Neosartorya fischeri*. These genes have been identified to code for enzymes involved in secondary metabolite production, protein kinases, transcriptional regulators, metabolic enzymes and other hypothetical proteins (Nierman *et al*., 2005). This suggests that *A. fumigatus*, being a human pathogen might be more evolved.

1.2.2.1. Aspergillosis

The term 'aspergillosis' is used to describe the broad spectrum of diseases caused by *Aspergillus* spp. This includes allergic bronchopulmonary aspergillosis (ABPA), a hypersensitivity reaction to fungal components and allergic fungal sinusitis which occur commonly in cystic fibrosis and asthma patients. Noninvasive aspergillomas or 'mycelial balls' embedded in a proteinaceous matrix may form in a pre-existing lung cavity following exposure to fungus, for instance the lung lesions in tuberculosis patients (Latgé, 1999) (Figure 4 A). Typically, aspergillomas do not spread to other sites in the body. However, they may grow larger, disrupting blood vessels in the cavity and resulting in internal bleeding and hemoptysis. The most fatal form of aspergillosis is invasive aspergillosis (IA) (Figure 4 B), which is prevalent among severely immunosuppressed people including patients with leukemia, AIDS, and transplant recipients. This infection process is characterized by the invasion of blood vessels followed by dissemination to other sites such as the bones, eyes, kidneys, skin, gastrointestinal tract and even central nervous system (Latgé, 1999; Dagenais and Keller, 2009).

A.

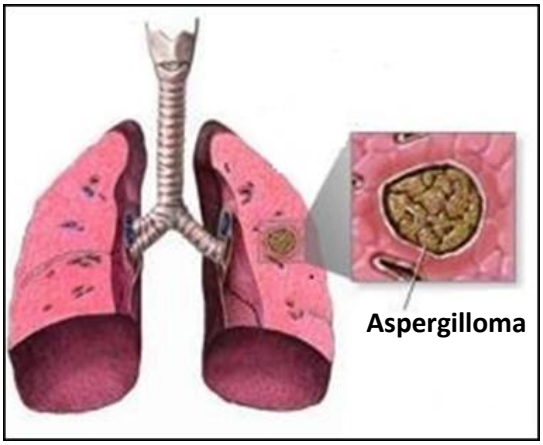

B.

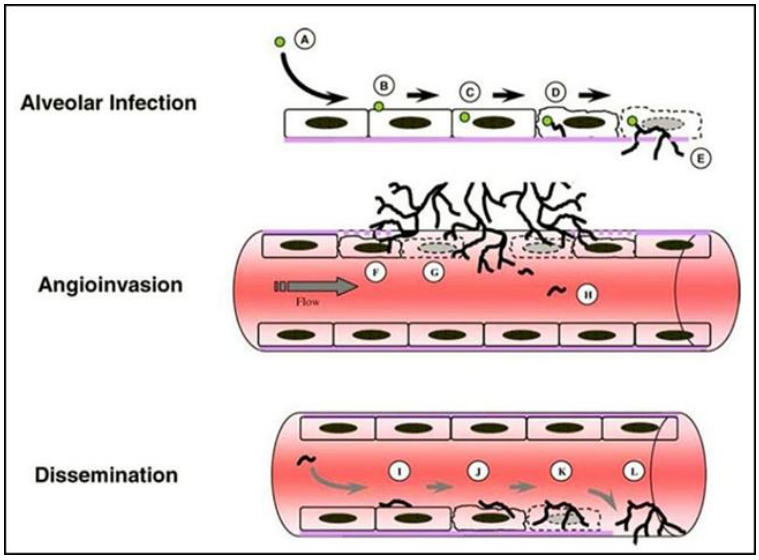

Figure 4. Different forms of aspergillosis. (A) Diagram showing colonization of a fungal mycelial ball 'aspergilloma' in a healed lung scar (Source: http://www.nlm.nih.gov/medlineplus/ency/imagepages/17263.htm). (B) Model illustrating invasive aspergillosis that occurs via three steps- alveolar infection, angioinvasion and dissemination (Filler and Sheppard, 2006).

1.2.3. Diagnosis

The high mortality rate associated with IA is mainly due to the difficulty in establishing a diagnosis at the early stages of infection. One of the first steps for diagnosis of invasive aspergillosis is high-resolution computed tomography (HRCT) (Logan and Müller, 1996). High resolution computer tomography (HRCT) scan allows earlier detection of pulmonary lesions in high-risk patients. The lesions are characterized by nodules, halo sign (early phase), an air crescent sign (usually after recovery from neutropenia) or a cavity (Figure 5).

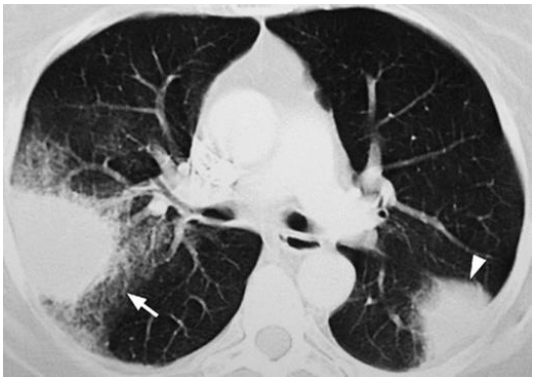

Figure 5. Transverse CT scan of a patient with invasive pulmonary aspergillosis. A large nodular mass with a characteristic halo sign (arrow) is seen in the right upper lobe, while a

smaller mass (arrowhead) with no well defined halo sign is seen in the lower left lobe (Pinto 2004).

Additional techniques to improve timely diagnosis of invasive aspergillosis are focused on the detection of circulating antigens such as galactomannan and 1,3-β-D-glucan released by the fungus by use of specific antigen tests. Commercial antigen assay kits that are currently used for diagnosis, make use of these unique fungal biomarkers to detect *Aspergillus* infection and monitor therapy. For instance, the Platelia *Aspergillus* assay is a double sandwich ELISA that detects galactomannan (GM), a complex sugar found in *Aspergillus* cell wall.

PCR detection of *Aspergillus fumigatus* DNA from body fluids using primers for conserved or specific genome sequences is also an additional method used for diagnosis of IA (Spreadbury *et al.*, 1993). However, PCR analysis is not yet a part of routine diagnostics. With the development of such non-culture based diagnostic tools, early diagnosis of aspergillosis is possible at greater accuracy (Verweij *et al*., 1999).

1.2.4. Antifungal therapy

The clinically relevant antifungals target fungal components that do not share considerable homology with human hosts to ensure elimination of fungal pathogen with minimal toxicity to the host. Currently, the three main classes of antifungal used for treatment against *Aspergillus* infections are polyenes, azoles and echinocandins.

Polyenes- This class of antifungals remains one of the oldest groups of drugs used for treating invasive aspergillosis. These are natural compounds derived from the bacterium *Streptomyces*. Amphotericin B (AmB) is one of the major polyene agents isolated from *Streptomyces nodosus* in 1955 by Gold *et al*. AmB binds to ergosterol, a functionally vital lipid in the fungal cell membrane and in addition leads to membrane permeabilization (Ellis 2002; Palacios *et al*., 2011) (Figure 6). Despite its broad spectrum activity, the drug was discontinued owing to the reported toxicity due to its affinity for cholesterol, the mammalian sterol counterpart (Joly *et al.*, 1992). However, new lipid formulations of amphotericin B such as liposomal AmB have minimized these side-effects and are currently part of treatment regime (Barrett *et al.*, 2003).

Azoles- These are synthetic cyclic organic compounds that target the ergosterol biosynthesis pathway in fungi. They inhibit the fungal cytochrome P450 dependent enzyme called lanosterol demethylase, encoded by the *ERG11* gene that catalyzes synthesis of ergosterol

from its precursor lanosterol. Inhibtion of this enzyme leads to depletion of ergosterol in the fungal cell membrane and accumulation of toxic sterol intermediates that affect membrane integrity and other vital functions, resulting in fungal death (Sheehan *et al*., 1999) (Figure 6). The triazoles represented by voriconazole, posaconazole and ravuconazole are associated with minimized drug-drug interactions and show enhanced activity, particularly against *Aspergillus* spp. (Maertens 2004). Currently, voriconazole is recommended as the first-line treatment for invasive aspergillosis (Walsh *et al*., 2008). Although, ravuconazole is yet to be approved for use by the FDA, it has reportedly promising fungicidal activity (Watt *et al*., 2013).

Echinocandins- These are a group of recently available antifungals including caspofungin, micafungin and anidulafungin. These are synthetic lipopeptides that inhibit the β-1,3-glucan synthase, an enzyme catalyzing the conversion of UDP into β-1,3-glucan which is an essential component of the fungal cell wall (Figure 6). Inhibition of β-(1,3)-glucan synthase activity leads to cell wall destabilization and osmotic lysis, resulting in cell death. Although echinocandins have a broad spectrum antifungal activity and are known to be fungicidal against *Candida*, they are mostly fungistatic towards *Aspergillus* (Espinel-Ingroff 1998; Ingham and Schneeberger, 2012).

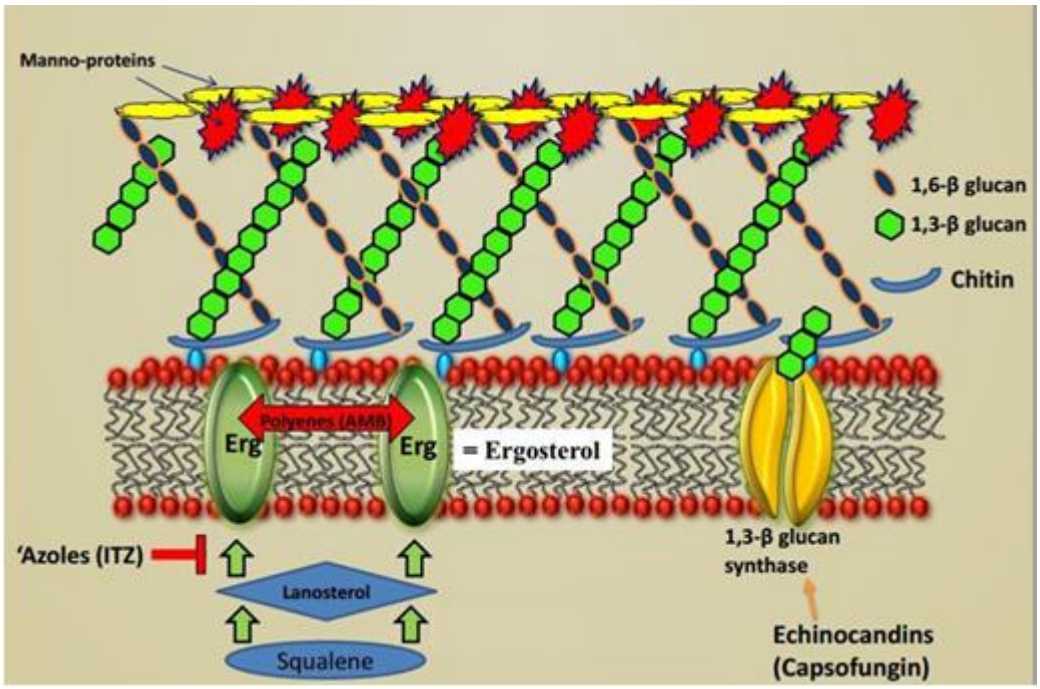

Figure 6. Mode of action of antifungals. Three classes of antifungals (polyenes, azoles and echinocandins) exert antifungal activity via distinct mechansims. Polyenes such as amphotericin B (AMB) simply bind to the plasma membrane-bound lipid, ergosterol and

inhibit its vital functions and also causes membrane permeabilization. Azoles such as itraconazole (ITZ) inhibit ergosterol biosynthesis by targeting the enzyme 14-alpha-demethylase leading to membrane instability. Echinocandin drugs such as caspofungin specifically inhibit the β-(1,3)-glucan synthase, thereby causing cell lysis (adapted from Ashley *et al*., 2006).

1.3. The fungal cell wall and its importance

The fungal cell is protected by a rigid but highly dynamic cellular structure known as the cell wall that is pivotal for its growth, survival and morphogenesis. The cell wall provides osmotic protection against hostile environmental stress such as temperature changes, pH, oxidative stress, nutrient limitations and other mechanical stresses (Bowman and Free, 2006). The cell wall also governs the interactions between the fungus and its host, modulating host immune reactions during infections. Additionally, it also mediates adhesive properties critical for colonization and invasion of host tissues as well as biofilm formation (Free, 2013). Thus, the fungal cell wall is not only crucial for maintain structural integrity in the face of extracellular stress, but also for pathogenicity. Since pathogenic fungi share a common biology with their mammalian hosts, finding molecular drug targets for antifungal therapy is challenging. Since the fungal cell wall is a unique cellular structure lacking in mammalian hosts and biologically important for the fungus, it has emerged as an attractive target for the development of antifungal drugs (Bowman and Free, 2006).

1.3.1. Cell wall organization and biosynthesis in *A. fumigatus*.

In general, the fungal cell wall constitutes a three-dimensional network of different polymers including chitin, glucans and mannoproteins. The central core of the cell wall of most fungi is fibrillar (alkali-insoluble) consisting of a lattice of β-glucans cross-linked to chitin. This glucan-chitin complex is covalently bound to other polysaccharides (α-glucans, mannans) forming the amorphous matrix (alkali-soluble). The amorphous composition of the cell wall varies specifically with the species (Latgé, 2010). For instance in *A. fumigatus*, it is composed of galactomannan and β-1,3/1,4-glucan, whereas in *C. albicans* it is mainly composed of β-1,6-glucan. Fibrillar components are usually located close to the plasma membrane, while amorphous polysaccharides are distributed especially on the outer side of the cell wall (Latgé 2010).

The cell wall of *A. fumigatus* is mainly composed of polysaccharides (∽ 90%) and proteins.

The major polysaccharides in the *A. fumigatus* cell wall include α-(1-3)-glucans (35-46%), β-(1,3)-glucans (20-35%), β-(1,3/1,4)-glucans (10%), chitins and galactomannans (20-25%) (Figure 7) (Abad *et al*., 2010).

Glucans- In *A. fumigatus*, the α-(1-3)-glucans are mostly part of amorphous cell wall polysaccharides (Henry *et al*., 2012). The α-(1-3)-glucans biosynthesis is mediated by three α-(1-3)-glucan synthase genes, namely *ags1*, *ags2* and *ags3* (Beauvais *et al*., 2005; Maubon *et al*., 2006). The β-(1,3)-glucans are synthesized by a plasma membrane bound β-1,3-glucan synthase complex. The catalytic subunit of the glucan synthase complex is encoded by the *fks1* gene, while its putative regulatory subunit is most likely encoded by *rho1* (Beauvais *et al*., 2001). The β-(1,3)-glucan synthase uses UDP–glucose as a substrate and extrudes nascent linear chain through the membrane, which on reaching the cell space are processed and cross-linked to form a scaffold for other polysaccharides (Gastebois *et al*., 2010). Besides, β-1,3-glucan also serves as an immunomodulatory molecule that is recognized by the innate immune pattern recognition receptor Dectin-1 on macrophages (Brown *et al*., 2002).

Chitin- It is a homopolymer of β-1,4-linked N-acetylglucosamine (GlcNAc) residues and an essential component of the fungal cell wall conferring shape and rigidity. Chitin synthesis occurs at the plasma membrane and then the nascent chitin chains are extruded into the cell wall space (Jiménez-Ortigosa *et al*., 2012). The chitin content is much higher is in the *A. fumigatus* mycelial cell wall than in yeast. The genome of *A. fumigatus* harbours at least eight chitin synthase genes (chs) namely, *chsA*, *chsB*, *chsC*, *chsD*, *chsE* (also called as *csmA*), *chsF*, *chsG* and *csmB* (Mellado *et al*., 1995; Mellado *et al*., 1996; Jiménez-Ortigosa *et al*., 2012).

Galactomannan- Another unique polysaccharide in the *A. fumigatus* cell wall is galactomannan. The galactomannans consist of a backbone of α-mannan chains with the side chain linked to β-galactofuranose residues. Therefore, galactomannan synthesis requires both mannosyl- and galactosyl-transferases (Nakajima and Ichishima, 1994). The synthesis of alpha-1,6-linked mannans in *Sachharomyces cerevisae* is initiated by α-1,6-mannosyltransferase encoded by the *ScOCH1* (stands for outer chain glycans) gene. In the *A. fumigatus* genome, four orthologues of *ScOCH1*gene have been identified. However, deletion of these mannosyl transferase orthologues did not show any marked phenotype different from the wild type, and only *A. fumigatus Afoch1* complemented the growth defects of *ScOCH1* deletion (Lambou *et al*., 2010). In *S. cerevisae*, an additional family of 3 genes: *ScMNN9*, *ScVAN1* and *ScANP1* encode a complex of type II membrane proteins termed as mannan

polymerase complex 1, which is responsible for elongation of the α-1,6-mannan chains (Jungmann and Munro, 1998). Comparative genome analysis has revealed that orthologues of these genes are conserved in *A. fumigatus*. However, the exact subcellular location for mannan synthesis and its mechanism of transfer to glucan chains remains uncharacterized (Latgé *et al*., 2005).

Galactomannan biosynthesis is regulated by galactofuranose metabolism which begins with the isomerization of UDP-galactopyranose to UDP-galactofuranose, the substrate for galactofuran synthesis. This process is catalyzed by the enzyme UDP galactopyranose mutase, encoded by the *glfA* gene in *A. fumigatus*. The Δ*glfA* mutant in *A. fumigatus* lacked galactofuranose and had thinner cell wall. The mutant also showed increased susceptibility to various antifungals and attenuated virulence in murine model of IA (Schmalhorst *et al*., 2008), suggesting the pivotal role of galactomannan in *A. fumigatus.*

GPI-anchored proteins- In *A. fumigatus,* the cell wall contains proteins linked with glycosyl phosphatidylinositol (GPI) moieties known as GPI anchors. The GPI anchor is a conserved post-translational modification found in eukaryotic cell surface proteins such as enzymes, receptors and adhesion molecules that serves to link these proteins to the plasma membrane (Li *et al*., 2007). The *A. fumigatus* genome harbours 115 putative GPI-anchored proteins, while the yeast genome encodes 88 GPI proteins (Cao *et al*., 2009). These are either found in the plasma membrane or the cell wall and accordingly have different biological functions. The plasma membrane anchored GPI proteins have enzymatic activities required for cell wall biogenesis, while the cell wall associated GPI proteins serve as anchors for linking cell wall polysaccharides (De Sampaïo *et al*., 1999; Klis *et al*., 2002). The first step of GPI anchor synthesis is initiated by the transfer of N-acetylglucosamine (GlcNAc) from UDP-GlcNAc to phosphatidylinositol (PI), which is catalysed by GPI–N-acetyl-glucosaminyltransferase (GPI–GnT) complex. In *A. fumigatus,* the gene *Afpig-a* is a homologue of *ScPIG-A/GPI3* which encodes for the UDP-glycosyltransferase subunit of the GPI-GnT complex, and is involved in GPI anchor biosynthesis. Surprisingly, deletion analysis of the *Afpig-a* gene reveals that the GPI anchor is not required for viability, but plays a role in morphogenesis, cell wall integrity and virulence of the pathogen (Li *et al*., 2007).

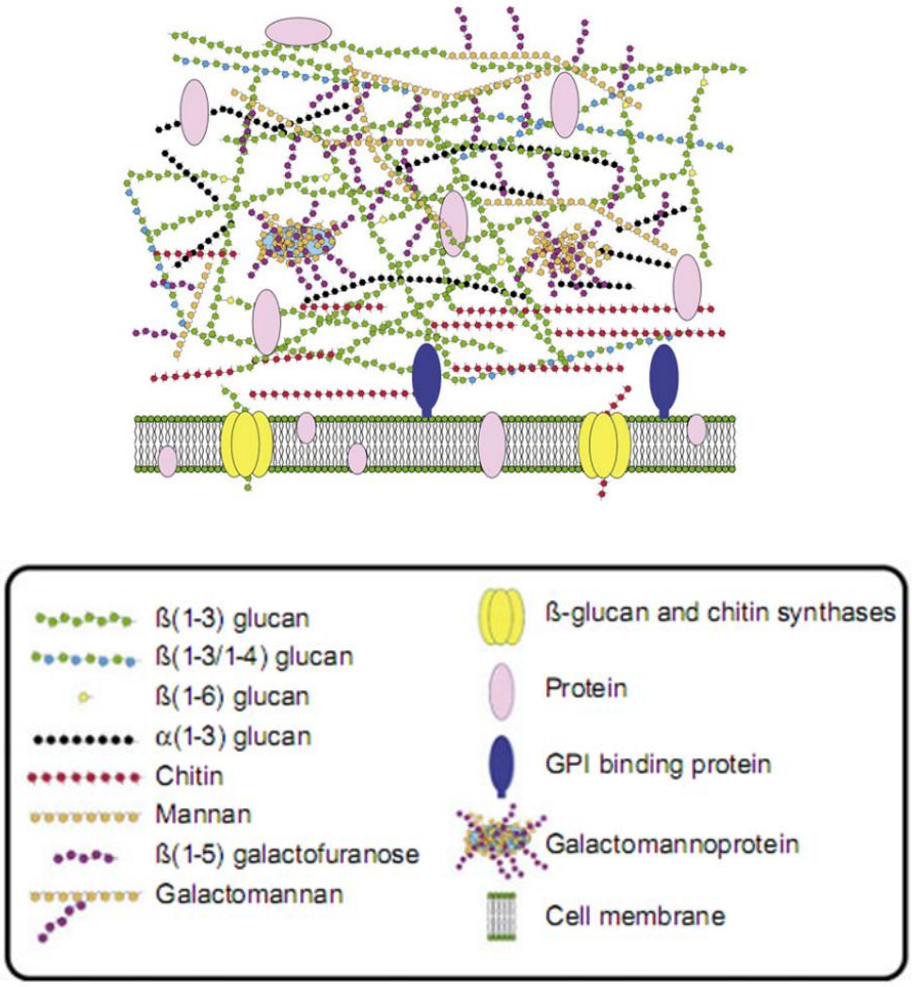

Figure 7. Schematic structure of the *A. fumigatus* cell wall. The *A. fumigatus* cell wall structure consists of a lattice of polysaccharides arranged in fibrillar and amorphous layers (Abad *et al*., 2010).

1.3.2. Cell wall remodelling: role of CWI Pathway

The fungus encounters a vast spectrum of stress conditions during its growth and morphogenesis. The cell surface stress acts as a stimulus for the cell wall which responds by remodelling its organization to counteract the extracellular stress (Levin 2005; Levin 2011). Besides environmental factors such as high temperature, pH and osmotic conditions, certain chemicals and drugs are known to trigger cell wall stress. Several chemical agents are known to perturb cell wall synthesisor inhibit protein glycosylation that affect linkages between major cell wall components (Hill *et al*., 2006). Some major wall-compromising agents include polysaccharide-binding agents (Congo red and Calcofluor white), echinocandin and SDS. The anionic detergent SDS disrupts membrane stabilizaion and rather than affecting cell wall directly. Therefore, it can be used to reveal cell wall defects that result in increased

accessibility of the detergent to plasma membrane (de Groot *et al*., 2001; Hill *et al*., 2006). Anionic dyes such as Congo red (CR) and Calcofluor white (CFW) have high affinity for nascent chitin chains and cellulose (Roncero and Durán *et al*., 1985; Herth, 1980). However, CR has a greater binding affinity towards β-1,3-glucans (Kopecká and Gabriel, 1992; Levin 2005). In vitro, both CR and CFW bind to nascent polysaccharide chains and thereby inhibit microfibril assembly in growing cells, resulting in cell wall weakening and lysis of hyphal tips (Ram and Klis, 2006).

The fungal cell employs the so-called cell wall integrity (CWI) signaling cascade that enables it to orchestrate changes in the cell wall composition in order to mount an appropriate stress response. This signaling pathway is best characterized in the model yeast *S. cerevisae* (Levin, 2005; Levin 2011). Briefly, this pathway comprises five transmembrane sensor proteins embedded in the cell surface, namely, ScWsc1-3 (Wall Stress Component), ScMidA and ScMtl1, guanine nucleotide exchange factors (GEFs) ScRom1/2, Rho1 GTPase, protein kinase C (ScPkc1) and a mitogen-activated protein (MAP) kinase module. The sensors are type I transmembrane proteins which act as mechanosensors probing the cell surface. They all contain a serine-threonine rich extracellular domain, a hydrophobic transmembrane domain and a short cytosolic tail (Levin 2005; Levin 2011). Additionally, the ScWsc family sensors harbour an N-terminal cysteine-rich residue, termed as the Wsc domain which is lacking in the ScMidA sensor (Ketela *et al*., 1999). Activation of the CWI pathway is initiated at the cell surface in response to stressors that are sensed by transmembrane sensors. These sensors then relay the signal downstream with the help of GEFs, which in turn stimulate nucleotide exchange on the ScRho1 GTPase. The activated GTPase then stimulates several downstream effectors involved in cell wall biogenesis. One of its primary effectors is ScPkc1, which regulates the MAPK cascade via ScBck1 (MAPKKK) and ScMkk1/2 (MAPKKs) and ultimately activate the end kinase ScMpk1 by dual phosphorylation of conserved threonine and tyrosine residues (Lee *et al*., 1993; Martin *et al*., 2000). Finally, the activated ScMpk1, via its repertoire of transcription factors, triggers the transcription of genes that regulate cell wall biogenesis (Levin, 2005; Levin 2011) (Figure 8).

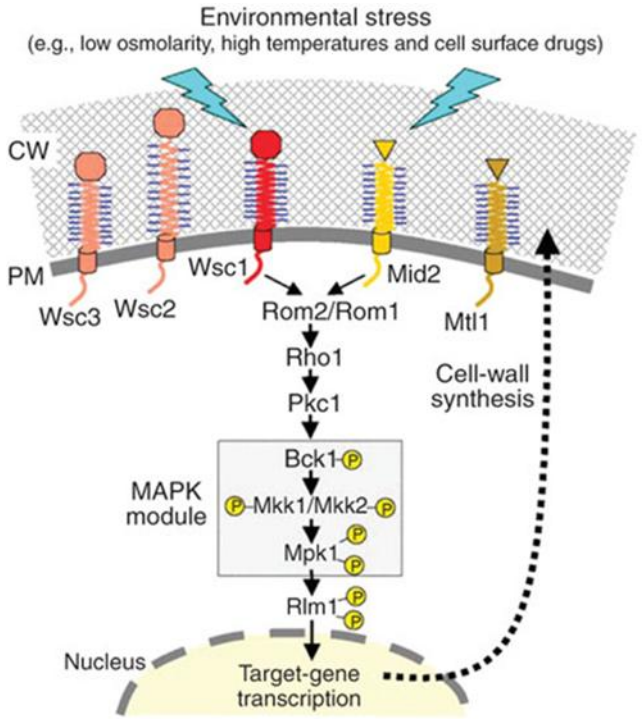

Figure 8. Model of CWI signalling in S. cerevisae. The sensors located in the plasma membrane (Wsc1-3p, Mid2p and Mtl1p) transduce the signal through the GEFs Rom1/2p to the central Rho1 GTPase, which then activates the Pkc1-dependent MAPK cascade consisting of Bck1, Mkk1/2 and Mpk1 (Heinisch *et al*., 2010).

1.3.2.1. CWI Signaling in *Aspergillus* spp.

Recently, it has become evident that the central signalling components of the CWI pathway are conserved from *S. cerevisae* to several filamentous fungal species including *Aspergillus* (Kwon *et al*., 2011; Dichtl *et al*., 2012; Futagami *et al*., 2011). Dichtl *et al*. have identified and characterized four potential cell wall stress sensors in *A. fumigatus*, namely AfWsc1, AfWsc2, AfWsc3 and AfMidA (Figure 9). These sensors appear to respond to different types of stimuli or stress as indicated by the differential sensitivity exhibited by the mutant strains. For instance, in *A. fumigatus*, the Δ*midA* is hypersensitive to thermal stress and the cell wall inhibitors Congo red and Calcofluor white, while Δ*wsc1* is sensitive to caspofungin (Dichtl *et al*., 2012). Similarly, in *A. nidulans*, the WscA and WscB have been identified as the homologues of the *S.cerevisae* Wsc family of sensors that activate CWI under hypo-osmotic and acidic pH conditions (Goto *et al*., 2009; Futagami *et al*., 2011).

In budding yeast, the cell wall stress signal is transduced via sensors to the downstream central regulatory component, Rho1 GTPase that belongs to a family of highly conserved

small, monomeric GTPases. The genome of *A. fumigatus* encodes six Rho-GTPases, namely AfRho1-4, AfCdc42 and AfRacA. Among these, only AfRho1, AfRho2 and AfRho4 have been characterized and implicated in cell wall maintenance and modulation (Dichtl *et al*., 2012). In *A. fumigatus*, the *Afrho1* gene has been shown to be essential for viability through doxycycline driven expression. While the AfRho4 GTPase is primarily involved in septum formation, the AfRho2, on the other hand, apparently exhibits functional redundancy with AfRho1 (Dichtl *et al*., 2012). The ScRho1 and ScPkc1 homologues in *A. nidulans*, represented by RhoA and PkcA respectively, are also shown to be involved in establishing polarity and cell wall integrity (Guest *et al*., 2004; Ronen *et al*., 2007; Teepe *et al*., 2007). Similarly, the AnRhoA and AnRhoB GTPases in *A. niger* are involved in viability as well as polar growth and cell wall maintenance respectively (Kwon *et al*., 2011). Furthermore, the tripartite MAPK module of the canonical CWI pathway in *S. cerevisae* is also conserved in *A. fumigatus* and represented by three protein kinases: AfBck1, AfMkk2 and AfMpkA (Valiante *et al*., 2008; Valiante *et al*., 2009; Dirr *et al*., 2010). The ScMkk1/2 homologue AfMkk2 is shown to be involved in cell wall integrity and virulence of the pathogen *A. fumigatus* (Dirr *et al*., 2010). The AfMpkA, on the other hand contributes to other cellular functions such as oxidative stress response, secondary metabolism and siderophore biosynthesis, besides regulating cell wall remodelling (Jain *et al*., 2011). Despite its role for stress resistance and growth in *A. fumigatus*, a mutant lacking *AfmpkA* function is not attenuated in virulence in a murine infection model in *A. fumigatus* (Valiante *et al*., 2008). In agreement with AfMpkA role, the MAPK homologue in *A. nidulans* is also involved in germination of spores and polarized growth. The mutant growth defects are mostly remedied upon osmotic stabilization suggesting that the mutant is impaired in CWI (Bussink and Osmani, 1999).

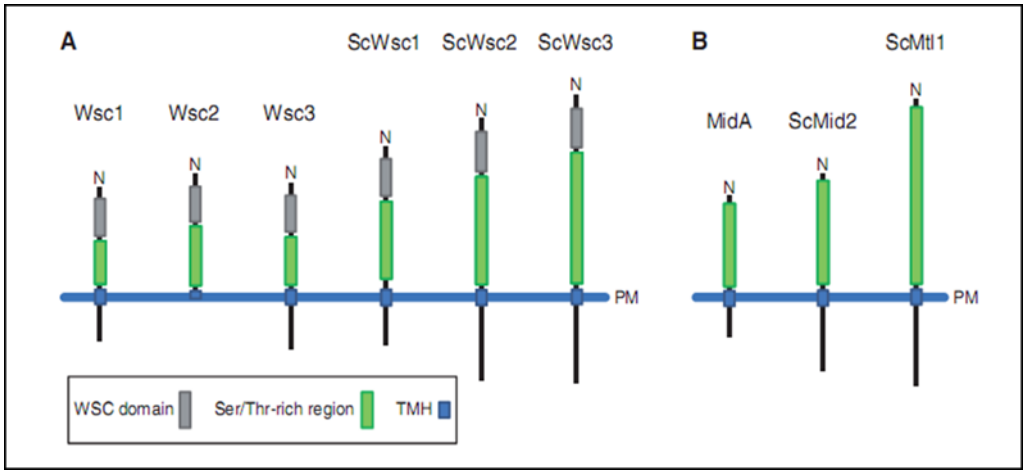

Figure 9. Domain structure of *S. cerevisae* CWI sensors and *A. fumigatus* orthologues. A. Members of the Wsc family of sensors possess a characteristic N-terminal Wsc domain followed by a serine/threonine region, a short transmembrane domain and cytosolic tail (absent in AfWsc2). B. Sensors not belonging to the Wsc family lack the N-terminal domain. N, N-terminus; PM, plasma membrane; TMH, transmembrane helix (Dichtl *et al*., 2012).

1.4. GEFs as activators of Rho GTPases

The Rho (Ras homologous) GTPases belong to the Ras superfamily of small guanosine triphosphatases (GTPases) and remain highly conserved among eukaryotes (Rossman *et al*., 2005). They function as molecular switches and adopt different conformational states in response to binding of GDP or GTP. When bound to GDP, they remain inactive and sequestered in cytoplasm. Upon binding to GTP, they become active, associate with plasma membrane and interact with several downstream effectors to regulate array of cellular functions such as organization of actin cytoskeleton, cell cycle progression and expression of various genes (Rossman *et al*., 2005). Cycling between theses two states is primarily regulated by two classes of molecules: GEFs (guanine-nucleotide exchange factors) and GAPs (GTPase-activating proteins). GEFs catalyze exchange of GDP for GTP and positively regulate Rho activity, while GAPs promote the intrinsic GTPase activity of Rho proteins, thereby acting as downregulators of Rho GTPases. In principle, activation of a Rho GTPase could occur through stimulation of a GEF or inhibition of a GAP (Schmidt and Hall, 2002). A third group of regulatory proteins called GDIs (guanine-nucleotide dissociation inhibitors) inhibit the GDP/GTP exchange reaction and maintain inactive pools of Rho GTPases in the cytosol (Dransart *et al*., 2005) (Figure 10).

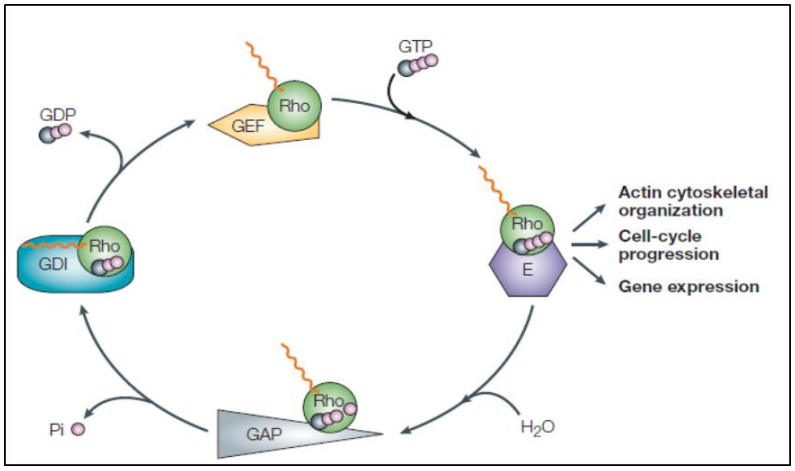

Figure 10. Regulation of Rho-GTPase activity. Rho GTPases are functional when bound to GTP and remain non-functional when bound to GDP. GTPase activating proteins (GAPs) stimulate intrinsic GTP hydrolysis activity and the release of terminal inorganic phosphate, Pi. Guanine nucleotide-dissociation inhibitors (GDIs) bind to the C-terminal isoprenyl chain (orange wavy line) and sequester them in cytosol. Gunanine-nucleotide exchange factors (GEFs) stabilize Rho-GTPases and stimulate exchange of GDP for GTP. Once activated, the Rho GTPases bind their effectors (E) (Rossman *et al*., 2005).

Interestingly, most of the Rho GEFs harbor a conserved domain structure characterized by the presence of a ~200 residue Dbl homology (DH) domain and an adjacent ~100 residue Pleckstrin homology (PH) domain. The DH domain, also known as the Rho GEF domain constitutes the catalytic domain responsible for exchange of GDP to GTP. The DH domains bind to switch regions of Rho GTPase and alter its nucleotide binding pocket. In contrast, the PH domain has been shown to bind phosphoinositides and probably mediates membrane localization of GEF proteins (Rossman *et al*., 2005) (Figure 11).

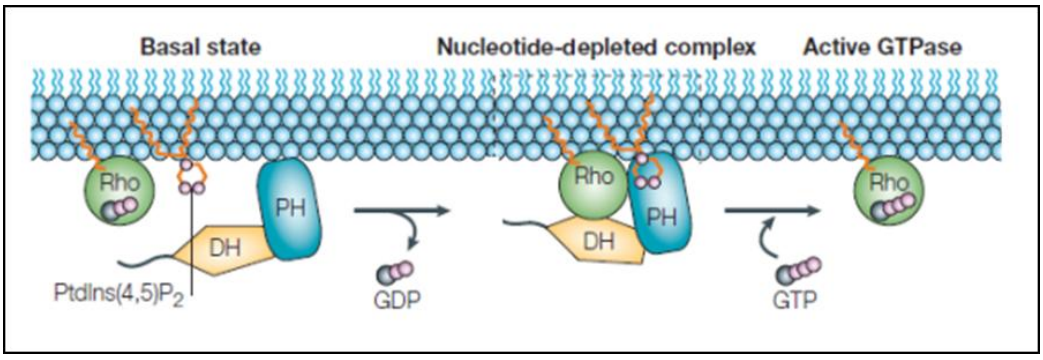

Figure 11. Model showing interactions between Rho GTPase and DH-PH domain of GEF. Interaction between membrane phosphoinositides and the PH domain allows binding of DH domain to Rho GTPase followed by dissociation of GDP and loading of GTP (adapted from Rossman *et al*., 2005). GDP- guanine dinucleotide phosphate; GTP, guanine nucleotide triphosphate; DH, Dbl homology; PH, Pleckstrin homology.

1.4.1. Role of Rho1 specific GEFs in CWI signaling

The ScRho1, the central regulator of CWI signaling is a homologue of the mammalian *rhoA* gene and shown to be essential in *S. cerevisae* (Madaule *et al*., 1987). In response to cell wall stress, the ScRho1 is activated by sensors via two GEFs ScRom1 and ScRom2. The homologous genes, *ScROM1* and *ScROM2* (RHO1 multicopy suppressor) were isolated as

multicopy suppressors of temperature-sensitive, dominant negative mutant allele of *ScRHO1* The ScRom1 and ScRom2 share overlapping functions and deletion of both GEFs is lethal. While the deletion of *ScROM1* resulted in wild type-like growth, *ScROM2* deletion showed temperature-sensitive growth that was partially suppressed by osmotic stabilization. Interestingly, a Δ*Scrom1*Δ*Scrom2* mutant strain expressing *ROM2* under the control of *GAL1* promoter exhibited cell lysis and temperature-sensitive growth under restrictive growth conditions i.e. in the absence of *GAL1* driven *ScROM2* expression (Ozaki *et al*., 1996). Similar phenotypes have been reported for a temperature-sensitive *Scrho1-104* mutant allele grown at restrictive temperature (Yamochi *et al*., 1994). Besides ScROM1 and ScROM2, another GEF, ScTUS1 is also implicated in regulating cell wall integrity in *S. cerevisae* via ScRHO1. Deletion of *Sctus1* also results in temperature-sensitive growth which is restored by osmotic stabilization. Furthermore, the growth defect of *Sctus1* deletion strain was suppressed by overexpression of *ScROM2*, *ScRHO1*, *ScRHO2* and *ScPKC1* (Schmelzle *et al*., 2002). Similarly, the homologues of ScRom1 and ScRom2 in *Schizosaccharomyces pombe* constituted by SpRgf1 and SpRgf2 respectively, are also implicated as SpRho1 GEFs involved in CWI signaling (Mutoh *et al*., 2005; Garcia *et al*., 2009). These studies also demonstrate that loss of GEF function mostly phenocopies the effects of loss of Rho1 and its downstream effector functions. In contrast to *S. cerevisae* and *S. pombe*, the *Candida albicans* genome contains only one ScRom1/ScRom2 homologue (orf19.906) which though remains uncharacterized, but is reported to be essential (personal communication of Aaron P. Mitchell to Candida genome database (CGD), 2009). Surprisingly, deletion of the *Cryptococcus neoformans* homologue ORF CNI04280 was not lethal. However, the Δ*Cnrom2* mutant showed abnormal morphology at restrictive growth temperature and attenuated virulence in a murine infection model (Tang *et al*., 2005; Fuchs *et al*., 2007). Similarly in filamentous fungi, NcRgf1 has been described as the specific GEF for NcRho1 in *Neurospora crassa* (Richthammer *et al*., 2012). According to these models, the GEFs act as functional links to transduce signal from various known and potentially unknown sensors to the Rho1 GTPase and therefore constitute the upstream activators of the CWI pathway in both yeasts and molds.

Several recent studies have elucidated the components of the CWI pathway in *Aspergillus* spp. including *A. fumigatus*, which indicates a similar signal transduction mechanism might exist in *A. fumigatus* (Guest *et al*., 2004; Kwon *et al*., 2011; Dichtl *et al*., 2012). This also pointed towards the existence of a relay molecule integrating signals from the *A. fumigatus* CWI sensors to activate the downstream MAPK cascade. Genome analysis of *A. fumigatus*

revealed a single homologue of ScRom1/Rom2, named as *Afrom2* (AFUA_5G08550). Characterization of AfRom2 and its role in stress response of the pathogen is one of the major topics of this study.

1.5. Echinocandin tolerance in *A. fumigatus*

When a fungal pathogen is exposed to an antifungal drug, the cells try to overcome growth inhibition by developing various resistance mechanisms leading to growth at higher drug concentrations and subsequent clinical resistance. In other cases, the fungal pathogen employs different factors such as altered metabolism or stress response pathways to withstand the killing effects of the drug, thereby determining its fungicidal or fungistatic status. Tolerance to a given drug is usually described as the phenomenon where an organism is able to survive the minimal inhibitory concentration (MIC) of the drug even though its growth is inhibited, thereby rendering it static (Sanglard 2003; Anderson 2005). However, if the tolerance mechanisms are compromised, the fungistatic effect of the drug is reversed and its efficacy is enhanced. For instance, the azoles are known to have fungistatic activity against *C. albicans*. However, in combination with the calcineurin inhibitor cyclosporine A (CsA), it exerts a potent fungicidal effect in vitro and shows increased efficacy with significantly reduced fungal burden in a rat model of endocarditis (Marchetti *et al*., 2000; Marchetti *et al*., 2003).

1.5.1. Fks1: the putative catalytic subunit of the β-1,3-D-glucan synthase complex and echinocandin target.

The echinocandins are non-competitive inhibitors of the conserved transmembrane enzyme complex, β-1,3-glucan synthase complex that production of β-1,3-glucan which constitutes an essential biopolymer responsible for structural integrity of the fungal cell wall. In *S cerevisae*, this enzyme complex consists of a catalytic and a regulatory subunit. The catalytic subunit is encoded by a pair of functionally redundant genes, *ScFKS1* and *ScFKS2* (for FK506 sensitive). The deletion of *ScFKS2* results in reduced glucan level which is compensated by upregulating *ScFKS2* expression. This is further supported by the lethality induced upon deletion of both *ScFKS1* and *ScFKS2* (Douglas *et al*., 1994; Mazur *et al.*, 1995). Another homologue of the β-1,3-glucan synthase subunit is encoded by the *ScFKS3* which is reportedly involved in the spore wall assembly (Ishihara *et al*., 2007). The genome of *C. albicans* encodes three homologues for ScFks1/Fks2, namely CaGsc1, Gsl1 and Gsl2, among which CaFKS1/GSC1 is essential and encodes the β-1,3-glucan synthase subunit (Douglas *et*

al., 1997; Mio *et al*., 1997). In contrast, *Aspergillus spp.* harbour only a single copy encoding the ScFks1 homologue. In *A. nidulans*, the glucan synthase subunit is encoded by the *fksA* gene which is reportedly involved in glucan synthesis (Kelly *et al*., 1996). The *A. fumigatus* homologue, AfFks1 is also an integral transmembrane protein and shares 90% identity with *A. nidulans* FksA. Additionally, the AfFks1 localizes primarily to hyphal tips and forms a complex with the AfRho1 GTPase (Beauvais *et al*., 2001). These findings are in agreement with the proposed model in budding yeast whereby ScRho1 regulates glucan synthesis via its effector ScFks1 (Levin, 2005). Although it is believed that echinocandins act via interaction with the enzyme subunit Fks1, the exact nature of binding remains unknown and the direct evidence supporting this interaction is still lacking (Walker *et al*., 2010).

Although the echinocandins exert fungicidal effect against *Candida* spp., they are largely fungistatic against *Aspergillus* spp. Treatment of *A. fumigatus* with caspofungin and anidulafungin leads to lysis of growing hyphal tips due to inhibition of glucan synthesis at the tips of hyphae (Walker *et al*., 2010; Beauvis *et al*., 2001; Ingham and Schneeberger, 2012). Although higher doses of respective echinocandins limited microcolony growth, there was reduced hyphal lysis and incomplete growth inhibition. Staining of caspofungin-treated *A. fumigatus* hyphae revealed that hyphal tips and sub-apical compartments are more vulnerable to echinocandin-mediated damage, while the remaining interior compartments are mostly viable, even under prolonged incubation up to 72 h with the drug (Bowman *et al*., 2002). Although in contrast to *C. albicans*, clinical resistance to echinocandins has not yet been reported in *A. fumigatus*. However, the mechanism conferring *in vitro* echinocandin resistance is mostly attributed to the point mutations in the AfFks1 subunit (Gardiner *et al*., 2005; Rocha *et al*., 2007). The fungistatic activity of echinocandins is rather surprising, considering that β-1,3-D-glucan is a principal component of the *Aspergillus* cell wall. In this context, understanding the importance of the β-1,3-glucan subunit Fks1 for viability, growth and antifungal response in *A. fumigatus* is highly imperative. Characterization of AfFks1 is also crucial to achieve greater insights into the echinocandin tolerance of the pathogen, and therefore, forms an important focus of this study.

2. Aims of the study

The mold *A. fumigatus* is able to colonize diverse habitats and is often challenged with extreme growth conditions. These stresses may arise either from natural environment or the host immune system in response to fungal infections or even antifungal drug activity. The fungal cell employs the cell wall integrity (CWI), a complex signalling cascade to remodel the structure of its cell wall to withstand such cell surface stress. Additionally, the cellular structure of this filamentous fungal pathogen is divided into distinct hyphal segments, which renders further protection. The septal walls successfully block any local damage caused by injuries to one or more hyphal compartments, while the successive compartments remain viable thereby promoting the survival of the pathogen. These defence mechanisms promote the survival of the pathogen and pose a challenge for existing antifungal arsenal used for treating invasive aspergillosis. Undoubtedly, compromising such mechanisms that boost the viability of this pathogen would be of utmost significance. The focus of this study is to gain further insight into such molecular mechanisms aiding viability, growth and antifungal resistance of this pathogen, with the sole objective to unravel molecular drug targets for developing effective antifungal therapy.

2.1. Characterization of *rom2* in *A. fumigatus*.

The *A. fumigatus* genome harbors a single homologue for ScRom1/2 which acts as a link between the upstream CWI sensors and ScRho1 GTPase in the CWI pathway. Based on the above literature and role of Rom2 homologues in other fungal species, we speculated a similar role for AfRom2. The AfRom2 being the sole homologue is assumed to articulate the phenotypes of the *A. fumigatus* CWI sensors and putative Rho GTPase(s). Therefore, the functional characterization of the putative GEF Rom2 is attempted to elucidate the role of AfRom2 in cell wall stress response, including antifungal resistance and establish its link to the previously identied CWI components in *A. fumigatus*.

2.2. Characterization of *fks1* in *A. fumigatus.*

The second part of this study aims to evaluate the significance of the echinocandin drug target, β-1,3-glucan synthase subunit Fks1 for viability, cell wall composition and antifungal tolerance of *A. fumigatus*. The echinocandins are fungistatic to *Aspergillus.* Therefore, it was hypothesized that either the cell wall component β-1,3-glucan is not essential for *A. fumigatus* viability or the echinocandins do not induce complete inhibition of β-1,3-glucan synthesis.

This has been addressed by studying the effects of downregulation of the *fks1* gene on *A. fumigatus* viability and growth phenotypes. Additionally, this study also emphasizes on the possible compensatory mechanisms that contribute to echinocandin tolerance in the pathogen, a theoretical concern for echinocandin therapy.

3. Materials and methods

3.1. Media and growth conditions

E. coli strain was grown at 37°C in LB medium containing 1% bacto-tryptone, 0.5% yeast extract and 1% NaCl pH 7.5 and for solid medium 1.5% bacto agar (214030; BD) was added (modified from Bertani 1951). For selection, LB was supplemented with 100 µg ml^{-1} ampicillin (171254; Calbiochem, Merck Chemicals, Germany).

A. fumigatus strains were grown on liquid and solid (supplemented with 2% bacto-agar) *Aspergillus* minimal media (AMM) containing salt solution, $MgSO_4.7H_2O$, trace elements (TE) and 1% (w/v) D-glucose (Hill and Kaffer, 2001). For growth on complete media, yeast glucose (YG) medium contained 0.5% (w/v) yeast extract (103303; M.P. Biomedicals, Irvine, CA) and 2% (w/v) D-glucose was used and pH was adjusted to either 6.0 or 7.0 as per requirement. For agar plates, medium was supplemented with 2% (w/v) bacto-agar (214030; BD, Franklin Lakes, NJ). Commercially available potato-dextrose agar (213400; Difco) and saboraud agar (210950; Difco) were used as such, while manually prepared saboraud dextrose agar (pH adjusted to 5.6) contained 0.5% tryptone/casein (8952.4; Carl Roth GmbH) as a substitute for pancreatic digest of casein, 0.5% peptic digest of animal tissue or peptone A (7181A; Neogen), 4% D-glucose and 1.5% bacto-agar (media composition adapted from Difco; 221988) while the liquid saboraud consisted of 0.5% tryptone/casein , 0.5% peptic digest of animal tissue or peptone A and 2% D-glucose (media composition adapted from Difco; 221014). For growth of mutants, media was supplemented with 0.5 µg ml^{-1} doxycycline (631311; Clonetech, Mountain View, CA) and 0.1 µg ml^{-1} pyrithiamine (sc-236525A; Santa Cruz Biotechnologies, CA) or 200 µg ml^{-1} hygromycin B (p21-014; PAA Laboratories, Pasching, Austria). Caspofungin diacetate (SML0425), calcofluor white (F3543), congo red (60910) and hydroxyurea (H86271) were obtained from Sigma-Aldrich (Taufkirchen, Germany). Sodium dodecyl sulphate (A3950) was obtained from AppliChem (Darmstadt, Germany).

3.2. Strain and Plasmid construction

E.coli strain DH5α (genotype F ϕ80d, lacZ ΔM15, endA1, recA1, hsdR17 (rK-mK-), supE44,thi-1, λ-, gyrA96, relA, Δ(lacZYA-, argF)U169) was used for cloning and plasmid propagation (Hanahan 1983).

The *A. fumigatus* strain Afs35 which is a derivative of strain D141 and lacks the homologous

end-joining component AkuA was used as wild-type in this study (Krappmann *et al*., 2006). The conditional $rom2_{tetOn}$ and $fks1_{tetOn}$ strains were constructed essentially as described recently (Dichtl *et al*., 2012). Briefly, the endogenous promoter of *rom2* (AFUA_5G08550) and *fks1* (AFUA_ 6G12400) were replaced by the $^{p}gpdA$ and $^{p}oliC$ doxycycline-regulated promoter cassettes respectively as described previously (Dichtl *et al*., 2012; Helmschrott *et al*., 2013). Approximately, 1 kb fragment of the 5'- flanking region located upstream of the *rom2* and *fks1* ORFs (amplified with primer pairs Prom2-5g08550-5-fwd and Prom2-5g08550-5-rev and Fks1-6g12400-5-fwd and Fks1-6g12400-5-rev respectively) and approximately 1 kb fragment of 3'-flanking region beginning with the start codon of ORFs of respective genes (amplified by primer pairs Prom2-5g08550-5-fwd and Prom2-5g08550-5-rev and PFks1-6g12400-3-fwd and PFks1-6g12400-3-rev respectively) were fused to the pyrithiamine-tetOn cassettes acquired by SfiI digestion of pJW123 and pJW128 respectively and transformed in strain AfS35. The C-terminally green fluorescent protein (GFP)-tagged Rom2 ($rom2\text{-}GFP_{gpdA}$) was expressed by cloning *rom2* (PCR amplified with primers Rom2-5g08550-fwd and Rom2-5g08550-fu-rev with chromosomal template DNA) into the PmeI site of pJW103 and transforming the resulting vector pSS001 in strain AfS35. The strain with the inducible expression of $rho1^{G14V}$ ($rho1^{G14V}_{tetOn}$) was constructed by transforming pCH003-G14V in AfS35. pCH003-G14V is a derivative of pCH003 that was created by site-directed mutagenesis using the mutagenesis primer Rho1-G14V-SphI and the Change-IT multiple mutation site-directed mutagenesis kit (USB Corporation, Cleveland, OH). pCH003 was constructed by cloning *rho1* (PCR amplified with primers Rho1-6g06900fufnew and Rho1-6g06900-rev) in pJW121. pJW121 was constructed by cloning the tetracycline-dependent transactivator, the *crgA* terminator and the *tetO7::Pmin* (a blunt-end fragment derived from pVG2.2 after digestion with EcoRI and PmeI) into the PmeI site of pSK379 (Meyer *et al*., 2011). pJW103 and pSK379 were described previously (Dichtl *et al*., 2010).

Strains for the doxycycline-inducible expression of the C-terminally 6X His-tagged full-length Rom2 and N-terminally hemagglutinin (HA)-tagged Rom2 with aminoacids 733 to 1199 [HA-Rom2(733-1199)] were generated by PCR amplifying full-length Rom2 with primers Rom2-5g08550-fwd and His-Rom2-5g08550-rev and Rom2 (733-1199) with the primers HA-Rom2GEF-5g08550-f and Rom2-5g08550-rev and cloning the respective PCR products in pSS005, yielding pSS006 and pSS009. pSS006 and pSS009 were subsequently transformed in strain AfS35. pSS005 is a derivative of pJW121 where the pyrithiamine resistance cassette was exchanged with a hygromycin B resistance cassette. To perform the

co-immunoprecipitation experiment, pSS009 [N-terminally HA-tagged Rom2 (733-1199)] was transformed in D141 strains constitutively expressing N-terminally GFP-tagged Rho1 or Rho3, which were previously described (Dichtl *et al*., 2010). Strains encoding the C-terminal GFP-tagged rom2 at the endogenous locus were constructed by transforming pSS011 in the respective parental strains (AfS35and $rom2_{tetOn}$ strain), yielding the *rom2-GFP* and $rom2\text{-}GFP_{tetOn}$ strains. pSS011 was cloned by digesting pSS001 with BstBI and pSS005 with BglII followed by blunt ending and further digestion with Acc65I. A pSS001 fragment harbouring the coding sequences of GFP and the C-terminal region of Rom2 was ligated to a pSS005 fragment harbouring the hygromycin B resistance cassette.

In order to downregulate *fks1* in Δ*hexA* and Δ*rho4* starins, the endogenous *fks1* promoter was of respective parental strains were replaced by $^{p}oliC$ promoter cassette as described above. The Δ*rho4* and Δ*hexA* deletion strains have been described previously (Dichtl *et al*., 2012; Beck *et al*., 2013). The deletion strain Δ*fks1* was generated by replacing the full-length ORF by a pyrithiamine-resistance (*ptrA*) cassette. Approximately 1 kb fragments flanking both upstream and downstream regions of *fks1* ORF were amplified from chromosomal DNA using primer pairs Fks1-6g12400-5-fwd and Fks1-6g12400-5-rev as well as Fks1-6g12400-3-fwd and Fks1-6g12400-3-rev which harboured incompatible SfiI sites. After digestion with SfiI, these fragments were ligated with pyrithiamine cassette and the resulting deletion deletion cassette was then transformed into AfS35. For each mutant strain, at least three independent clones were isolated and verified by PCR as well as phenotypic analysis.

Table 1. All the oligonucleotide primers used in this study are listed in Table 1 (Part I and II).

I. AfRom2 characterization:

Primer	Sequence
Rom2-5g08550-5-fwd	TTGCGGCCGCTCCTTAGGCGCGTGACGG
Rom2-5g08550-5-rev	CGGGCCATCTAGGCCGCTTCTACCTCTGACAG
Prom2-5g08550-3-fwd	GTGGCCTGAGTGGCCATGGCCGATCTCGGTGGCC
Prom2-5g08550-3-rev	TTGCGGCCGCCGACCCGTGAGAGCAGGGC
Rom2-5g08550-fwd	ATGGCCGATCTCGGTGGCC

Rom2-5g08550-fu-rev	GCCGCCGCTTGTTGTTGTTGGGGCTTGTTC
Rho1-6g06900fufnew	AGGCGGCATGGCTGAAATCCGCCGCAAG
Rho1-6g06900-rev	TTACAAAATAGTGCACTTGCCCTTC
Rho1-G14V-SphI	GTCATCGTTGGCGATGTCGCATGcGGTAAGACTTGTC TTC
His-Rom2-5g08550 rev	TCAGTGGTGGTGGTGGTGGTGGGAGCCGCGGCCGCCT TGTTGTTGTTGGGGCTTGTTC
HA-Rom2GEF-5g08550-f	ATGTACCCATACGATGTTCCAGATTACGCTGCCAGC CTTCACGGCGATG
Rom2-5g08550-rev	TCATTGTTGTTGTTGGGGCTTG
Rom2-5g08550-3-cast	GACATTGACCGTCTATTCACG
Rom2-5g08550-pro-cast	CTTTGAGCTCAAGACCAGTG
ptrA-3-fwd	GTCCCGTATGTAACGGTGG
seq-tetOn-fwd	AAGTGAAAGTCGAGCTCC

II. AfFks1 characterization:

Primer	Sequence
Fks1-6g12400-5-fwd	TTGCGGCCGCCTAACTGCAACCGCATAGCG
Fks1-6g12400-5-rev	CGGGCCATCTAGGCCAGATGAACGAAGGTAGGGAGG
PFks1-6g12400-3-fwd	GTGGCCTGAGTGGCCATGTCGGGATATCAACAAGGG
PFks1-6g12400-3-rev	TTGCGGCCGCAAGAACAGTGCCAGTTGGCG
PFks1-6g12400-5-cast	GTCTCATTACGAGCCATGCAG
PFks1-6g12400-3-cast	CGGACCTGGTTGGCTTCG
ptrA-3-fwd	GTCCCGTATGTAACGGTGG

tetOn-rtTA-fwd	CACCATGTCTAGACTGGACAAG
Fks1-6g12400-int-fwd	GGATGCATGGCTGTCCAGGAACTGACAG
Fks1-6g12400-fu-rev	GCCGCCGCGCTCGTTGCAGTAGCCACGC
ptrA-5-rev	CGTTACCAATGGGATCCCG

Table 2. *A. fumigatus* strains used in this study

Strain	Relevant gene modification or plasmid	Parental strain	Reference
AfS35	*akuA::loxP*	D141	Krappmann *et al.* (2006)
$rom2_{tetOn}$	*Prom2::ptrA-tetOn*	AfS35	This study
$rho1^{G14V}{}_{tetOn}$	pCH003-G14V	AfS35	This study
$rom2\text{-}His_{tetOn}$	pSS006	AfS35	This study
$HA\text{-}rom2(733\text{-}1199)_{tetOn}$	pSS009	AfS35	This study
rom2-GFP	pSS011	AfS35	This study
$rom2\text{-}GFP_{tetOn}$	pSS011	$rom2_{tetOn}$	This study
$rom2\text{-}GFP_{gpdA}$	pSS001	AfS35	This study
$GFP\text{-}rho1_{gpdA}$	pJW103-Rho1	D141	Dichtl et al. (2010)
$GFP\text{-}rho3_{gpdA}$	pJW103-Rho3	D141	Dichtl et al. (2010)
$GFP\text{-}rho1_{gpdA}$ $HA\text{-}rom2(733\text{-}1199)_{tetOn}$	pSS009	$GFP\text{-}rho1_{gpdA}$	This study
$GFP\text{-}rho3_{gpdA}$ $HA\text{-}rom2(733\text{-}1199)_{tetOn}$	pSS009	$GFP\text{-}rho3_{gpdA}$	This study
AfS35-GFP	pJW656-sGFP-phleo	AfS35	This study
$fks1_{tetOn}$	*fks1(p)::ptrA-oliC-tetOn*	AfS35	This study
Δfks1	*fks1::ptrA*	AfS35	This study
Δ*hexA*	*hexA:: loxP-hygro*^{R}*/tk*	AfS35	Beck & Ebel (2013)

Δ*hexA*+ *hexA*	pSK379-*hexA(p)-hexA*	Δ*hexA*	Beck & Ebel (2013)
Δ*hexA*-GFP	pJW656-sGFP-phleo	Δ*hexA*	This study
Δ*hexA-fks1*$_{tetOn}$	*fks1(p)::ptrA-oliC-tetOn*	Δ*hexA*	This study
Δ*rho4*	*rho4::loxP-hygro*^{R}*/tk*	AfS35	Dichtl *et al*. (2012)
Δ*rho4* + *rho4*	pSK379-*rho4(p)-rho4*	Δ*rho4*	Dichtl *et al*. (2012)
Δ*rho4* –GFP	pJW656-sGFP-phleo	Δ*rho4*	This study
Δ*rho4-fks1*$_{tetOn}$	*fks1(p)::ptrA-oliC-tetOn*	Δ*rho4*	This study

3.3. General molecular biological methods

3.3.1. Genomic DNA isolation from *A. fumigatus*

A. fumigatus condia were grown in liquid AMM at 37ºC on a 180 rpm shaker for approximately 16-24 h and harvested using sterile filter paper. Approximately 20 mg of mycelia was added into a sterile 2ml lysing matrix A tubes (116910050; MP Biomedicals) containing a ceramic bead and 0.25ml chemically inert quartz (107536; Merck, Darmstadt, Germany). For each reaction, 225 µl of yeast cell lysis solution (MPY80200; Epicentre Biotechnologies) was added and homogenized using FastPrep-24 at a speed of 6 m/s for 40 seconds. This was followed by incubation at 65ºC for 30 minutes and then on ice for 5 minutes. Then 112.5 µl of MPC Protein precipitation reagent (MPY80200; Epicentre Biotechnologies) was added and the tube was centrifuged at 10,000 rpm for 10 minutes. The supernatant was transferred to a fresh sterile microcentrifuge tube and mixed with 375 µl isopropanol. This was followed by centrifugation at 13,000 rpm for 15 minutes. The pellet was washed with 500 µl 70% EtOH at 13,000 rpm for 15 minutes at 4ºC. The pellet containing genomic DNA was dried at 55ºC and finally dissolved with ddH_2O containing RNase. The DNA concentration was measured using Nanodrop spectrophotometer and analyzed on 1% agarose gel.

3.3.2. PCR

Pfu-DNA polymerase (EP0502; Fermentas) was used for preparative PCR reactions according to manufacturer's protocol. Alternatively, control PCRs and colony PCRs were

performed with Taq-polymerase (EP0401; Fermentas). LongAmp™ *Taq* DNA polymerase (M0323S; NEB) was used to amplify fragments ≥ 5 kb. Customized oligonucleotides were ordered from GATC Biotech. A standard PCR reaction consisted of an initial denaturation step over two minutes at 95°C, 30 cycles with each cycle consisting of 30 s denaturation at 95°C, 30 s primer annealing at 50-60°C (depending on primer pair composition) and 1-6 min DNA elongation at 72°C (elongation time depended on the length of the amplified fragment), and a final elongation step at 72°C over 10 min. Usually, genomic DNA or in case of colony PCRs *E. coli* transformants were used as template for the reactions.

3.3.3. Restriction digestion, phosphorylation, dephosphorylation and ligation

Ligation reactions were performed with T4 DNA ligase (EL0011, Fermentas) and incubated at 16ºC overnight or using rapid DNA ligation kit (K1422, Fermentas) for 5 minutes at room temperature. For dephosphorylation of vectors and phosphorylation of PCR products Fast AP alkaline phosphatase (EF0651; Fermentas) and T4 polynucleotide kinase (EK0031; Fermentas) were used respectively. Dephosphorylation of vector was performed by incubating with enzyme at 37ºC for 20 minutes followed by heat inactivation at 75ºC for 5 minutes. Phosphorylation of PCR fragments was performed by incubating at 37ºC for 45 minutes followed by heat inactivation at 75ºC for 10 minutes. Restriction enzymes were ordered from Fermentas and digestions were performed as per instructions manual.

3.3.4. Transformation in *E. coli*

Chemically competent E. coli cells were prepared and DNA transformation was performed as described (Inoue *et al*., 1990). Briefly, the recombinant plasmid was added to *E.coli* DH5α competent cells aliquot and incubated on ice for 30 minutes. This was followed by a brief heat shock at 42ºC for 90 seconds and further incubation on ice for 2 minutes. Then 1 ml of LB media was added to the aliquot and incubated for atleast 45 minutes followed by centrifugation at 13,000 rpm for 2 minutes. The pellet was dissolved in 100 µl supernatant and plated out on LB agar plate supplemented with 100 µg ml^{-1} ampicillin.

3.3.5. Plasmid Isolation

Plasmid DNA was isolated from E. coli DH5α competent cells with the PureYieldTM

plasmid midiprep system (Promega). Briefly, a bacterial colony was grown overnight in 60-100 ml LB media supplemented with ampicillin and the cells were collected by centrifugation

at 5,000xg for 10 minutes. The pellet was resuspended in 3ml cell resuspension solution and mixed with 3ml of cell lysis solution and incubated at room temperature for 3 minutes. The lysate was mixed with 5 ml cold neutralization solution and centrifuged at 11,000 x g for 15 minutes. The supernatant was transferred into the spin column assembly placed on a vacuum manifold port and allowed to pass through the column assembly. The clearing column was removed and 5 ml endotoxin removal wash solution was added to the binding column and allowed to pass through by applying vacuum. This was followed by addition of 20 ml column wash solution which was allowed to pass through and the binding membrane was dried for 30-60 seconds. The column was removed from vacuum port and placed in a 50 ml falcon tube. The plasmid DNA was eluted with 600 µl of nuclease-free water that was added onto the membrane and incubated for 5 minutes at room temperature. The plasmid was collected by centrifugation at 2,000 x g for 5 minutes.

3.3.6. Transformation in *A. fumigatus*

The protocol for *A. fumigatus* transformation was adapted from Punt *et al*., 1987 with slight modifications. *A. fumigatus* conidia were grown for 16-24 h in liquid AMM at 180 rpm shaker at 37ºC and harvested by filtration through sterile Miracloth (Calbiochem, CA). The mycelia was washed with citrate buffer (pH 5.5) containing 150 mM KCl, 580 mM NaCl and 50 mM sodium citrate dehydrate and digested with 30 ml enzyme solution containg either 30 mg/ml Novozyme 234 solution or 66 mg/ml Vinotaste®Pro (Novozymes) in citrate buffer for 45 minutes. The digest was then filtered through Miracloth to generate protoplasts. The protoplast suspension was incubated with STC 1700 buffer (1.2 M sorbitol, 10 mM Tris pH 5.5, 50 mM $CaCl_2$ and 35 mM NaCl) on ice and washed twice at 1700 x g for 12 minutes each at 4ºC. The supernatant was discarded and protoplast pellet was resuspended in remaining 500 µl buffer. 30 µl DNA was added to the aliquots containing 200 µl protoplast suspension and incubated on ice for 30 minutes. Fusion was accomplished by addition of PEG 4000 mix containing 60% PEG 4000, 50 mM $CaCl_2$ and 50 mM Tris-HCl pH 7.5. Following transformation, the fused protoplasts were concentrated by centrifugation at 1700 x g for 12 minutes at 4 ºC and added to aliquots of molten soft agar containing 1.2 M sorbitol, mixed well and overlaid on AMM agar plates supplemented with 1.2 M sorbitol with or without 0.5 µg ml^{-1} doxycycline and appropriate selection marker.

3.4. Microbiological methods

3.4.1. Growth tests and susceptibility assays

To evaluate the doxycyline dependent growth, 1.5×10^3 conidia were added at the center of each well containing 2 ml of AMM agar supplemented with varying concentration of doxycycline as indicated in 24-well plates and incubated for 36 h at 37°C. Radial growth assay was performed by inoculating 1.5×10^3 conidia at the centre of AMM agar plate with or without 0.5 and 5 µg/ml doxycycline, incubated for at least 3 days at 37°C and colony diameter was measured every 24 h.

Drop dilution assays were performed in a series of 10-fold dilutions derived from a starting suspension of 5×10^6 conidia ml^{-1}. Aliquots of 3 µl were spotted onto agar plates. Media was supplemented with or without doxycycline and cell wall perturbing agents such as CR, CFW as indicated. For antifungal E-tests, 25 x 10^3 conidia were spread on a plate and Etest strips were overlaid and the plate was incubated for 48 h at 37°C. E-test strips were obtained from bioMérieux (Marcyl'Etoile, France).

3.5. Biochemical methods

3.5.1. Colorimetric alkaline phosphatise assay

This assay was performed as described previously (Cabib and Duran, 1975; Paravicini *et al*., 1992) with slight modifications. Conidia suspension containing 1.5 x 10^3 conidia was spotted on AMM agar plate and incubated for 36 h at 37ºC and then shifted to 48ºC for 6 h. The plate was then overlaid with soft agar containing 1% agar supplemented with alkaline buffer (containing 1 M glycine (pH 10.0), 1 M $MgCl_2$ and 250 mM $ZnCl_2$) and 10 mM chromogenic substrate BCIP (5-bromo-4-chloro-3-indolyl-phosphate) and incubated at 48ºC for further 2 h. Mutant colony with lysed cells appeared blue within 30-45 min, whereas wild-type colony remained unstained even after 2h.

3.5.2. Protein extraction and Western blot

Freshly harvested conidia were inoculated in 10 ml of AMM supplemented with 0.5 µg ml^{-1} doxycycline if required, and cultured in a tube rotator at 37ºC for 24 h. 100 µg ml^{-1} calcofluor white was added to respective cultures and further incubated for 30 minutes. Mycelium was harvested and resuspended in prewarmed 2X Laemmli buffer [95ºC; 2% (w/v) SDS, 5% (v/v) mercaptoethanol, 60 mM Tris/HCl (pH 6.8), 10% (v/v) glycerol, 0.02 (w/v) bromophenol blue] and extracted using a FastPrep-24 (M.P. Biomedical, Irvine, CA) with a speed of 5.5

ms^{-1} for 40 s followed by heat denaturation at 98ºC for 5 min. Samples were separated using 12% or 7.5% SDS-PAGE as indicated and transferred to nitrocellulose membrane (Whatman, Germany) at 200 mA for 2 h at room temperature. Blots were blocked in 5% milk in TBS-T and analyzed with the anti-phospho-p44/42 MAPK rabbit monoclonal antibody (1:2000) (Cell Signaling Technologies, Boston, MA; 4370) or a polyclonal rabbit anti-GFP antibody (a kind gift from Carsten Bornhövd, Munich, Germany). Monoclonal antibodies directed against mitochondrial manganese superoxide dismutase MnSOD (AFUA_4G11580) or asf22 (AFUA_6G06770) was used as loading control (kind gifts from Frank Ebel). The membranes was washed with 1X TBS-T and reprobed with goat polyclonal secondary antibodies against rabbit (1:10000) and mouse (1:10000) (Bio Rad, Hercules, CA). Immunodetection was accomplished using the ECL detection kit (Milipore).

3.5.3. Relative quantification of phosphorylated MpkA

Developed Super RXX-rayfilms (Fujifilm, Tokyo, Japan) were scanned with a GS-800 calibrated densitometer and analyzed with Quantity One 4.5.0 (Bio-Rad, Hercules, CA). The relative signal intensity (percentage of total adjusted volume of all phosphorylated MpkA signals) and respective standard deviations were calculated for each sample.

3.5.4. Coimmunoprecipitation with HA-Rom2 (733-1199)

Conidia of the D141 strain expressing the N-terminally GFP-tagged Rho1 and Rho3 and harbouring the doxycycline-inducible HA-tagged Rom2 (733-1199) construct were inoculated in AMM (5×10^5 conidia ml^{-1}) and cultured in a shaker at 37°C. After 24 h, either no or 50 µg ml^{-1} doxycycline was added, and the cultures were incubated for another 4 h at 37°C. Mycelium was harvested and washed twice with washing buffer (50 mM Tris-HCl [pH7.6], 20 mM NaCl, 1 mM phenylmethylsulfonyl fluoride [PMSF]). Five hundred milligrams of mycelium was added to 0.85 ml lysis buffer (50 mM Tris-HCl [pH7.6], 20 mM NaCl, 1 mM NaF, 2 mM $MgCl_2$, 1% [v/v] Triton X-100, 10% [v/v] glycerol, 1µg ml^{-1} complete EDTA-free protease inhibitor (04693159001; Roche Diagnostics, Risch, Switzerland) in a Lysing Matrix C tube and lysed with a FastPrep-24 (M.P.Biomedical; Irvine,CA) for 10 times at 5.5 ms^{-1} for 40 s. The samples were centrifuged for 15 mins at 21,000 x g at 4°C, and 2 ml supernatant was added to 20 µl anti-HAagarose (26180; Thermo FisherScientific, Rockford, IL) and incubated in an end-over-end mixer at 4°C. After 5 h, the agarose was transferred to a spin column and washed two times with 0.5 ml agarose washing

buffer (25mM Tris-HCl [pH7.2], 0.15 M NaCl, 1mM NaF, 2mM $MgCl_2$, 0.05% [v/v] Tween 20, 1X complete EDTA-free protease inhibitor). The agarose was heated at 95°C for 5 mins in 25 µl non-reducing sample buffer (26180; ThermoFisherScientific, Rockford, IL). The eluate was supplemented with 1.5µl 2-mercaptoethanol and 1 µl of a 100X complete EDTA-free protease inhibitor stock solution. The supernatant (2.5 µl per lane) and eluate (7.5 µl per lane) were analyzed on 12% SDS-PAGE by Western blot. Primary antibodies directed against the HA tag (monoclonal antibody) (H9658; Sigma-Aldrich, St.Louis, MO) or GFP (polyclonal antibody, rabbit; a kind gift from Carsten Bornhövd, Munich, Germany) were used.

3.5.5. Immunostaining

To prepare samples for galactomannan and β-glucan staining, conidia from wild type and mutant strains were co-incubated on glass cover slips in 1 ml of AMM for 14 h at 37°C. Coverslips were then fixed with 3.7 % formaldehyde in PBS and washed thrice in PBS. Samples were subsequently blocked with 1 % goat serum in PBS (supplemented with 0.1 % Tween-20 when indicated) for 30 min followed by three washes with PBS/T. The galactomannan-specific mAb (L10-1; diluted 1:50 in PBS/T) and β-glucan-specific mAb (2G8; diluted 1:10 in PBS/T) that have been described previously (Heesemann *et al.*, 2011 and Torosantucci *et al.*, 2005 respectively) were used as primary antibodies. Samples were incubated with the primary monoclonal antibody (mAb) in a humid chamber for 30 min and washed thrice with PBS/T, followed by a staining with Cy3-labelled anti-mouse secondary antibody (Dianova, Hamburg, Germany) or Alexa Fluor 488 conjugated goat anti-mouse IgG (A-11001, Life Technologies, Darmstadt, Germany) diluted 1:50 and 1:200 in PBS/T respectively. The coverslips were then washed thrice with PBS/T and mounted with Vecta Shield mounting medium (Vector Laboratories, Burlingame, USA) for fluorescence microscopy.

3.5.6. Galactomannan quantification assay

The Platelia *Aspergillus* Ag Kit (62794; Bio-Rad Laboratories, Hercules, U.S.A.) was used to determine the galactomannan concentration in culture supernatants. Briefly, 3 x 10^4 conidia from respective strains were incubated in 1 ml AMM at 37°C. After 10.5 h, 80 % of the medium was replaced with fresh medium and incubated for additional 35 h at 37°C. Subsequently, supernatants were collected and centrifuged at 13,000 rpm for 15 min to eliminate residual soluble components. Samples were diluted 1:500 in ddH_2O prior to

galactomannan quantification according to manufacturer's instructions. The viability of the overnight grown cultures was measured using PrestoBlue cell viability reagent (A-13261; Life Technologies, Darmstadt, Germany), diluted 10 % in AMM and incubated for further 2.5 h at 37°C. The change in coloration of supernatant was quantified using a FLUOstar Optima fluorescence plate reader (BMG Labtech, Ortenberg, Germany) with optimized settings (excitation filter 550 nm, emission filter 590 nm and gain value 1100). Samples were used in triplicates.

3.6. Sequence analysis and bioinformatic tools

The sequences were derived from the following genome databases: the Aspergillus genomedatabase (http://aspergillusgenome.org), the Saccharomyces GenomeDatabase (http:// www.yeastgenome.org), and the Central Aspergillus DataRepository (CADRE) (http://www. cadre-genomes.org.uk). Conserved protein sequence signatures were predicted using InterProScan (http://www.ebi.ac.uk/Tools/pfa/iprscan). The Pfam database (http://pfam. sanger.ac.uk) was used to identify proteins with functional domains in *A.fumigatus*. Multiple sequence alignments and phylogenetic trees were generated with MAFFT (http://www.ebi.ac. uk/Tools/msa/mafft/). The phylogenetic tree was visualized with TreeVector (http://supfam. cs.bris.ac.uk/TreeVector/). Identities and similarities of MAFFT alignments were calculated with Sequences Identities And Similarities (SIAS) (http://imed.med.ucm.es/Tools/sias.html).

3.7. Microscopy

3.7.1. Microscopic examination of hyphal growth and morphology

Representative microscopic bright-field images of hyphal growth and morphology were taken with an Axiovert 25 inverted microscope (Carl Zeiss Microimaging, Göttingen, Germany). Briefly, 5 x 10^3 conidia were inoculated in 24-well plates in 1ml AMM supplemented with the indicated amount of doxycycline and caspofungin. Images were taken with a Canon EOS 600D camera (Tokyo,Japan).

3.7.2. Live cell imaging

To determine the localization of Rom2-GFP, the strain was cultured in an eight well-chambered µ-Slide (80826; Ibidi, Martinsried, Germany) containing 5 x 10^2 conidia in 300 µl of AMM in each well. Live cell images were taken after approximately 15 h of incubation at

37°C. Living hyphae were analyzed with UltraView LCI spinning disc confocal system (PerkinElmer; Waltham, MA) fitted on an Eclipse TE300 microscope (Nikon, Tokyo, Japan) in a temperature-controlled chamber. Images were taken with a black/white ORCA ER camera (Hamamatsu, Hamamatsu City, Japan).

3.7.3. Fluorescence microscopy

To quantify the effect of septa on caspofungin-mediated killing, conidia of the indicated strains expressing cytosolic GFP were cultured on glass cover slips in 24-well plates in 1 ml media at 37°C. After 12 h incubation, 50% of the medium was replaced with fresh medium containing caspofungin diacetate (0.1 µg ml^{-1} final concentration). After additional 2 h incubation, the samples were fixed and stained with calcofluor white to detect presence of septa. Experiments were performed in either AMM or YG as indicated. When required, YG was supplemented with 0.025 % (v/v) diepoxyoctane (DEO) or 9 mM hydroxyurea (HU). Samples were quantified using a Leica DMLB fluorescence microscope (Leica Microsystems, Wetzlar, Germany). The hyphae were counted as alive when showing GFP fluorescence throughout or partially alive if GFP fluorescence was detected in at least one hyphal compartment or dead when showing no GFP fluorescence at all.

For calcofluor white staining, samples were fixed with 3.7% formaldehyde and washed with 1X PBS in formaldehyde. Coverslips were overlayed with 1 mg ml^{-1} CFW in ddH2O for 3 min. Coverslips were subsequently washed with 1X PBS in formaldehyde and mounted on glass slides with Vectashield Mounting Medium (H-1000; Vector, Burlingame, U.S.A.). Images were taken with a Leica SP5 confocal laser-scanning microscope (Leica Microsy stems, Wetzlar, Germany). Analysis of fluorescence intensity was performed using the LAS AF Software provided by Leica. A vector was drawn perpendicular to the hyphal surface and the average of all values of signal intensity between the base and peak of the curve was calculated. The mean fluorescence instensity of atleast 60 cell wall intersections each of both wild type and $fks1_{tetOn}$ was quantified.

4. Results

4.1. Characterization of Rom2 GEF in cell wall integrity of *A. fumigatus.*

4.1.1. Identification of ScRom1/Rom2 homologue in *A. fumigatus* and domain analysis.

In order to identify the homologue of ScRom1/Rom2 in *A. fumigatus* genome, a BLASTP search using the query sequence was performed in the genome database of *A. fumigatus* (Arnaud *et al*., 2010). The search resulted in only one homologue (AFUA_5G08550) with a length of 1,199 amino acids which has an identity and similarity of 28% and 41% with ScRom1 and 31% and 43% with ScRom2, respectively. Therefore, the protein sequence encoded by AFUA_5G08550 was named Rom2.

Next, the domain architecture of Rom2 was determined using InterProScan (Zdobnov and Apweiler, 2001). As expected, the Rom2 harboured conserved domains similar to ScRom1/Rom2- a dishevelled, Egl-10, and pleckstrin (DEP) domain (PF00610), followed by a Rho GEF domain (PF00621) and a citron homology (CNH) domain (PF00780) from the N terminus to C terminus respectively. The PH domain if present is not annotated (Table 3). A PFAM search for proteins containing the Rho GEF domain (PF00621) in *A. fumigatus* listed six proteins, including Rom2 (Figure 12). However, none of the other GEF domain proteins contained a DEP domain, and only one, AFUA_5G07430, harbored a CNH domain. AFUA_5G07430 is similar to the GEFs SpRgf3 (*S. pombe* Rho gef3) and NcRGF3 (*N. crassa* RGF3) of *S. pombe* and *N. crassa*, respectively. SpRgf3 is a GEF of SpRho1 and controls β-(1,3)-D-glucan biosynthesis and cytokinesis (Mutoh *et al*., 2005; Tajadura *et al*., 2004), while NcRgf3 of the filamentous fungus *N. crassa* was shown to be a specific GEF for NcRho4 and implicated in septum formation (Justa-Schuch *et al*., 2010).

Table 3. Domains annotated in *A. fumigatus* Rom2 protein as revealed by InterProScan analysis.

Protein domain	Position
DEP	334-403
RhoGEF/ DH	503-689
CNH	882-1169

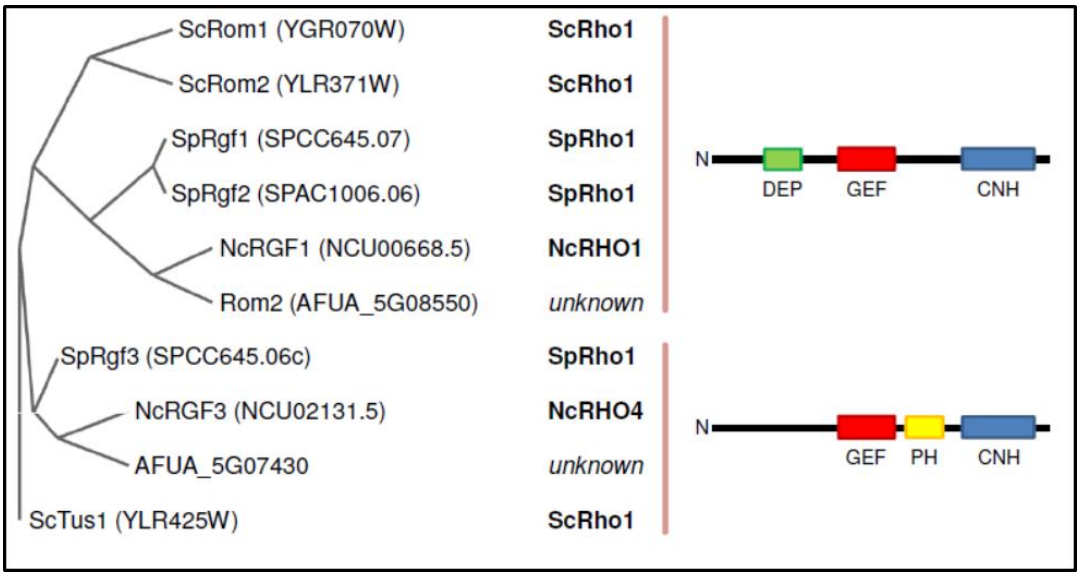

Figure 12. Sequence alignment of the putative Rho1 GEF in *A. fumigatus* with other fungal homologues. Phylogenetic tree of Rho GEF domain (PF00621)-containing proteins of *S. cerevisiae* (Sc), *S. pombe* (Sp), *N. crassa* (Nc), and *A. fumigatus* with similarity to ScRom1/2. The protein sequences of the respective genes were aligned, and the guided tree was generated with MAFFT and visualized with TreeVector. The known interacting Rho GTPases for each GEF and the conserved protein domain structures are listed.

4.1.2. Generation of a conditional *rom2* mutant.

In *S. cerevisae*, a double deletion of *ScROM1* and *ScROM2* is lethal. The same is true for a double deletion of *rgf1*$^{+}$ and *rgf2*$^{+}$ in *S. pombe*. Despite several attempts to create a deletion mutant of *rom2* in *A. fumigatus*, a viable clone harboring the respective mutation could not be isolated. This suggested that similar to its other orthologues, *rom2* is also an essential gene in *A. fumigatus*. Therefore, a conditional *rom2* mutant (*rom2*$_{tetOn}$) was constructed by replacing the endogenous *rom2* promoter with a doxycycline-inducible promoter (Figure 13 A and B).

Surprisingly, the conditional *rom2* mutant was viable under repressive conditions on minimal medium. The addition of 0.25 to 0.5 µg ml^{-1} doxycycline reconstituted wildtype-like growth on solid medium, while the addition of higher doxycycline concentrations significantly repressed sporulation (Figure 14 A). However, in absence of doxycycline, the radial growth of the mutant was strikingly impaired and sporulation was completely abolished. Overexpression of *rom2* slightly reduced radial growth, while sporulation was significantly reduced compared to the wild type (Figure 14 B and D). Further, it was speculated that if Rom2 acts as a putative GEF for Rho1, overexpression of *rom2* would phenocopy the constitutive activation of *rho1*.

To test this hypothesis, a strain expressing a constitutive active allele (*rho1*$^{G14V}_{tetOn}$) under a doxycycline-inducible promoter was constructed. The expression of the constitutive active *rho1*^{G14V} resulted in a slightly reduced radial growth compared to the wild type. Sporulation was also drastically reduced, but the colony morphology appeared less compact compared to the strains overexpressing *rom2* (Figure 14 C and E).

A.

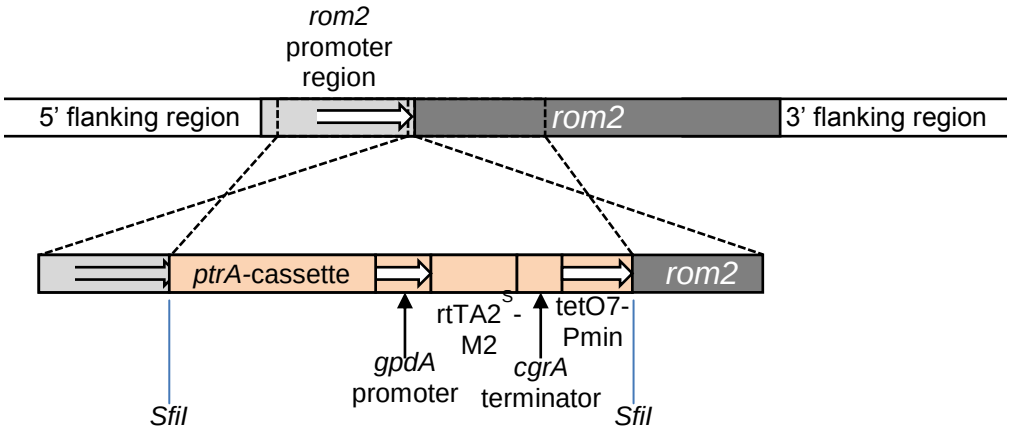

B.

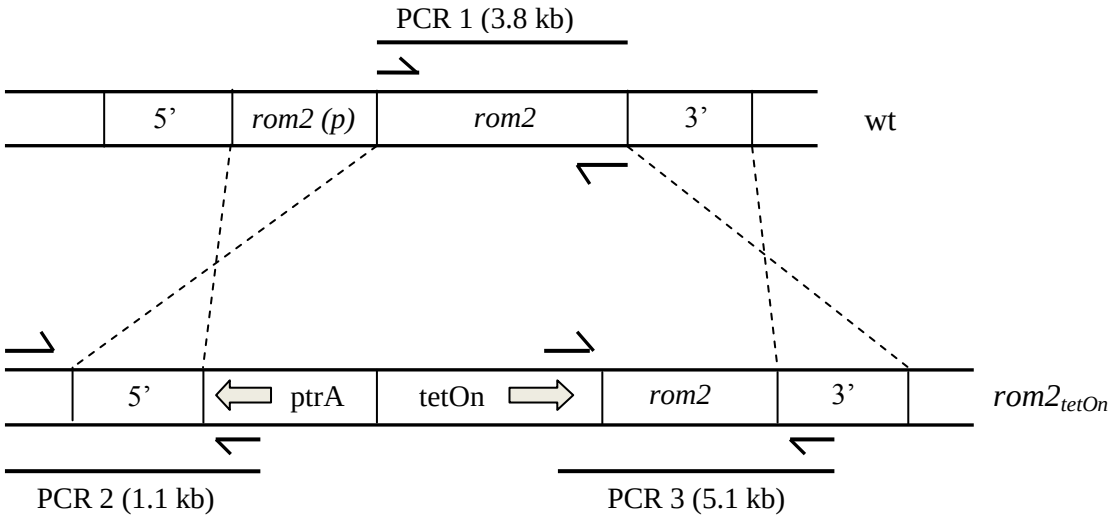

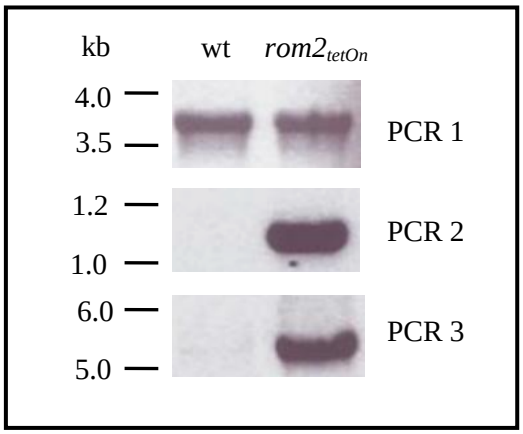

Figure 13. Generation of a conditional rom2 mutant and PCR verification of mutant clone. (A) The promoter of rom2 was replaced by homologous recombination with a doxycycline-inducible promoter system. The 5'- and 3'- flanking regions were ligated to the doxycycline-inducible promoter system using the indicated SfiI restriction sites. (B) Graph showing the promoter locus in wild-type (wt) and *rom2*$_{tetOn}$ mutant. Primer binding sites and length of respective amplicons are indicated. PCR amplifications correspond to regions indicated by PCR 1-3.

A.

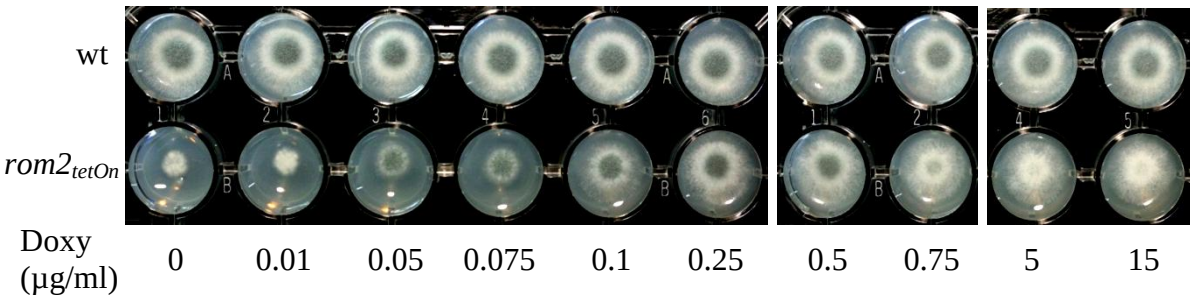

B.

C.

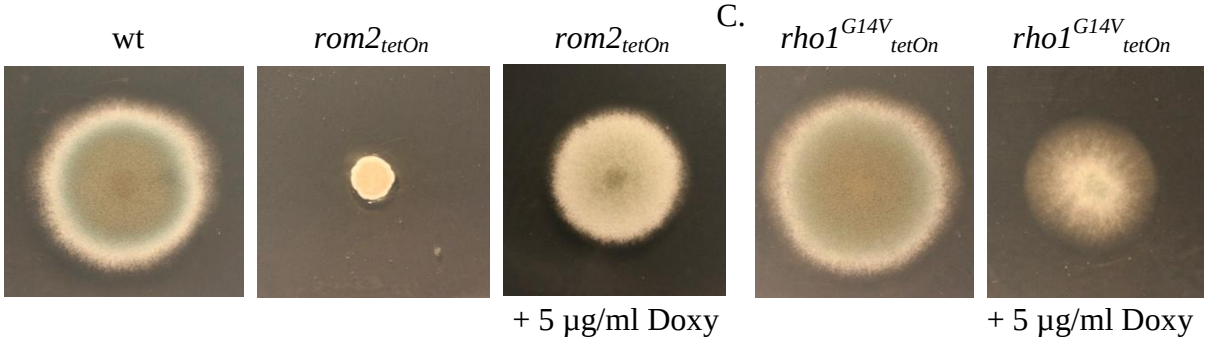

D. E.

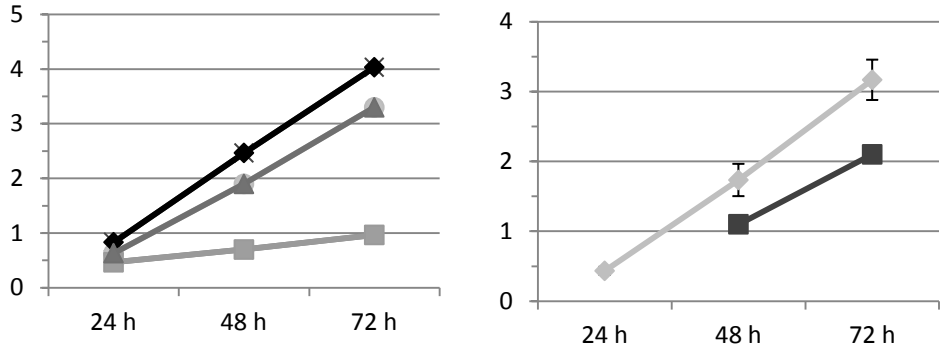

Figure 14. Doxycycline-dependent growth phenotypes of the conditional *rom2*$_{tetOn}$ mutant. (A to C) A total of 1.5x10^3 conidia of the indicated strains were spotted on AMM agar supplemented with the indicated amount of doxycycline (Doxy) and incubated for 36h (A), 72h (B), or 96h (C) at 37°C. (D and E) Mean radial colony diameter of strain AfS35 (black symbols and lines in panel D) and *rom2*$_{tetOn}$ strain with and without 5 µg/ml doxycycline (dark and light gray symbols and lines, respectively in panel D) and *rho1*$^{G14V}_{tetOn}$ strain with and without 5 µg/ml doxycycline (light gray and black symbols and lines, respectively in panel E) measured after indicated time periods. The AMM agar was additionally supplemented with pyrithiamine to avoid loss of rho1$^{G14V}_{tetOn}$ construct (C). Error bars indicate standard deviation. wt, wild type.

4.1.3. Evaluation of *rom2* expression levels in the conditional *rom2*$_{tetOn}$ mutant.

In order to evaluate the expression levels of *rom2*$_{tetOn}$ under basal, optimal and overexpression conditions, the sequence expressing a C-terminal GFP tag was integrated at the endogenous *rom2* loci in the wild type and conditional *rom2*$_{tetOn}$ mutant. These strains named the *rom2-GFP* and *rom2-GFP*$_{tetOn}$ strains respectively, were analyzed by fluorescence microscopy and Western blotting (Figure 15). The growth and conidiation of both wild type and induced *rom2-GFP* strains were identical, suggesting that the GFP-tagged Rom2 was fully functional. As expected, the ~160 kDa Rom2-GFP band was not detected in the parental wild type or non-induced *rom2-GFP*$_{tetOn}$ strain. The endogenous expression of Rom2-GFP in the *rom2-GFP* strain appeared to be equivalent to the expression induced by 0.1 µg ml^{-1} doxycycline in in the *rom2-GFP*$_{tetOn}$ strain in liquid medium (Figure 15). In agreement, the fluorescence of Rom2-GFP driven by its endogenous promoter was also too weak to detect with a conventional fluorescence microscope, thereby suggesting that endogenous expression

of *rom2* is rather weak.

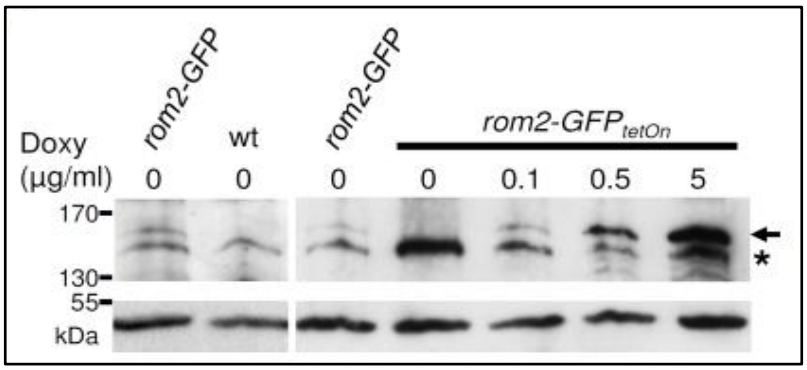

Figure 15. Relative induced expression levels of Rom2. Conidia of indicated strains (10^6 conidia ml-^{1}) was cultured at 37°C for 20 h. Protein extracts were analyzed by western blot with antibodies directed agaisnt GFP (top panel) and Aspf22 (loading control; bottol panel). The arrow indicates Rom2-GFP, while the asterisk (*) indicates an unspecific band.

4.1.4. Downregulation of *rom2* expression results in hypersusceptibility to cell wall-perturbing agents.

To evaluate the importance of *rom2* in CWI of *A. fumigatus*, the sensitivity of the conditional *rom2* strain under repressive growth conditions was analyzed in presence of cell wall perturbing agents such as Congo red, Calcofluor white and SDS. As shown in Figure 16 A, repression of *rom2* resulted in an increased sensitivity to these agents compared to the wild type. These growth defects were overcome by supplementing the medium with 5 µg ml^{-1} doxycycline. The mutant growth was also tested in presence of other drugs such as farnesol (1 mM) that was previously shown to interfere with CWI signaling (Dichtl *et al*., 2010) and the N-glycosylation inhibitor, tunicamycin (10 µg ml^{-1}) that is presumed to contribute to cell wall weakening by preventing the incorporation of glycosylated proteins (de Groot *et al*., 2005). In contrast to other agents, the *rom2$_{tetOn}$* mutant was not affected by farnesol or tunicamycin under repressive conditions (Figure 16 A).

While the wild type could grow at high temperatures, the repressed mutant strain showed severe temperature sensitivity at 48°C. This growth defect was partially rescued by the addition of an osmotic stabilizer (1.2 M sorbitol), suggesting that the growth inhibition is associated with impaired CWI (Figure 16 B). In agreement with this result and in contrast to the wild type, the repressed *rom2$_{tetOn}$* strain stained positive in a colorimetric alkaline

phosphatase assay suggesting leakage of cytoplasm when exposed to elevated temperature (Figure 16 C).

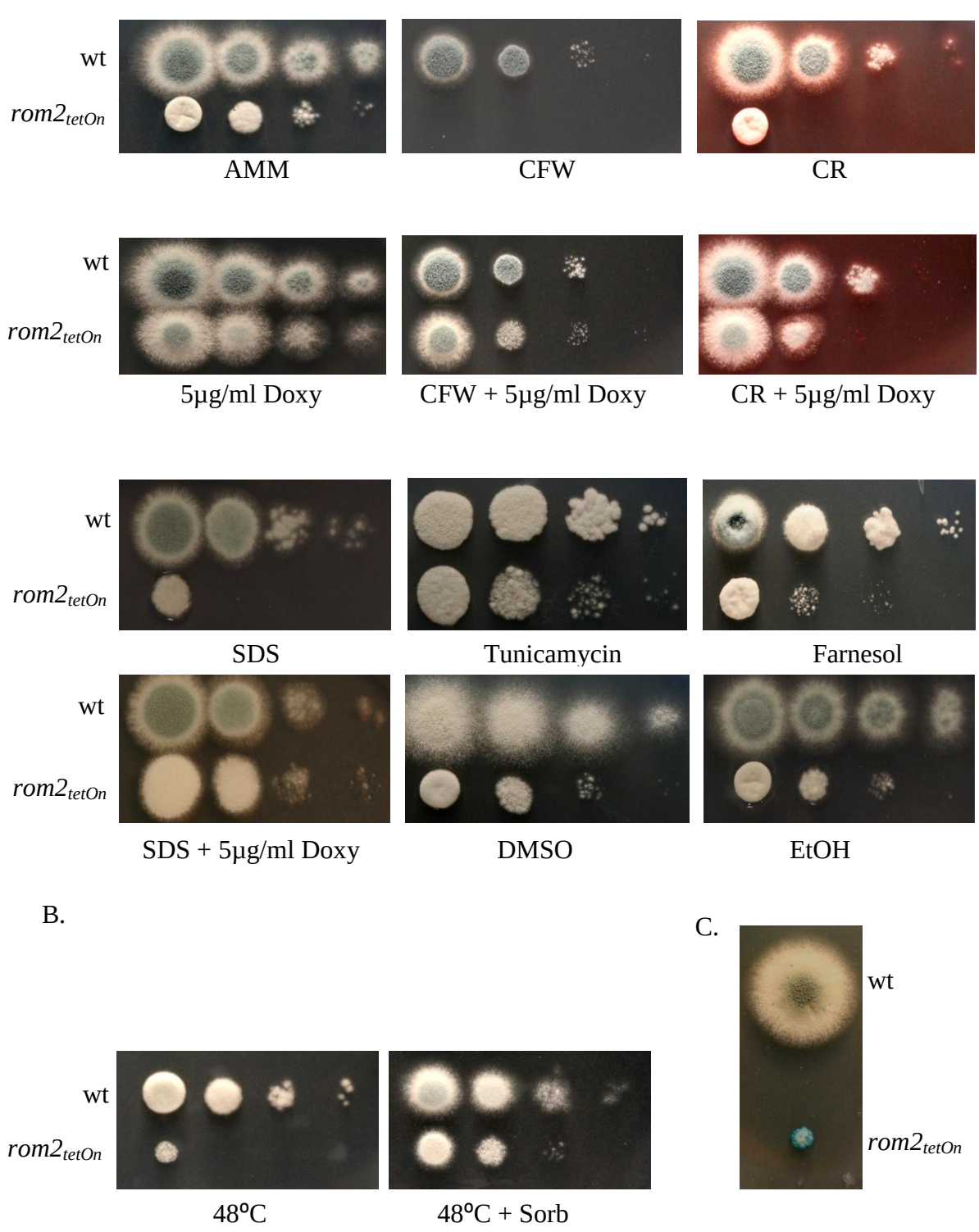

Figure 16. Repression of *rom2* results in increased susceptibility to cell wall perturbing agents and heat stress induced cytoplasmic leakage. (A) 3 µl conidia suspension from a

10-fold series dilution starting with $5x10^6$ conidia ml^{-1} of the indicated strains were spotted onto AMM agar plate supplemented with 8 µg ml^{-1} Congo red (CR), 40 µg ml^{-1} Calcofluor white (CFW), 1 mM farnesol [control 50 µl 100% ethanol (EtOH)], 0.005% SDS and 10 µg ml^{-1} tunicamycin [control 250 µl DMSO)] or doxycycline (Doxy). Plates were incubated at 37°C for 36 h. (B) To test heat sensitivity, AMM agar plates were incubated at 48°C for 48 h with and without 1.2 M sorbitol (Sorb). (C) Colorimetric alkaline phosphatase assay indicating cytoplasmic leakage in *rom2*$_{tetOn}$ mutant. $1.5x10^3$ conidia were spotted on AMM agar plate and incubated at 37°C for 36 h and then shifted to 48°C for 6 h. The agar plate was then overlaid with soft agar supplemented with 5-bromo-4-chloro-3-indolylphosphate and incubated for another 30min at 48°C. Cell lysis (enzymatic activity) is visualized by blue coloration.

4.1.5. Reduced expression of *rom2* impairs growth on complete media.

Surprisingly, the rom2$_{tetOn}$ mutant failed to grow on complete media such as yeast glucose (YG), saboraud dextrose and or potato dextrose agar (Figure 17 A). However, supplementing the media with doxycycline reconstituted wild type- like growth. Additionally, supplementing complete media with 1.2 M sorbitol partially rescued growth, suggesting this phenotype to be associated with lack of CWI (Figure 17 A). The major difference between minimal medium and complete medium such as yeast extract is the inclusion of reduced nitrogen sources. Since the yeast extract composition is not well defined, several possible reduced nitrogen sources were tested for growth inhibition of the mutant. Therefore, the growth of *rom2*$_{tetOn}$ mutant was analyzed on minimal media lacking nitrogen source (in this case $NaNO_3$) and supplemented with equimolar concentrations of different reduced nitrogen sources like ammonium salt (chloride) and free amino acids such as L-arginine under both repressive and inducing conditions. Interestingly, the mutant did not grow in presence of these nitrogen sources, indicating these sources to be responsible for the mutant growth failure on complete media (Figure 17 B). Additionally, microscopic analysis of the mutant growth in liquid culture revealed that the presence of rich nitrogen sources such as NH_4Cl or yeast extract significantly inhibits hyphal germination (data not shown).

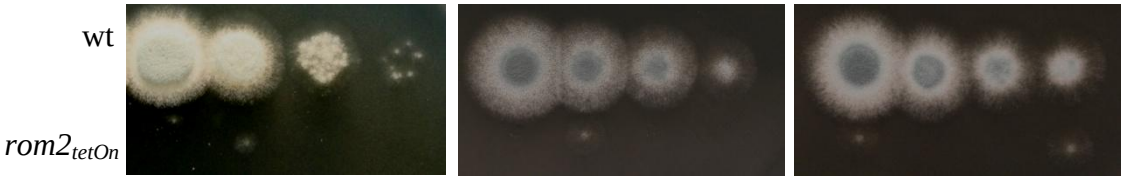

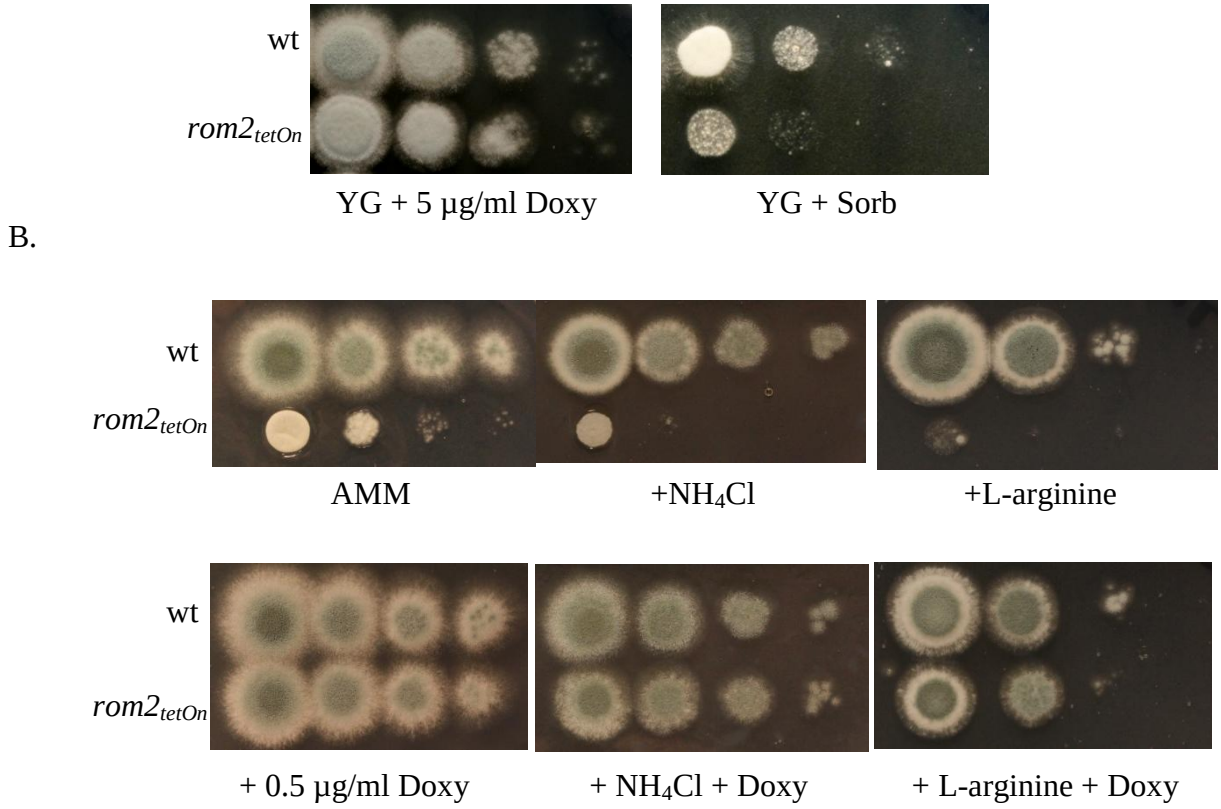

Figure 17. Downregulation of *rom2* expression results in impaired growth on complete media. (A and B**)** In a series of 10-fold dilutions derived from a starting suspension of 5x 10^6 conidia ml^{-1} of the indicated strains, aliquots of 3µl were spotted onto agar plates. (A) Aliquots were spotted onto YG, potato dextrose or saboraud dextrose agar supplemented with doxycycline and sorbitol as indicated. (B) 3 µl drops were spotted on AMM agar supplemented with or without reduced nitrogen source such as NH_4Cl and L-arginine in presence and absence of 0.5 µg ml^{-1} doxycycline (Doxy).

4.1.6. Effects of repression or overexpression of *rom2* on hyphal growth and development.

In order to examine the effects of *rom2* on the germination and hyphal growth under induced and repressed conditions, the mutant strain was cultured without and with 0.5 and 5 µg ml^{-1} doxycycline for microscopic examination. As shown in Figure 18 A, repression of *rom2* resulted in slightly delayed germination and growth, while overexpression of *rom2* with 5 µg/ml doxycycline restored wild type-like growth. On shifting the mutant strain to 48°C, the swollen conidia and germ tubes of *rom2* cultured without doxycycline rapidly ruptured. On the contrary, induction of *rom2* in presence of 0.5 µg ml^{-1} doxycycline exhibited wild type-like growth without any cell lysis. Surprisingly, overexpression of *rom2* delayed growth and

resulted in a 'hyperbranching' phenotype only when shifted to 48°C (Figure 18 B; lower panel). However, this overexpression phenotype was not observed in the culture grown at standard growth temperature i.e. 37°C for the same amount of time (Figure 18 A). Expression of the constitutively active *rho1*^{G14V} allele that is deficient in GTP hydrolysis also significantly delayed germination and hyphal development which was already visible at 37°C (Figure 18 A).

A.

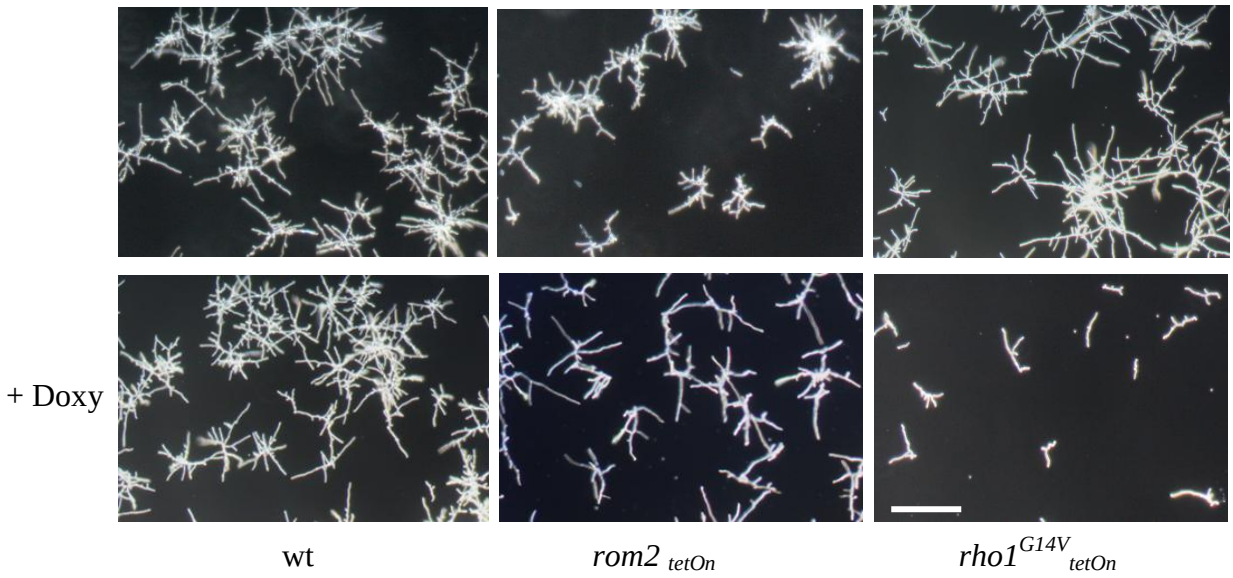

B.

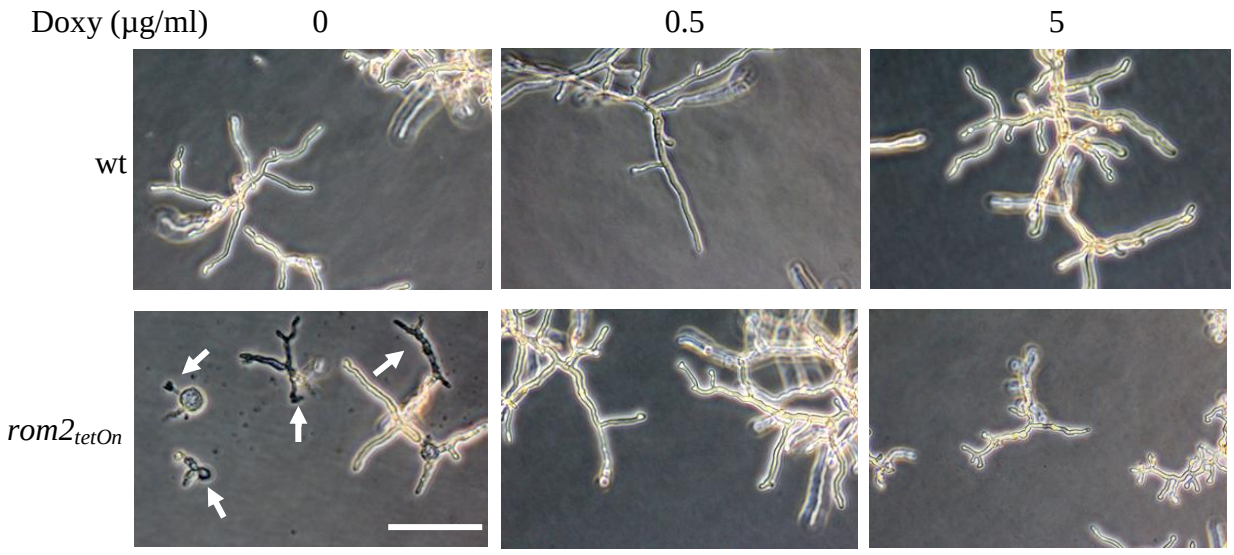

Figure 18. Defects in germination and hyphal growth incduced by repression or over expression of *rom2* and expression of constitutively active *rho1* mutant allele. (A and B)

$5x10^3$ conidia ml^{-1} from indicated strains were inoculated in well plates in liquid AMM supplemented with 0, 0.5 or 5 µg ml^{-1} of doxycycline (Doxy) as mentioned. (A) The well plate was incubated at 37°C for 16 h. Bar 250 µm. (B) The plate was incubated at 37°C for 12h and then shifted to 48°C for 4 h. Bar 100 µm.

4.1.7. Rom2 is required for caspofungin resistance but dispensable for azole tolerance.

Previously, it has been demonstrated that the CWI signaling is required for antifungal drug tolerance and disrupting the signaling components increases sensitivity to azoles and echinocandins (Dirr *et al*., 2010, Dichtl *et al*., 2012). In *S. cereviase*, the stress sensor Wsc1 mediates tolerance to echinocandin by activating CWI via Rom2 (Philip and Levin, 2001). To examine the effects of *rom2* repression and overexpression on antifungal resistance, commercially available epsilometer (E-test) strips for echinocandin (caspofungin () and azole (posaconazole and voriconazole) were used. The E-test is a well established method for assessing antimicrobial resistance. A predefined gradient of antibiotic concentrations on a plastic strip is used to determine the Minimum Inhibitory Concentration (MIC) of the respective agent. Repression of *rom2* resulted in a significantly increased susceptibility to caspofungin as compared to wild type, as evident from the reduced MIC (Figure 19 A). However, the sensitivity of the mutant to posaconazole and voriconazole remained unaltered (Figure 19 B and data not shown). Interestingly, overexpression of *rom2* did not further increase the resistance to caspofungin. In agreement with this result, expression of $rho1^{G14V}$ also did not affect caspofungin sensitivity (Figure 19 A).

A.

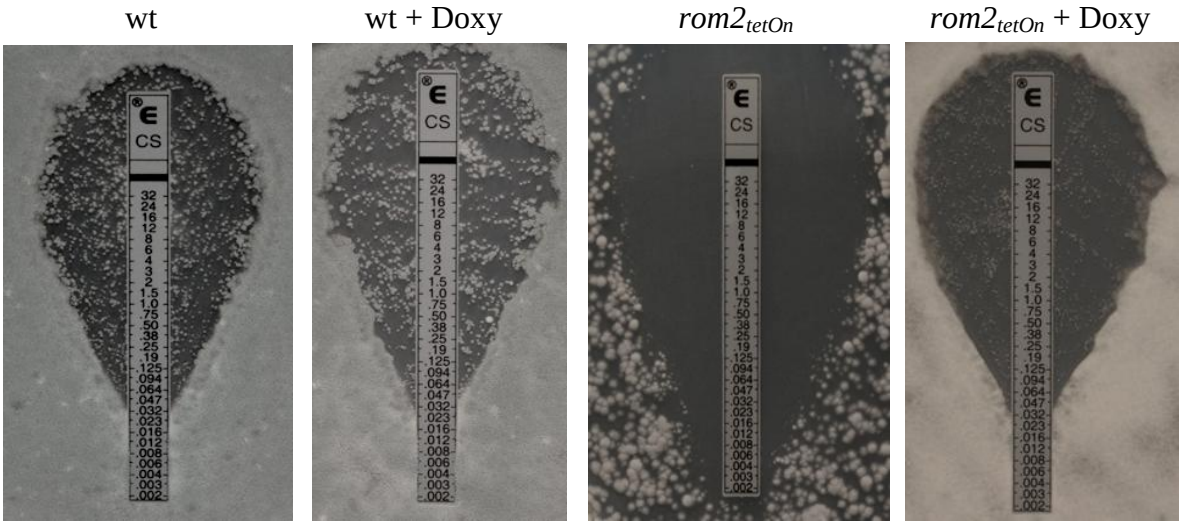

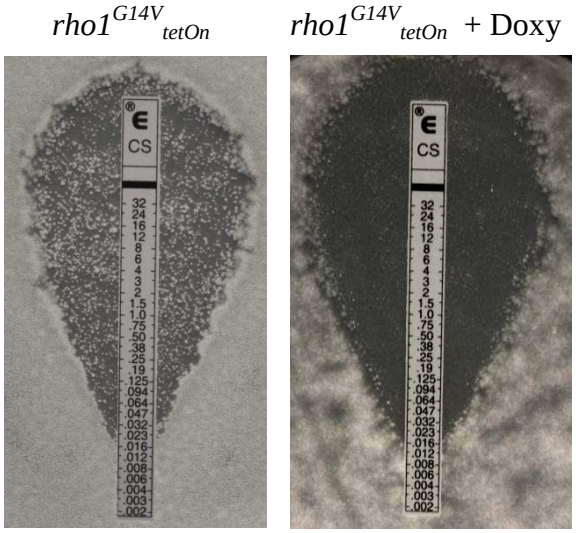

B.

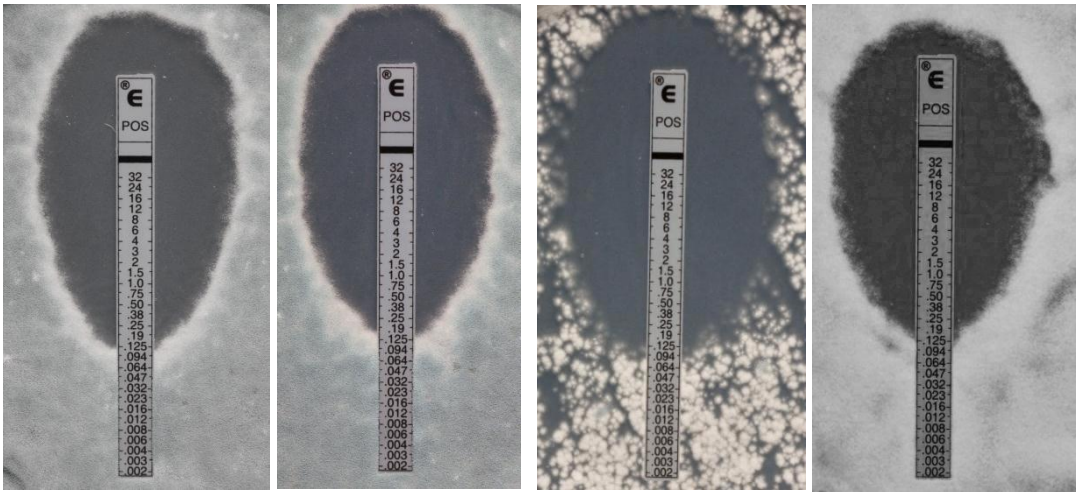

Figure 19. **Rom2 is required for echinocandin but not azole tolerance**. A total of 2.5x10^4 conidia of the indicated strains were spread on AMM agar plates supplemented with or without 5 µg ml^{-1} doxycycline (Doxy), as indicated. (A) Caspofungin or (B) posaconazole E-strips were applied and plates were incubated for 48h at 37°C. The agar plates for *rho1*$^{G14V}_{tetOn}$ were additionally supplemented with 0.1 µg ml-1 pyrithiamine to avoid loss of construct.

4.1.8. Rom2 localizes to hyphal tips and newly formed septa but is not essential for septum formation.

It was previously shown that GFP-tagged Rho1 preferentially localizes to hyphal tips (Dichtl *et al.*, 2010). Therefore, it was assumed that if Rom2 was a putative GEF and interaction partner of Rho1, it should show a similar localization pattern. To visualize the sub-cellular localization of Rom2, a C-terminally GFP-tagged Rom2 driven by the strong constitutively

active *gpdA* promoter was expressed and named as *rom2-GFP*$_{gpdA}$. The GFP positive clones isolated showed reduced sporulation, corresponding to the overexpression phenotype of Rom2 and had weak GFP fluorescence. Rom2-GFP clearly localized to cell membrane and preferentially to hyphal tips (Figure 20 A). Interestingly, Rom2-GFP also concentrated at the sites of newly formed septa (Figure 20 B), suggesting its role in septum formation. If this was true, then mutant lacking Rom2 activity would have no septa. Therefore, the presence of septa in the *rom2*$_{tetOn}$ strain cultured under repressive condition was examined. But, it was found that the mutant possessed multiple septa which dismissed the direct involvement of Rom2 in septum formation (Figure 20 C).

A.

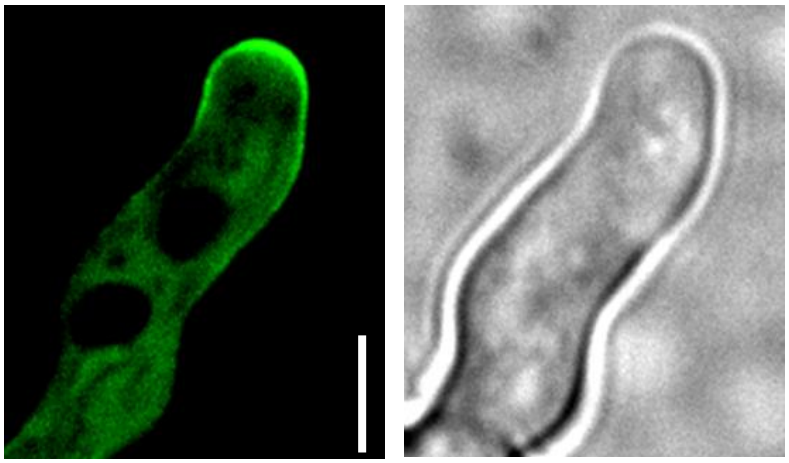

B.

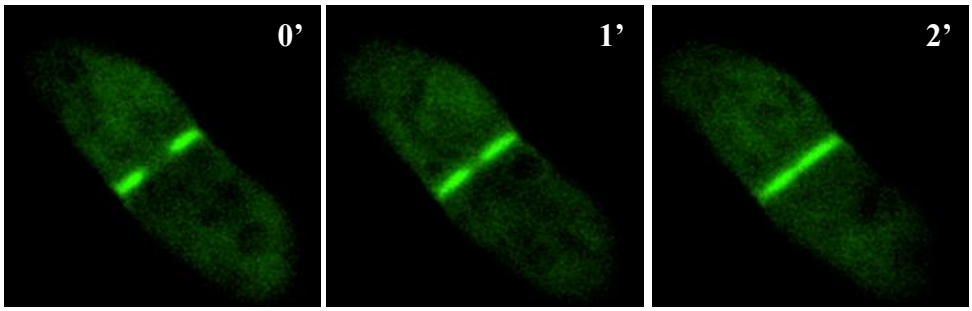

C.

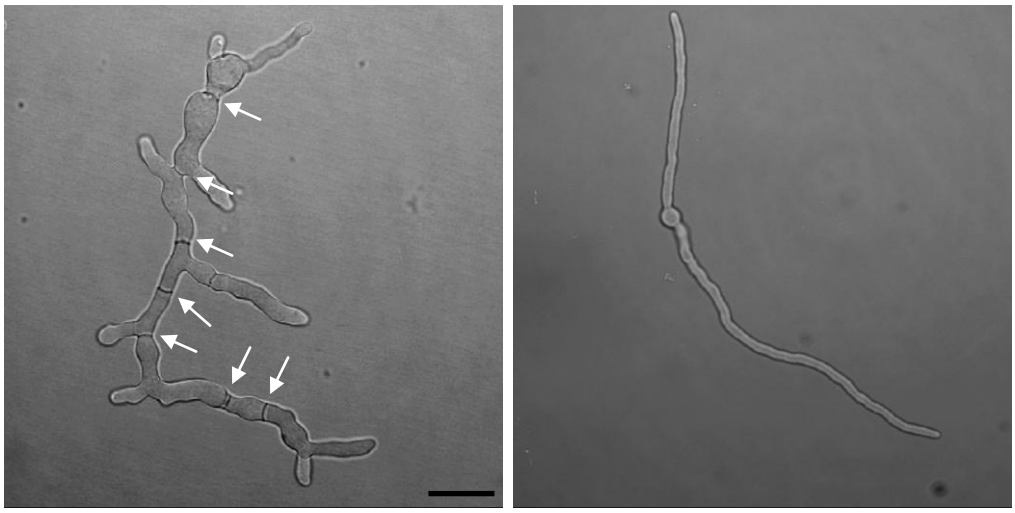

Figure 20. GFP-tagged Rom2 localizes to the hyphal tips and septa. (A and B) $5x10^2$ conidia of a wild-type strain expressing a C-terminally GFP-tagged Rom2 were inoculated in AMM and cultured at 37°C for approximately 15 h. Fluorescence and bright-field images were taken with a spinning disc confocal microscope and represent one optical section of living hyphae. (B) The timelapse pictures of the forming septum were taken after 0, 1, and 2 min as indicated. Bar, 5 µm. (C) Bright-field microscopy images of repressed *rom2*$_{tetOn}$ (left) and Δ*rho4* (right) showing presence and absence of septa (indicated by white arrows) respectively. Bar, 10 µm.

4.1.9. Repression of *rom2* results in increased basal activation of MpkA.

In *A. fumigatus*, the MAP kinase MpkA is shown to be phosphorylated and activated by cell wall stress (Dirr *et al*., 2010; Dichtl *et al*. 2012). Similar observations have been made in other fungal species (Martín *et al*., 2000; Madrid *et al*., 2006). In agreement, previously it has been shown that the cell wall stressor CFW induces MpkA activation in both wildtype and Δ*wsc1*. However, this activation is reduced in Δ*midA* supporting that MidA is required for calcofluor white induced stress tolerance (Dichtl *et al*. 2012). Therefore, in order to assess the effect of downregulation of *rom2* on the downstream MpkA activation, the basal and induced phosphorylation of MpkA were evaluated in *rom2*$_{tetOn}$ strain under repressive growth conditions and wild type. Interestingly, repression of *rom2* resulted in a significant basal MpkA phosphorylation under the uninduced condition in contrast to wild type. This phosphorylation level was not further increased by CFW induction in *rom2*$_{tetOn}$ strain, while the wild type showed drastic increase in MpkA phosphorylation in response to CFW (Figure 21 A and B). The phosphorylation of another MAP kinase, MpkB has also been reported

under cell wall stress conditions (Dirr *et al*., 2010). Interestingly, the MpkB phosphorylation was also observed in the *rom2*$_{tetOn}$ strain under basal conditions which was further enhanced upon calcofluor white-induced stress. In contrast, MpkB phosphorylation was only induced by CFW in the wild type, suggesting activation of MpkB is also triggered by cell wall stress (Figure 21 A).

A.

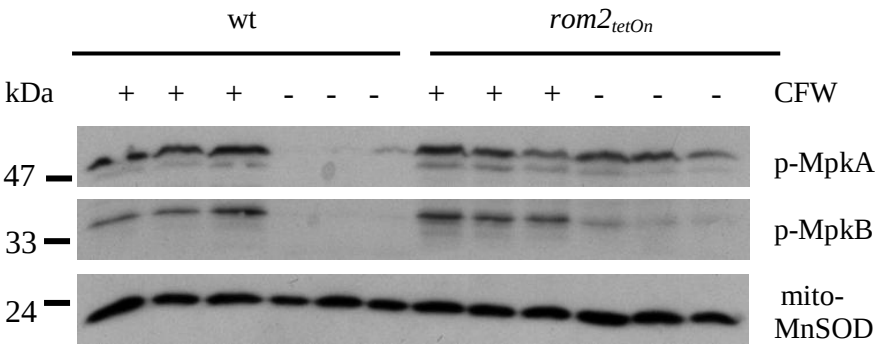

B.

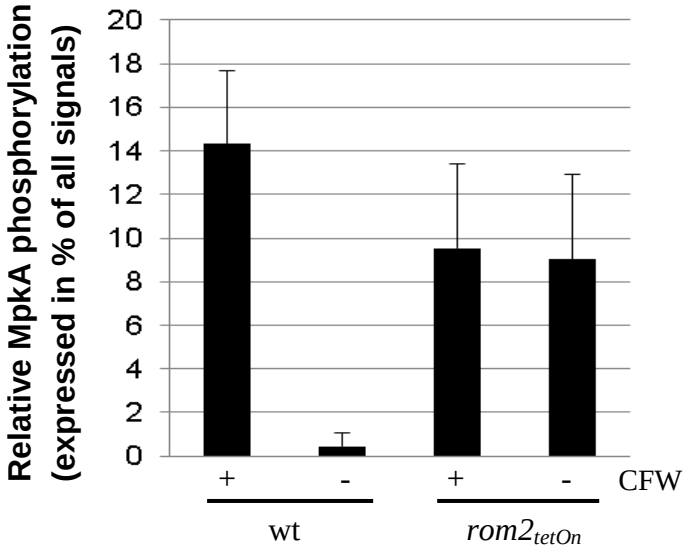

Figure 21. Basal and induced phosphorylation of MpkA in *rom2*$_{tetOn}$ under repressive growth condition. (A and B) Conidia of the wild type (wt) and *rom2*$_{tetOn}$ strain were inoculated in triplicate in AMM (10^5 conidia ml^{-1}) and cultured at 37°C in a tube rotator. After 24 h, 100 µg ml^{-1}Calcofluor white (CFW) was added to samples (indicated by '+' sign) and incubated for 30 min. Protein extracts were analyzed by SDS-PAGE and Western blotting with antiphospho-p44/42 MAPK antibodies directed against phosphorylated MpkA (p-MpkA) and phosphorylated MpkB (p-MpkB). Antibodies directed against the mitochondrial MnSOD were used for a loading control. (B) The relative quantity of phosphorylated MpkA expressed as a percentage of all signals (listed in Table 4) is indicated.

Error bars indicated the standard deviations of triplicate samples.

Table 6. Relative quantification of MpkA phosphorylation bands in wild type and *rom2*$_{tetOn}$.

Sample	Volume OD*mm^2	Adjusted Volume OD*mm^2	%Adj. Vol.	Average
Wild type	10.44718331	3.330593249	13.94	14.31
(+)	6.734824046	2.656263151	11.12	
	8.797934319	4.269195189	17.87	
Wild type	2.472840306	0.019773277	0.08	0.46
(-)	2.496519801	0.036713577	0.15	
	2.761131894	0.273021050	1.14	
rom2$_{tetOn}$	6.841793766	3.283498735	13.75	9.52
(+)	4.960110943	2.085170299	8.73	
	4.623325785	1.457251911	6.10	
rom2$_{tetOn}$	7.158953891	2.913260957	12.20	9.03
(-)	6.138127549	2.446396454	10.24	
	5.078288147	1.115641408	4.67	

4.1.10. Effects of N-terminal truncated Rom2 overexpression on hyphal growth and sporulation.

While this Rom2 study was in progress, the group of Stephan Seiler showed that NcRgf1, a homologue of ScRom2 in *Neurospora crassa* is a specific GEF for NcRho1. They also reported that *in vitro*, the N-terminal part of NcRgf1 containing the DEP domain negatively regulates its GEF activity. They validated through yeast two-hybrid data as well as GEF activity that the GEF domain of NcRGF1 could induce nucleotide exchange on NcRHO1 only if the N-terminal part harbouring the DEP domain was not included in the construct. (Richthammer *et al*., 2012). This prompted the speculation if AfRom2 exerts a similar self-inhibitory mechanism in *A. fumigatus*. According to this model, the overexpression of

truncated Rom2 lacking the N-terminal DEP domain would exert more severe effects on hyphal growth and development than the full-length protein. In order to test this hypothesis, two mutant strains that ectopically expressed the full-length protein (C-terminally His tagged) and N-terminally HA-tagged Rom2 (733-1199) lacking the N-terminal part including the DEP domain under a doxycycline-inducible promoter, repectively, were generated. As expected, overexpression of the full-length Rom2 yielded growth phenotypes that phenocopied the overexpression of the conditional *rom2* mutant i.e. strikingly reduced sporulation and slightly reduced radial growth (Figure 22 A). In contrast, overexpression of the HA-Rom2 (733-1199) resulted in a significantly more severe growth phenotype with drastically reduced radial growth and absence of sporulation (Figure 22 A). Additionally, overexpression of Rom2 (733-1199) also had more drastic effects on germination and hyphal growth compared to the overexpression of the full-length Rom2 in liquid media (Figure 22 B).

A.

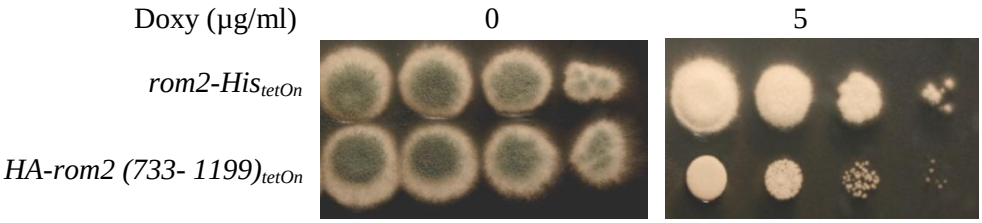

B.

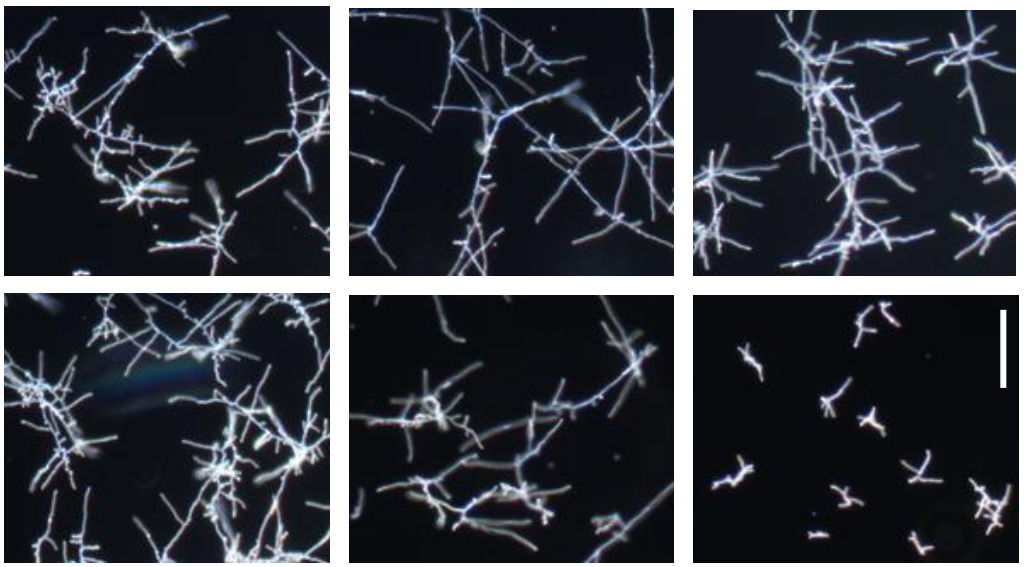

Figure 22. Differential growth effects of HA-Rom2 (733-1199) and full-length Rom2. (A) Aliuots of 3 µl conidial suspension in a series of ten-fold dilution starting from $5x10^6$ were spotted on agar plates supplemented with 0 or 5 µg ml^{-1} doxycycline (Doxy) and 100 µg ml^{-1} hygromycin to avoid loss of respective constructs. Plates were incubated at 37°C for 48 h. (B) Total $5x10^3$ conidia ml^{-1} from indicated strains were incubated for 16 h at 37°C in liquid AMM supplemented with no doxycycline (upper panel) or 5 µg ml-1 doxycycline (lower panel). Bar, 250 µm.

4.1.11. Interaction of Rom2 with Rho1.

In order to confirm that Rom2 interacts with Rho1, a Co-IP assay was performed and analysed if Rho1 was pulled down by the active HA-Rom2 (733-1199) protein lacking the N-terminal part of Rom2. Furthermore, in order to assess that Rom2 is a Rho1-specific GEF, constitutively expressing GFP-tagged Rho1 and Rho3 strains which previously showed similar subcellular localization were used (Dichtl *et al*., 2010). These strains were transformed with the construct expressing doxycycline inducible HA-Rom2 (733-1199) ectopically. As expected, GFP-Rho1and not GFP-Rho3 was co-immunoprecipitated with HA-Rom2 (733-1199) when induced with doxycycline for 4 h. In absence of doxycycline, HA-Rom2 (733-1199) was not expressed and hence GFP-Rho1 was not pulled down (Figure 23).

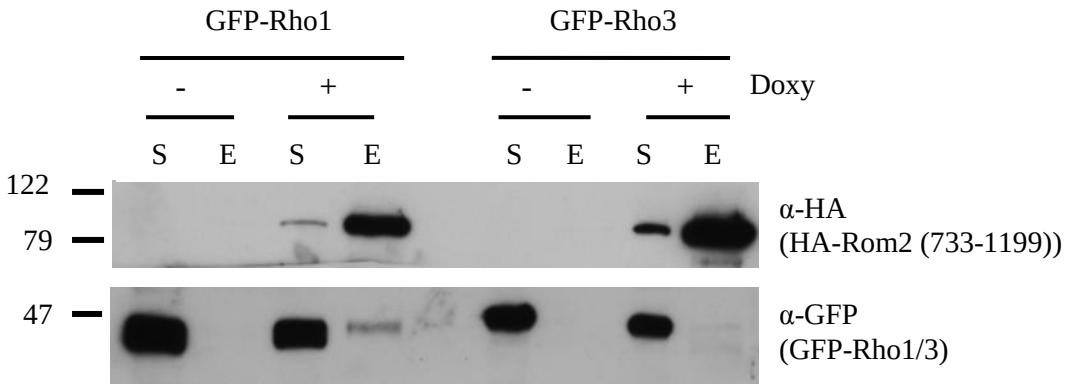

Figure 23. Interaction of HA-Rom2 (733-1199) with GFP-Rho1. Conidia of strains constitutively expressing GFP-Rho1 or GFP-Rho3 and conditionally expressing HA-Rom2 (733-1199) were inoculated in AMM and incubated on a rotary shaker at 37°C. After 24 h, HA-Rom2 (733-1199) expression was induced with 50 µg ml^{-1} doxycycline (+) or not (-) and the cultures were incubated for another 4 h at 37°C. The soluble fractions (S) of mycelium

extracts were subjected to anti-HA agarose. After two wash steps, bound protein was eluted (E). Portions (0.125%) of the soluble fraction (S) and 30% of the elution (E) were analyzed by SDS-PAGE and Western blotting with anti-HA (α-HA) and anti-GFP (α-GFP) antibodies.

4.1. Characterization of the β-1,3-glucan synthase subunit Fks1 of *A. fumigatus.*

4.2.1. Generation and growth of conditional *fks1* mutant.

The genome of *A. fumigatus* contains a single copy of gene encoding the β-1,3-glucan synthase, *fks1* (AFUA_ 6G12400) which has been previously described to be essential (Firon *et al*., 2002). Therefore, in order to further investigate the role of *fks1* and downregulate its expression, a conditional *fks1* mutant was constructed. For this approach, an improved version of the doxycyline-inducible 'TetOn' promoter system as described previously was employed (Helmschrott *et al*., 2013). The endogenous promoter of *fks1* was replaced with this conditional promoter, resulting in a doxycycline-regulated *fks1*^{tetOn} mutant (Figure 24 A). The *fks1*$_{tetOn}$ mutant was though viable under repressive conditions, but highly impaired in sporulation and radial growth as compared to wild type. The mutant was very slow-growing under repressive conditions, but wild type-like growth rate was reconstituted upon addition of ≥ 0.5 µg ml^{-1} doxycycline (Figure 24 B and C).

A.

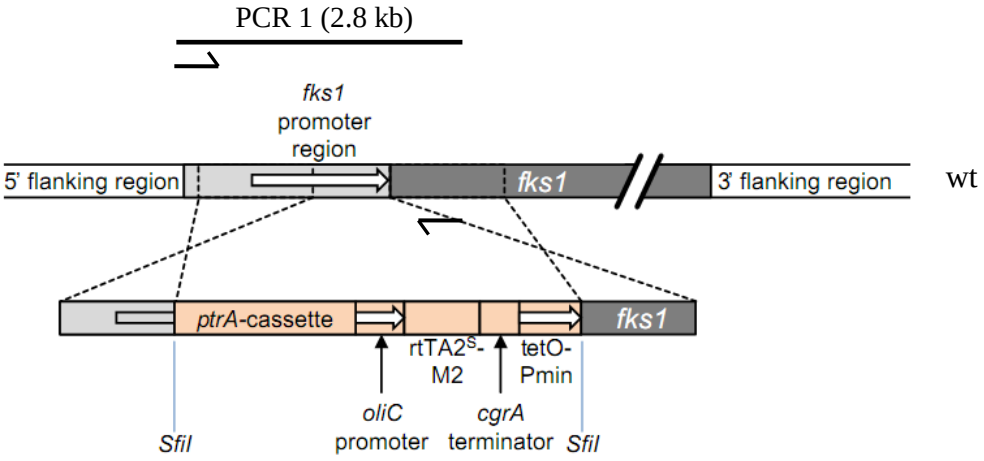

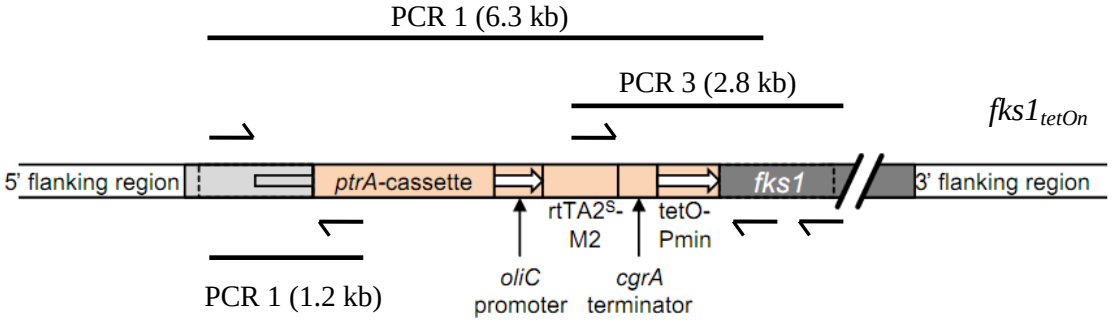
PCR 1 (6.3 kb)
PCR 3 (2.8 kb)
fks1tetOn
5' flanking region
ptrA-cassette
fks1
3' flanking region
rtTA2S-M2
tetO-Pmin
PCR 1 (1.2 kb)
oliC promoter
cgrA terminator

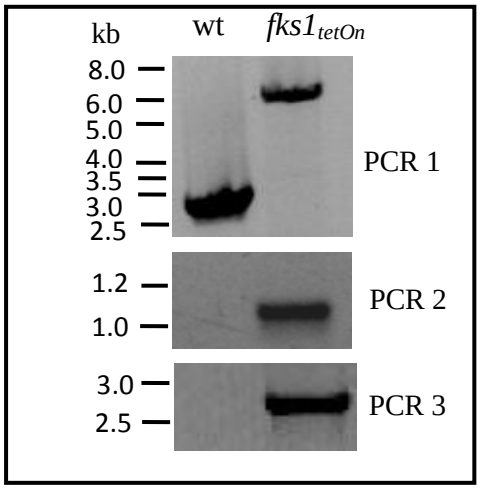
kb
wt
fks1tetOn
8.0
6.0
5.0
4.0
3.5
3.0
2.5
PCR 1
1.2
1.0
PCR 2
3.0
2.5
PCR 3

B.


wt
fks1tetOn
Doxy (µg/ml)
0
0.01
0.05
0.1
0.25
0.5
1
5
15

C.

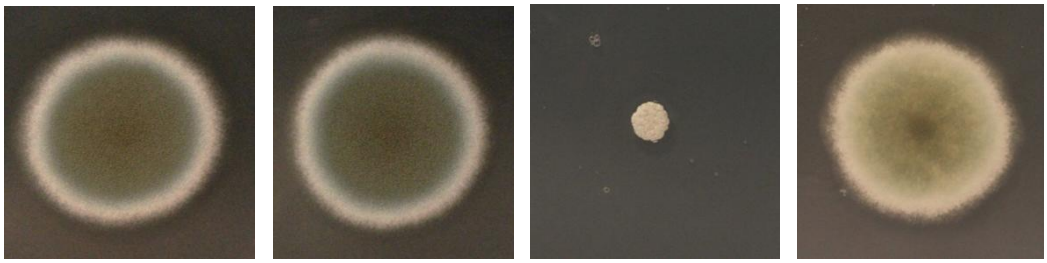
wt
wt+ Doxy
fks1tetOn
fks1tetOn + Doxy

D. E.

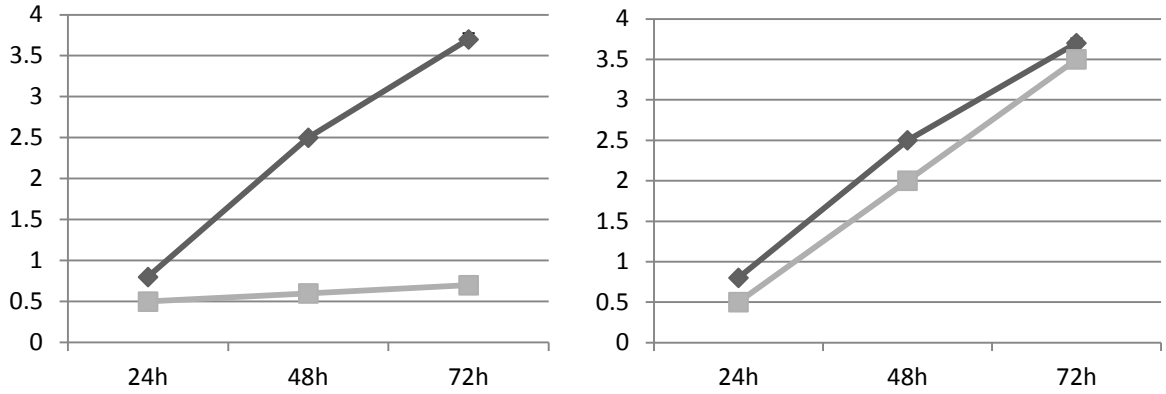

Figure 24. Generation and doxyxyline-dependent growth phenotype of conditional *fks1*$_{tetOn}$ mutant. (A) Graph showing the promoter locus in wild-type (wt) and *fks1*$_{tetOn}$ mutant. The native promoter of *fks1* was replaced by homologous recombination with a doxycycline-inducible promoter system. Primer binding sites and length of respective amplicons verifying the *tetOn* promoter integration are indicated by PCR 1-3. (B) 1.5 x 10^3 conidia of the indicated strains were spotted on AMM agar supplemented with the indicated amount of doxycycline (Doxy) and incubated at 37 °C for 36 h. (C, D and E) 1.5 x 10^3 conidia of the indicated strains were spotted at the center of AMM agar plates supplemented without or 0.5 µg/ml doxycycline (Doxy) and incubated at 37 °C for 72 h. (D and E) Mean radial growth diameter of wild type (in dark gray lines and symbols) and *fks1*$_{tetOn}$ (in light gray lines and symbols) strains without (D) and with 0.5 µg/ml doxycycline (E).

4.2.2. Downregulation of *fks1* mimics echinocandin effect on wild type.

The *fks1* gene encodes the β-1,3-glucan synthase in *A. fumigatus* which is also the known target of the echinocandin class of antifungals. Therefore, the growth morphology upon *fks1* repression was analyzed to assess if it phenocopies the growth inhibition induced by echinocandins on wild type. Microscopic examination of the *fks1*$_{tetOn}$ strain under repressive conditions revealed irregular, slowly growing and frequently branching hyphae. Additionally, the mutant colonies showed frequent lysed hyphal tips. Importantly, these growth alterations caused by reduced *fks1* expression strikingly resembled those of wild type exposed to echinocandins, which also resulted in delayed growth, more frequent branching and cell lysis. On the other hand, these growth defects were not observed in the *fks1*$_{tetOn}$ mutant upon addition of doxycycline (Figure 25).

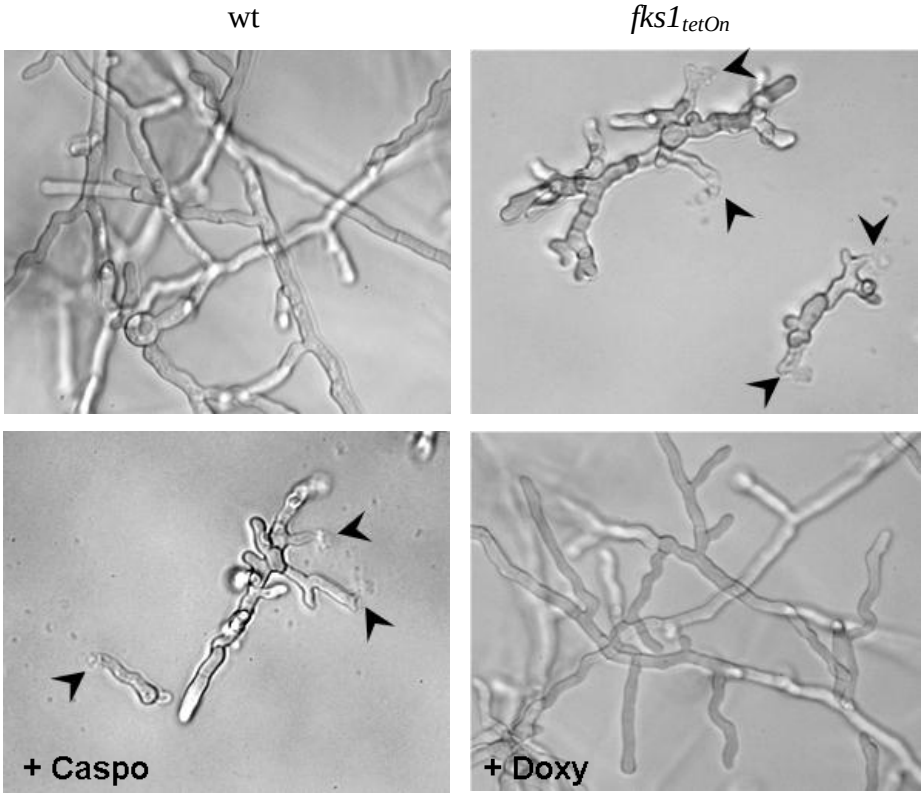

Figure 25. Cellular morphology of *fks1*$_{tetOn}$ repressed mutant phenocopies the effect of echinocandins. Distinct similarities in morphology (320X) were observed between caspofungin-treated and untreated wild type (wt) and *fks1*$_{tetOn}$ mutant strains cultured under repressed and induced conditions respectively. Conidia (5 x 10^3/ ml) from the indicated strains were inoculated in liquid AMM and incubated at 37 °C for 18 h. Media was supplemented with 1 µg/ml caspofungin (Caspo) or 0.5 µg/ml doxycycline (Doxy) as mentioned. The arrows indicate lysed hyphal tips and cytoplasmic leakage.

4.2.3. Effect of *fks1* downregulation on cell wall integrity and antifungal resistance.

Fks1 is reportedly required for synthesis of the cell wall component β-1,3-glucan in *A. fumigatus*, which is also important for structural integrity of the cell wall (Beauvais *et al*., 2001). In order to ascertain the importance of β-1,3-glucan for cell wall integrity, growth of the *fks1*$_{tetOn}$ mutant was analyzed under repressive growth conditions and in presence of cell wall perturbing agents. As shown in Figure 26 A, repression of *fks1* resulted in increased susceptibility to SDS and Calcofluor white. Interestingly, susceptibility to other cell wall perturbing conditions, i.e., Congo red and heat were not significantly altered (Figure 26 A and B).

Next, the effect of the loss of Fks1 activity on antifungal drug resistance was also assessed. The minimal inhibitory concentration (MIC) of echinocandins and azoles, respectively, were analyzed with commercial Epsilometer tests (Etests). Reduced *fks1* expression did not significantly alter the MIC to the azole antifungals (Figure 27; lower panel). Interestingly, the growth of the repressed *fks1*$_{tetOn}$ mutant was not affected at all by caspofungin in contrast to wild type which showed a distinct MIC. But when induced with doxycycline, the mutant showed a MIC similar to wild type (Figure 27; upper panel).

A.

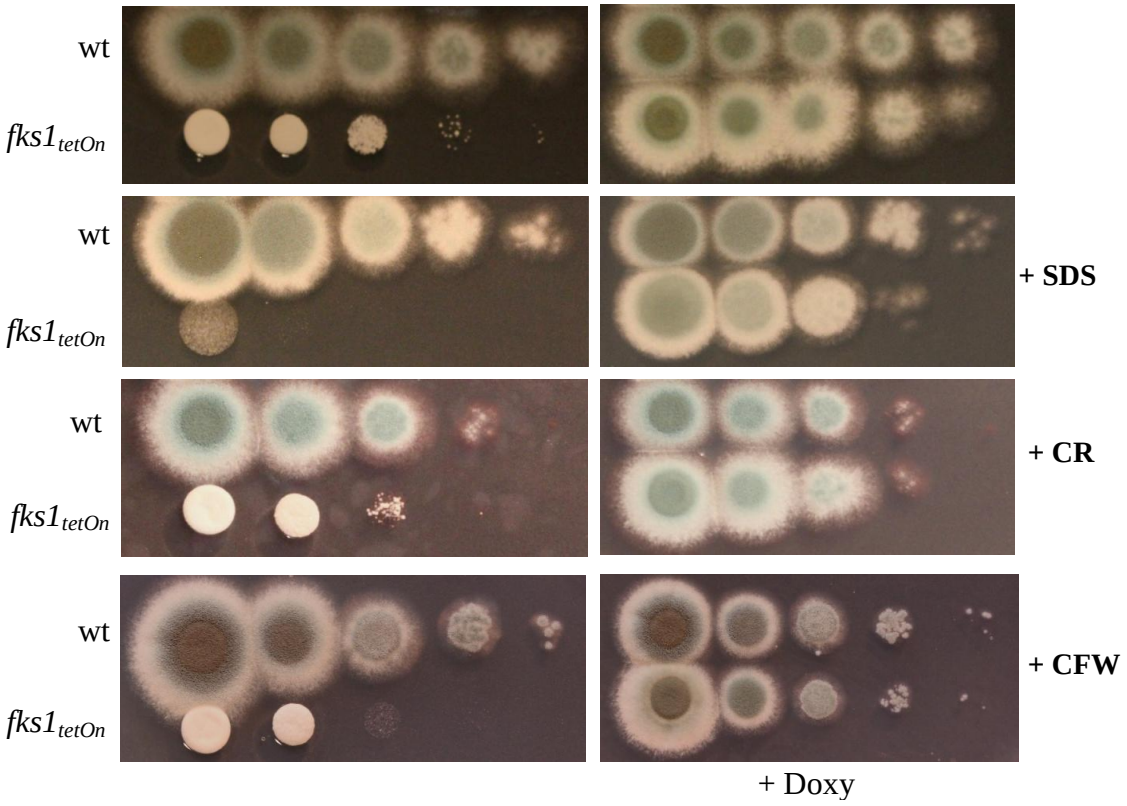

B.

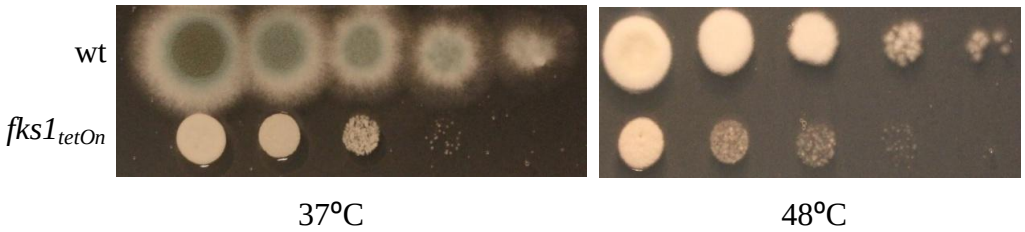

Figure 26. Susceptibility of the repressed *fks1*$_{tetOn}$ mutant to cell wall perturbing conditions. (A and B) Aliquots of 3 µl conidia suspension derived from a series of ten-fold dilution with a starting suspension of 5 x 10^7 conidia/ml were spotted onto AMM agar plates. The plates were supplemented with sodium dodecyl sulfate (SDS; 0.005 % (w/v)), Congo red

(CR; 8 µg/ml), Calcofluor white (CFW; 40 µg/ml), or doxycycline (Doxy; 0.5 µg/ml). (A) The plates were incubated for 36 h at 37°C except for CFW supplemented plate which was incubated for 48 h. (B) The agar plates were incubated at 37 °C for 36 h or at 48 °C for 48 h.

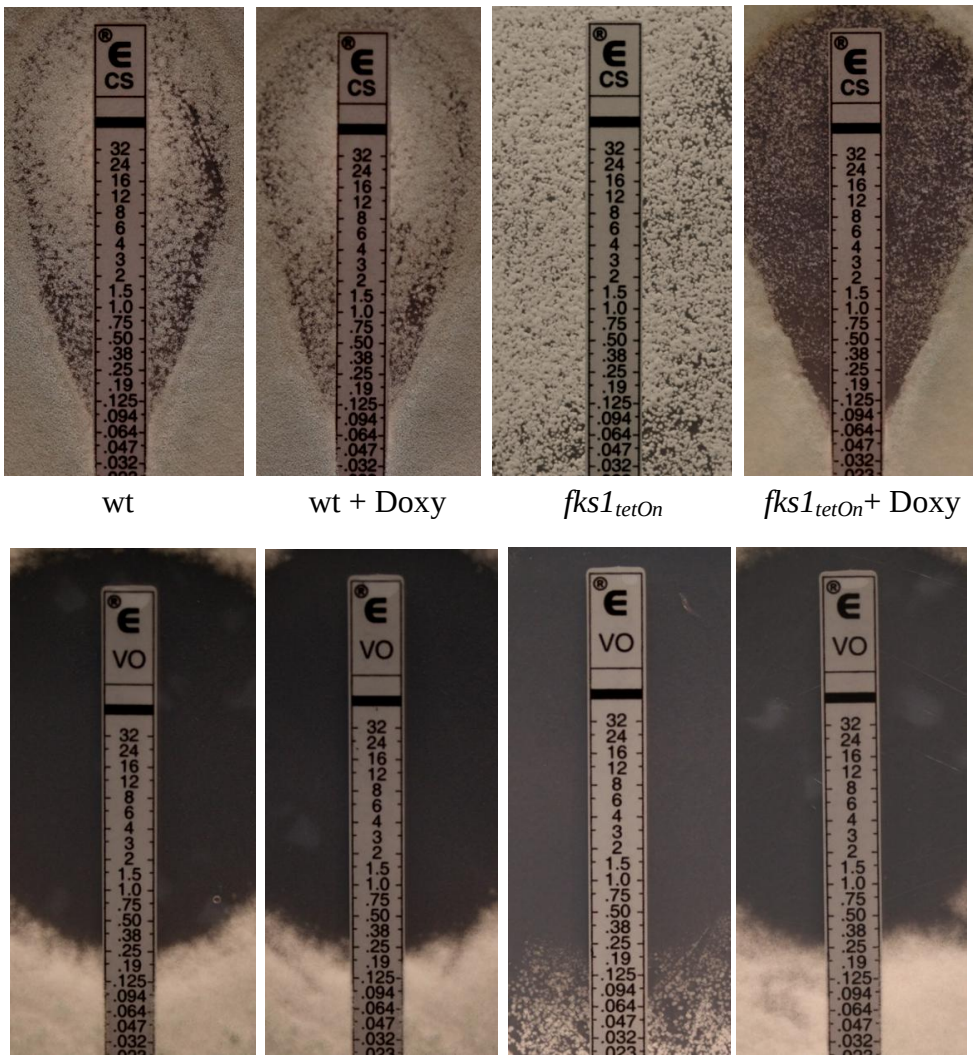

Figure 27. Downregulation of *fks1* renders the mutant resistant to echinocandin, while invariant to azole. A total of 2.5 x 10^5 conidia from indicated strains were spread on AMM agar plates supplemented with no or 0.5 µg/ml doxycyline (Doxy). Caspofungin (CS; upper panel) or voriconazole (VO; lower panel) E-test strips were applied and the agar plates were incubated at 37 °C. Representative photos were taken after 43 h.

4.2.4. Effect of repression of *fks1* on cell wall organization.

β-1,3-glucan is not only an essential cell wall component, but also acts as a scaffold for otherpolysaccharides, for e.g. galactomannan which is covalently bound to the glucans

(Fontaine *et al*., 2000). Therefore, it was speculated that a reduced β-1,3-glucan could also influence the cell surface galactomannan integration. In order to investigate the effects of downregulating *fks1* on cell wall composition, a β-glucan-specific monoclonal antibody (mAb, 2G8) was used to immunostain cell wall β-1,3-glucan (Torosantucci *et al*., 2005) (performed in close collaboration with Dr. med. Karl Dichtl). Conidia of the $fks1_{tetOn}$ strain together with wild type conidia were inoculated on cover slips in liquid media under repressive conditions (no doxycycline). Clear morphologic differences allowed discrimination between wild type and $fks1_{tetOn}$ hyphae. As expected, the wild type but not $fks1_{tetOn}$ hyphae were stained with the 2G8 mAb, suggesting that reduced *fks1* expression results in a decrease in β-1,3-glucan in the cell wall (Figure 28 A). Next, a galactomannan-specific mAb (L10-1) was used to stain *Aspergillus* hyphae cultured under similar conditions (Heesemann *et al*., 2011) (performed in close collaboration with Dr. med. Karl Dichtl). As shown in Figure 28 B, in contrast to wild type hyphae which showed an even galactomannan staining pattern throughout the cell surface, the $fks1_{tetOn}$ hyphae were weakly stained with the L10-1 mAb. This suggested that the mutant was affected in integrating galactomannan into the cell wall. Interestingly, the $fks1_{tetOn}$ hyphae showed diffused galactomannan staining marked by halos around the mutant hyphae (Figure 28 B), pointing towards elevated galactomannan release by the mutant. Additionally, it has been shown previously that echinocandin treatment induces a compensatory increase in chitin content of fungal cell wall including *A. fumigatus* to mediate cell wall integrity (Fortwendel *et al*., 2010; Walker *et al*., 2008). Similar to the echinocandin-induced effect, the $fks1_{tetOn}$ mutant showed significantly increased cell wall chitin under repressive growth conditions as compared to wild type (Figure 28 C).

A.

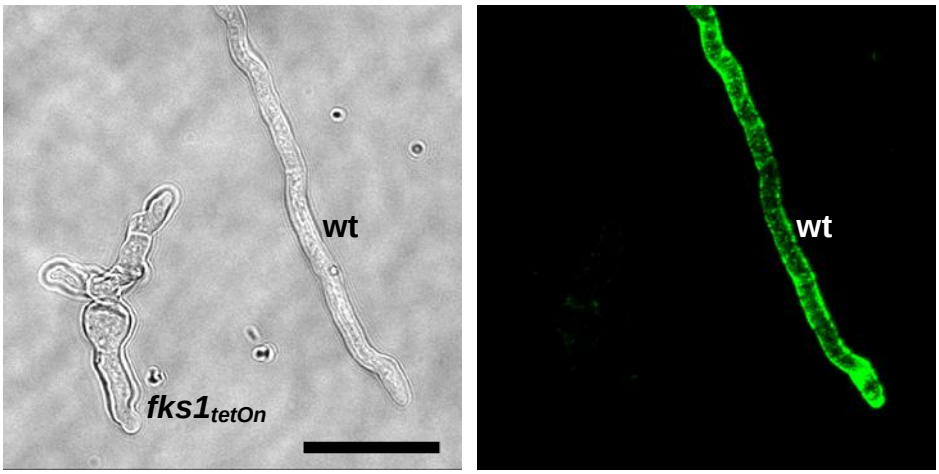

B.

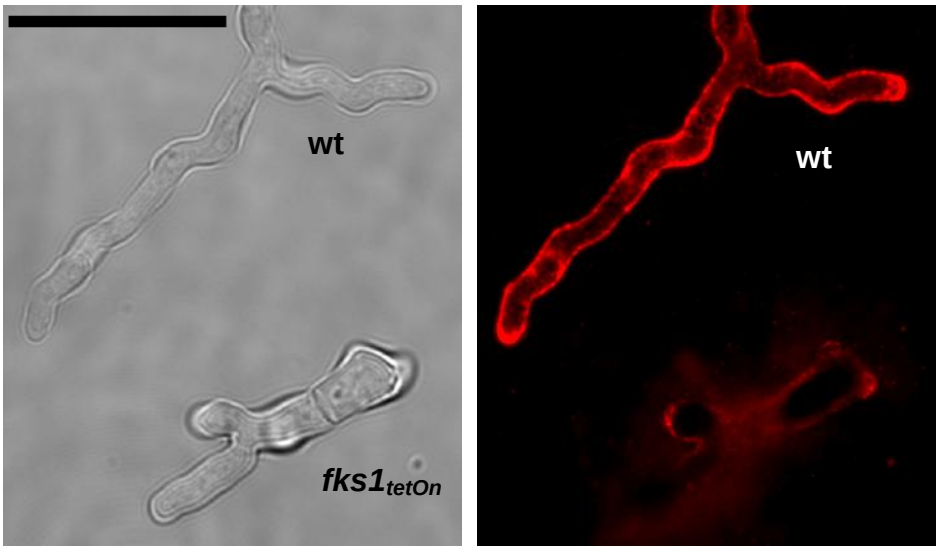

C.

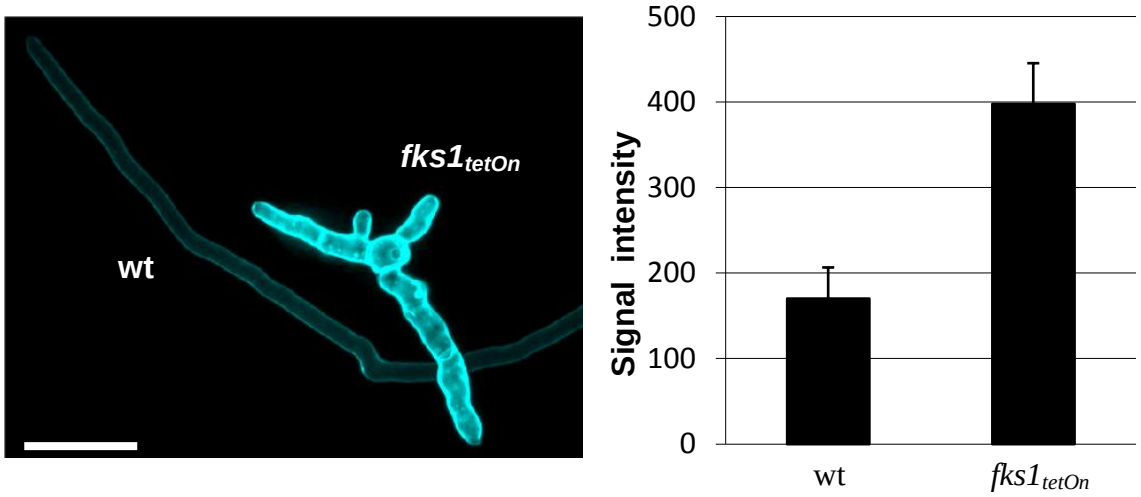

Figure 28. Reduced β-1,3-glucan and galactomannan but increased chitin staining observed for repressed *fks1*$_{tetOn}$ mutant. Conidia of wild type and *fks1*$_{tetOn}$ were inoculated in AMM on cover slips and cultured at 37 °C for 14 h. Cells were subsequently fixed, stained and analyzed with a confocal laser scanning microscope. (A and B) Representative bright field (left panels) and immunofluorescent images (right panels) of hyphae stained with β-glucan-specific 2G8 mAb (A) and galactomannan-specific L10 mAb (B). (C) Representative image of hyphae stained with chitin-specific calcofluor white dye (left panel) and the relative mean fluorescence intensity quantified from 60 cell wall intersections of wild type and *fks1*$_{tetOn}$ hyphae (right panel). Bar, 20 µm.

4.2.5. Downregulation of *fks1* induces increased galactomannan shedding.

Detection of the biomarker galactomannan in body fluids is relevant for clinical diagnosis of invasive aspergillosis (Kousha *et al*., 2011). The galactomannan staining of the *fks1* mutant demonstrated that inhibition of β-1,3-glucan reduces integration of galactomannan into the cell wall. This raised an obvious question about the consequent galactomannan release into the medium i.e. if it is decreased due to reduced synthesis or degaradation within the cell or increased due to the failure of being covalently linked to the cell wall in absence of β-1,3-glucan. Hence, the commercially available Platelia™ *Aspergillus* ELISA kit was employed to measure the galactomannan released into cell culture supernatants of wild type and the conditional *fks1*$_{tetOn}$ strain cultured under repressive and induced conditions. The metabolic activity was also quantified as an index of viability of the strains by a resazurin-based assay. As expected, the growth and metabolic activity of the wild type and the induced *fks1*$_{tetOn}$ strain significantly surpassed the *fks1*$_{tetOn}$ strain cultured under repressive conditions (Figure 29 A and B). Despite significant showing low metabolic activity and fungal biomass, higher galactomannan concentration was detected in the repressed *fks1*$_{tetOn}$ culture supernatant as compared to other strains (Figure 29 C). This suggests that inhibition of β-1,3-glucan synthesis results in increased galactomannan shedding.

A.

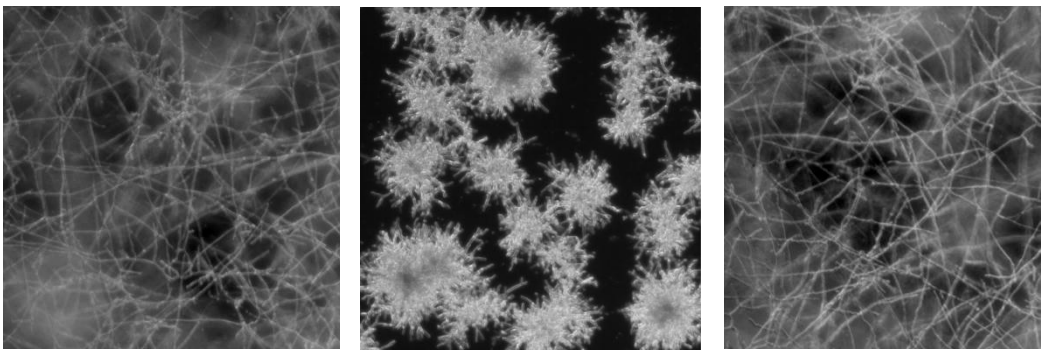

wt *fks1*$_{tetOn}$ *fks1*$_{tetOn}$ + Doxy

B.

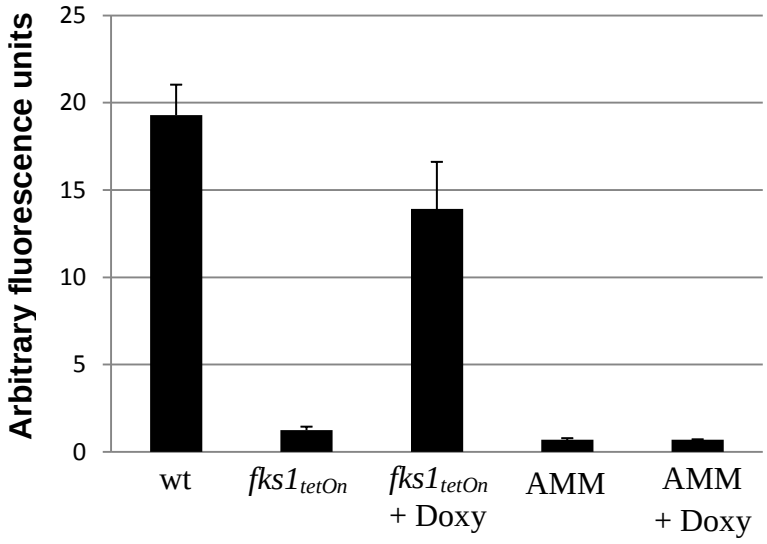

C.

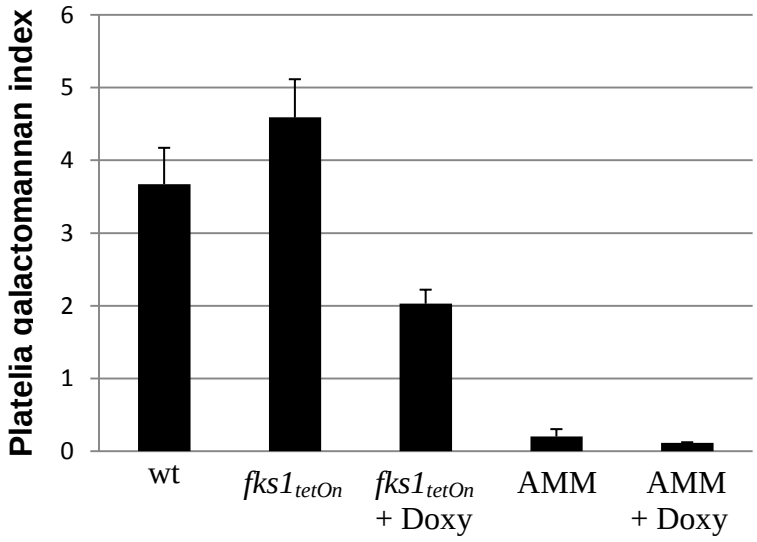

Figure 29. Reduced *fks1* expression triggers increased galactomannan shedding. (A-C) 3 x 10^4 conidia/ml from indicated strains were inoculated in triplicates in well plates at 37°C. When indicated, medium was supplemented with 0.5 µg/ml doxycycline (Doxy). Supernatants were collected and analyzed with a commercial galactomannan antigen test as described in Materials and methods. (A) Representative microscopic images of wild type (wt) and $fks1_{tetOn}$ strains cultured under repressed and induced conditions were taken after 46 h incubation at 37°C. (B) The viability of the strains measured by a resazurin-based dye. (C) Galactomannan index quantified from culture supernatants of indicated strains. (B and C) Error bars indicate standard deviations. Medium (AMM) and medium supplemented with 0.5 µg/ml doxycycline (AMM + Doxy) were used as negative controls.

4.2.6. The β-1,3-glucan synthase is dispensable for *A. fumigatus* viability.

As shown in Figure 27 (upper panel), growth of *fks1*$_{tetOn}$ mutant was not impaired at all by the echinocandin caspofungin. A possible explanation for this phenomenon could be that the β-1,3-glucan synthase is not essential in *A. fumigatus* in contrast to previous reports. To test this hypothesis, an *A. fumigatus fks1* deletion mutant was generated and cultured (performed in close collaboration with Dr. med. Karl Dichtl). For this, an *fks1* deletion cassette harboring a pyrithiamine resistance marker was generated (Figure 30 A) and surprisingly, the transformation yielded only wild type-like clones. Interestingly, when the conidia of the clones were subsequently streaked on agar plates under selective and non-selective condition, a differential heterokaryotic phenotype was observed under respective conditions. Several of these transformants yielded tiny and slowly growing white colonies without conidiation when raised specifically under selective conditions (Figure 30 B left panel). This growth phenotype was very similar to that of the *fks1*$_{tetOn}$ strain cultured under repressive growth conditions. In contrast, when raised under non-selective conditions i.e. in absence of pyrithiamine, these clones showed a wild type-like growth thereby suggesting that these transformants were heterokaryotic progenitors (Figure 30 B right panel). Similar heterokaryotic clones were isolated from several independent transformations and the gene replacement cassette was validated with PCR (Figure 30 A). Upon prolonged incubation on agar plates under selective conditions, the tiny white clones grew into huge swollen colonies with a popcorn-like appearance. These colonies were covered with caramel-colored droplets, probably due to continuous cytoplasmic bleeding (Figure 30 C).

The microscopic examination of the Δ*fks1* hyphae revealed that they were morphologically similar to wild type cultured in the presence of echinocandins or the *fks1*$_{tetOn}$ strain cultured under repressive conditions i.e. characterized by slow growth, frequent branching and hyphal tip lysis (Figure 31 A). Additionally, in contrast to wild type, the Δ*fks1* hyphae were not immunostained with 2G8 mAb, suggesting the strain lacked β-1,3-glucan in the cell wall (Figure 31 B). Taken together, these results demonstrated that the β-1,3-glucan synthase is not essential in *A. fumigatus.*

A.

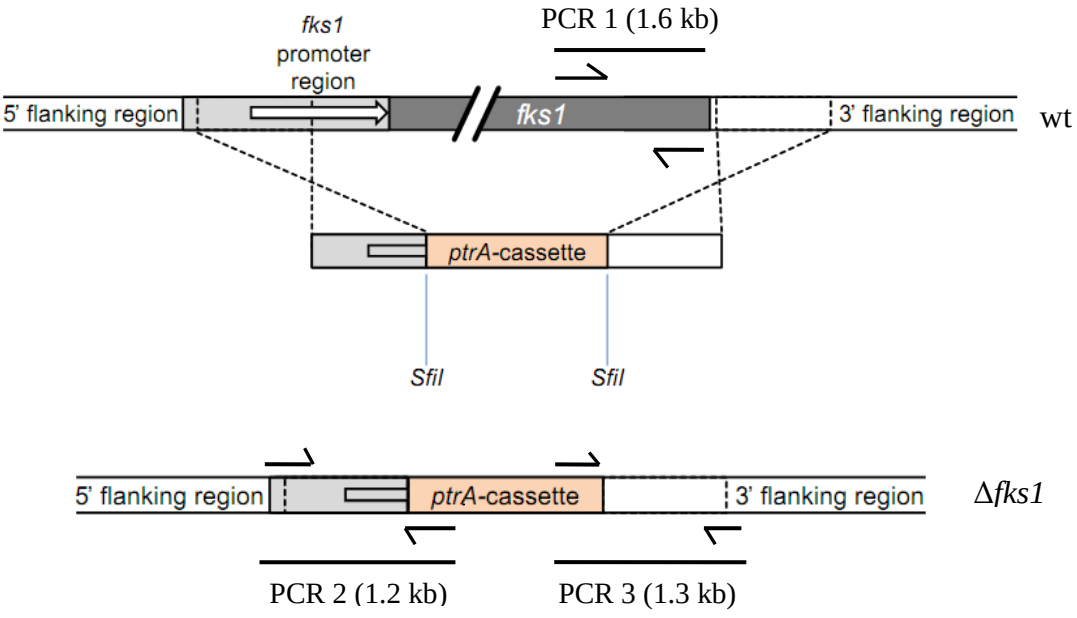
fks1
promoter
region
PCR 1 (1.6 kb)
5' flanking region
fks1
3' flanking region
wt
ptrA-cassette
SfiI
SfiI
5' flanking region
ptrA-cassette
3' flanking region
Δfks1
PCR 2 (1.2 kb)
PCR 3 (1.3 kb)

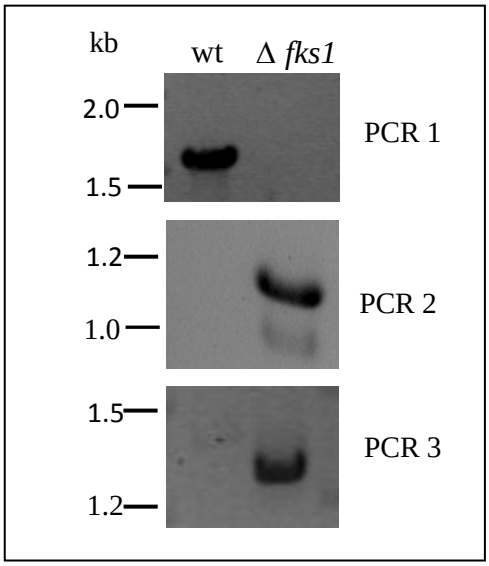
kb
wt
Δ fks1
2.0
1.5
PCR 1
1.2
1.0
PCR 2
1.5
1.2
PCR 3

B.

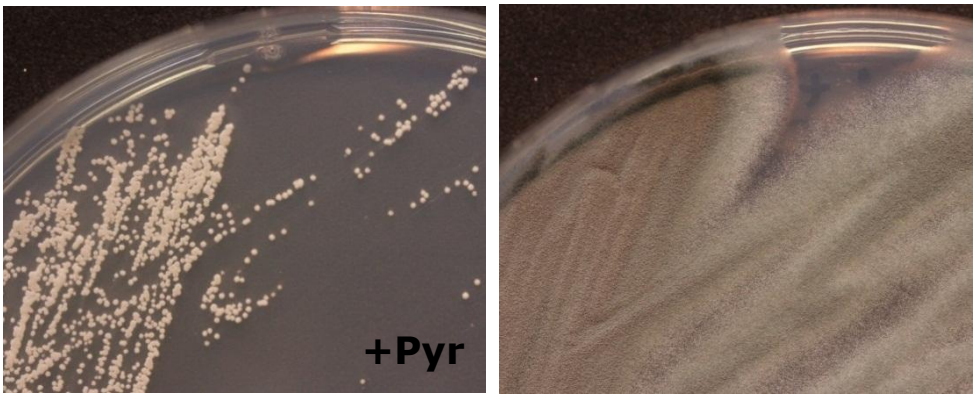
+Pyr

C.

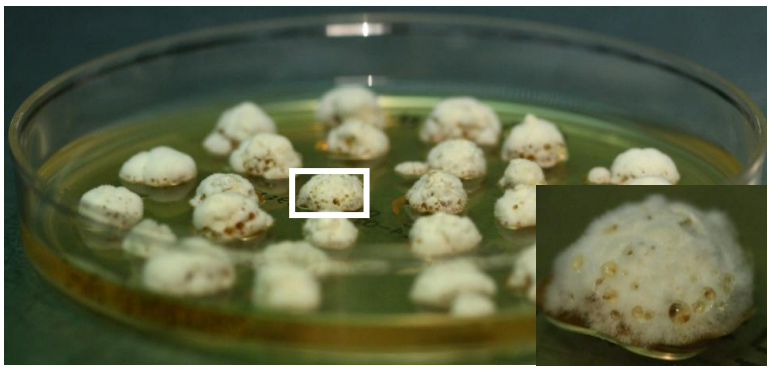

Figure 30. Construction of Δ*fks1* mutant. (A) An *fks1* deletion mutant was generated by replacing the respective ORF with a pyrithiamine resistance marker (*ptrA*) and validated with PCR. (B) Conidia of a heterokaryon Δ*fks1* transformant were streaked on AMM agar plates supplemented with no or 0.1 µg/ml pyrithiamine hydrobromide (Pyr). The plates supplemented without and with pyrithiamine were incubated at 37 °C for 36h and 48 h respectively. (C) Δ*fks1* isolates incubated on a Saboraud dextrose agar plate at 37°C for 30 days exhibiting cytoplasmic bleeding phenotype (inset).

A.

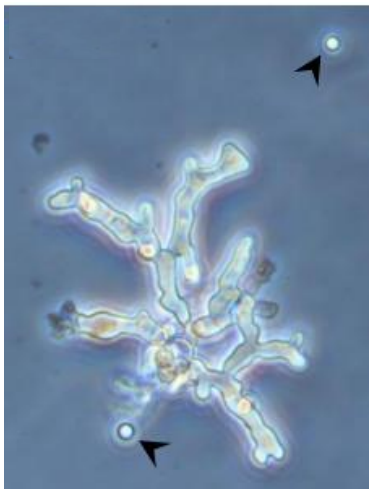

B.

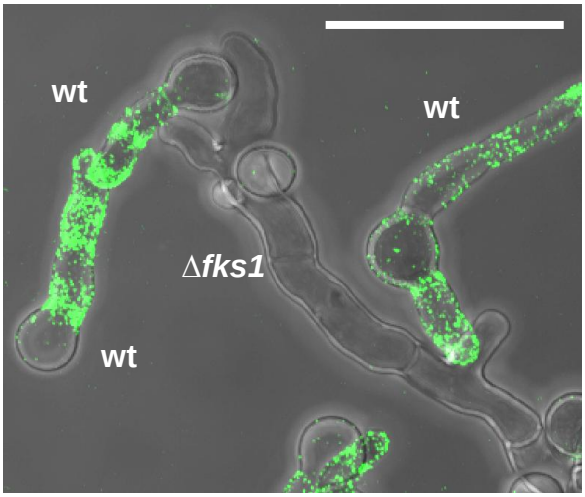

Figure 31. Phenotypic characterization of Δ*fks1* mutant. (A) Microscopic morphology of a heterokaryon Δ*fks1* cultured in AMM supplemented with 0.1 µg/ml pyrithiamine hydrobromide at 37°C for 22 h. The black arrow heads indicate wild type conidia. (B) Conidia of a heterokaryon Δ*fks1* transformant cultured in AMM on coverslip for 22 h at 37°C and immunostained with a β-glucan-specific mAb 2G8. Bar, 20 µm.

4.2.7. Septa and sealing of septal pores promote survival of *Aspergillus* microcolonies exposed to echinocandins.

As shown in Figure 27, *Aspergillus* is still able to grow at echinocandin concentrations above the MIC. This phenomenon is called 'trailing growth'. Interestingly, a Δ*rho4* mutant which is lacking the GTPase Rho4 shows no trailing growth (Dichtl *et al*., 2012). Therefore, it was speculated that the striking fungicidal effect of echinocandins on the Δ*rho4* mutant might be attributed to the lack of Rho4 GTPase activity and its importance for septum formation (Si *et al*., 2010; Dichtl *et al*., 2012). To investigate the significance of septa for echinocandin tolerance, the activity of caspofungin on microcolonies of wild type and the Δ*rho4* mutant was analyzed. Furthermore, for microscopic analysis of caspofungin mediated lysis, strains constitutively expressing GFP to discriminate between lysed and intact hyphae were used. The presence of septa in respective strains was detected by chitin-specific Calcofluor white staining. As shown by GFP fluorescence in caspofungin treated and untreated samples (Figure 32 A and B), the wild type hyphae harbored mostly intact hyphal compartments (sGFP-positive) that were clearly separated from the dead hyphal compartments (sGFP-negative) even after 2 h of caspofungin treatment. In contrast, the Δ*rho4* hyphae treated with caspofungin lacked septa and were completely dead (sGFP-negative). These results were in agreement with the quantitative analysis of hyphal lysis which revealed about 90 % of the wild type microcolonies to be fully or partially viable and about 95 % of the Δ*rho4* microcolonies that were completely dead after 2 h of caspofungin treatment (Figure 32 C). Due to the absence of septa, no partially viable Δ*rho4* microcolonies were found. Notably, approximately 5 % of the Δ*rho4* microcolonies survived caspofungin treatment. This is in a similar range as the number of fully intact wild type microcolonies after caspofungin treatment. We additionally analyzed the susceptibility of a Δ*hexA* strain to caspofungin. This strain although harbors septa, but lacks septal "plugs" known as Woronin bodies that function to seal the septal pores in response to cellular damage (Beck and Ebel, 2013; Beck *et al*., 2013). Compared to wild type, about 75 % of Δ*hexA* microcolonies were viable after caspofungin treatment and several partially intact hyphae were observed similar to wild type (Figure 32 C and D). In absence of caspofungin treatment, the frequency of completely dead microcolonies of wild type, Δ*rho4* and Δ*hexA* strains was below 4 % (Figure 32 D).

In agreement with the above results, the Δ*rho4* and Δ*hexA* strains also showed abolished or reduced growth in presence of caspofungin, as compared to wild type and complemented strains (Figure 33 A). To further validate that the increased susceptibility of the Δ*rho4* and Δ*hexA* strains to caspofungin is specifically attributed to inhibition of β-1,3-glucan synthesis, Δ*rho4* $fks1_{tetOn}$ and Δ*hexA* $fks1_{tetOn}$ double mutant strains were generated and analyzed under

induced and repressive conditions (performed in close collaboration with Dr. med. Karl Dichtl). As shown in Figure 33 B, repression of *fks1* expression in a Δ*rho4* or Δ*hexA* background resulted in growth inhibition similar to the effects observed under caspofungin treatment. Thus, these results demonstrated an important role for *Aspergillus* hyphae for echinocandin tolerance and also suggested a model whereby the absence of β-1,3-glucan synthesis and subsequent lysis is partially compensated by septa.

A.

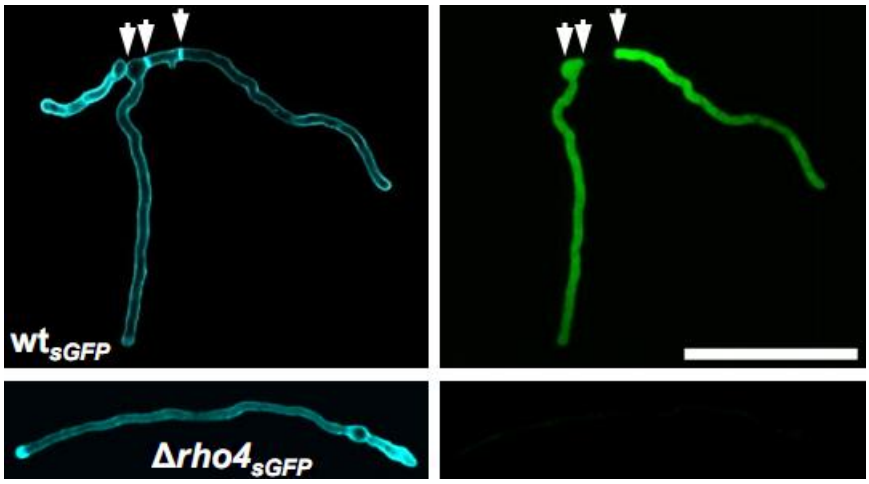

B.

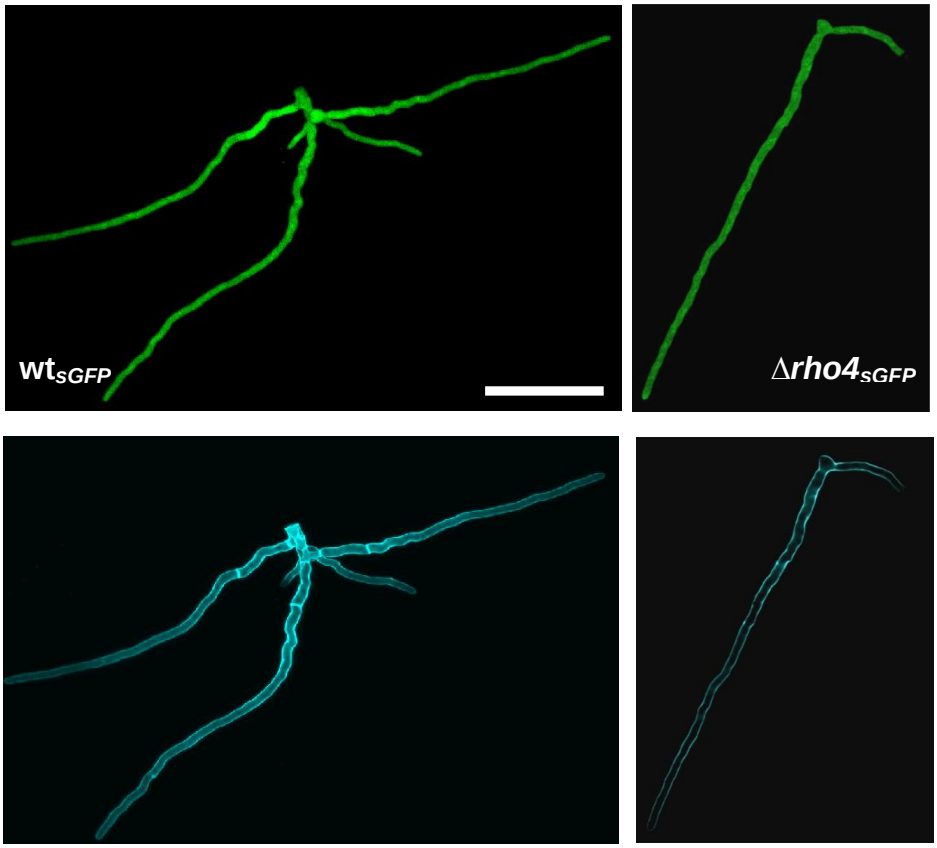

C.

.

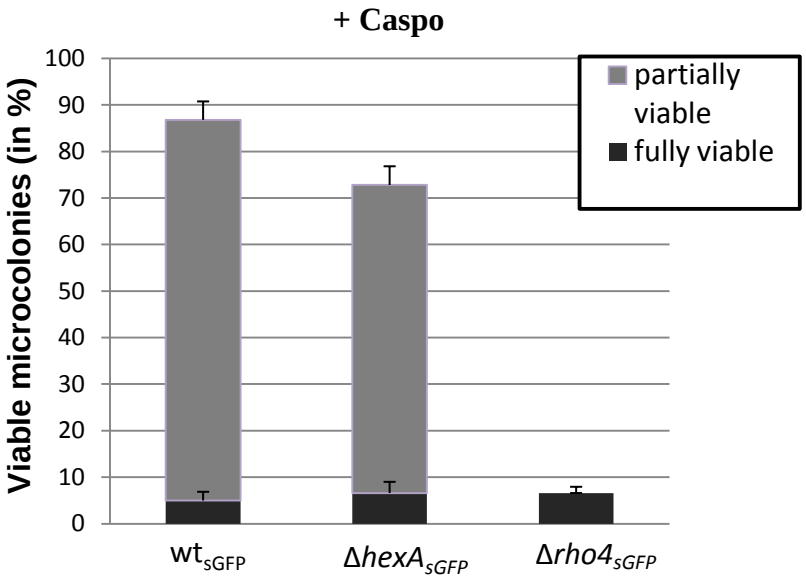

D.

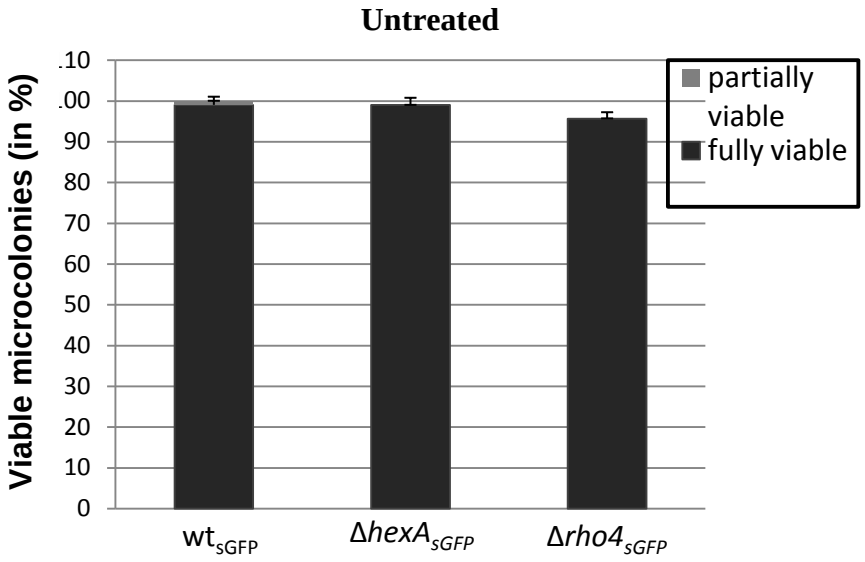

Figure 32. Lack of functional septa results in increased susceptibility to echinocandin. (A-D) Conidia of the indicated sGFP-expressing strains were inoculated in AMM on cover slips and cultured at 37 °C. After 11 h, 0.1 µg/ml caspofungin (Caspo) was added when indicated. After additional 2 h incubation, cells were fixed and analyzed. (A and B) Representative confocal microscopy images of indicated strains untreated (B) and treated with 0.1 µg/ml caspofungin (A). Left panel, cytoplasmic sGFP; right panel, Calcofluor white staining of the cell wall. Arrows indicate septa. Bar, 50 µm. (C and D) Quantification of fully (black) and partially (gray) viable microcolonies. For each strain, at least 3 x 100 microcolonies were analyzed.

A.

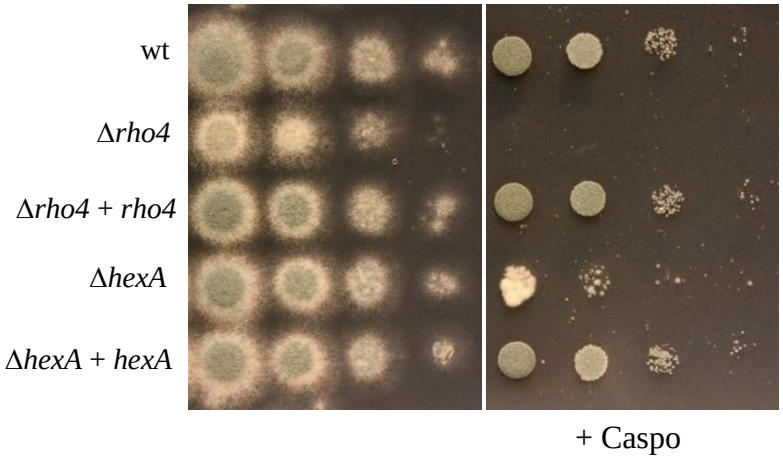

B.

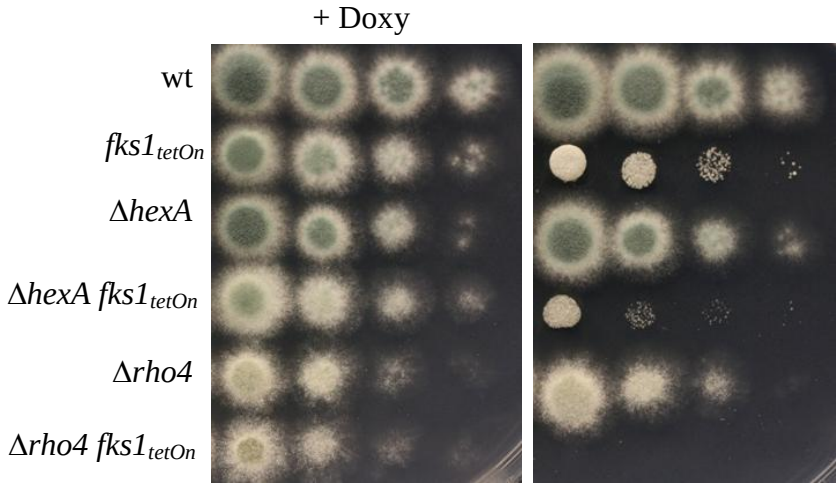

Figure 33. Survival of β-1,3-glucan depleted *Aspergillus* relies on functional septa. (A and B) Aliquots of 3 µl derived from a starting suspension of 5 x 10^6 conidia/ml of the indicated strains were spotted onto AMM agar. When indicated, AMM was supplemented with 0.1 µg/ml caspofungin (Caspo) or 0.5 µg/ml doxycycline (Doxy). Agar plates were incubated at 37 °C for 36 h (A, with caspofungin) or 48 h (B, with doxycycline).

4.2.8. Echinocandins exhibit synergistic activity with septum formation inhibitors.

Since it was observed that septal blockade is important to survive the echinocandin effect in *Aspergillus*, the effect of pharmacologic inhibition of septum formation on the efficacy of echinocandin antifungals became relevant to probe. Previously, it has been shown that the DNA-damaging agents diepoxyoctane (DEO) and hydroxyurea (HU) inhibit septum formation in *A. nidulans* (Harris and Kraus, 1998). According to the model proposed above, such inhibitors should enhance the fungicidal effect of echinocandins against *Aspergillus*. Therefore, in order to validate this speculation, the synergistic effect of these two compounds

with the echinocandin caspofungin was evaluated (performed in close collaboration with Dr. med. Karl Dichtl). In agreement with the results obtained with *A. nidulans*, the wild type hyphae rarely formed septa in presence of sublethal doses of DEO or HU (data not shown). Consequently, both inhibitors significantly reduced the number of viable microcolonies upon caspofungin treatment as compared to the agents used alone (Figure 33 A and B). In congruence, there was a marked dose-dependent reduction in the trailing growth as well was MIC of wild type observed on caspofungin E-tests with DEO (Figure 33 C).

A.

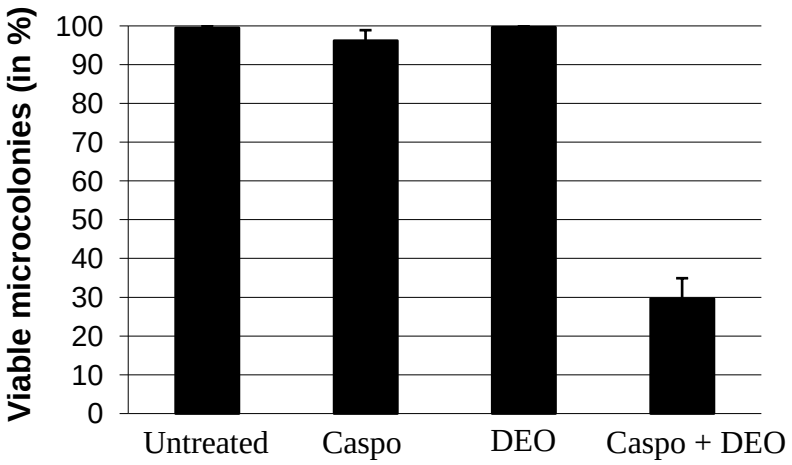

B.

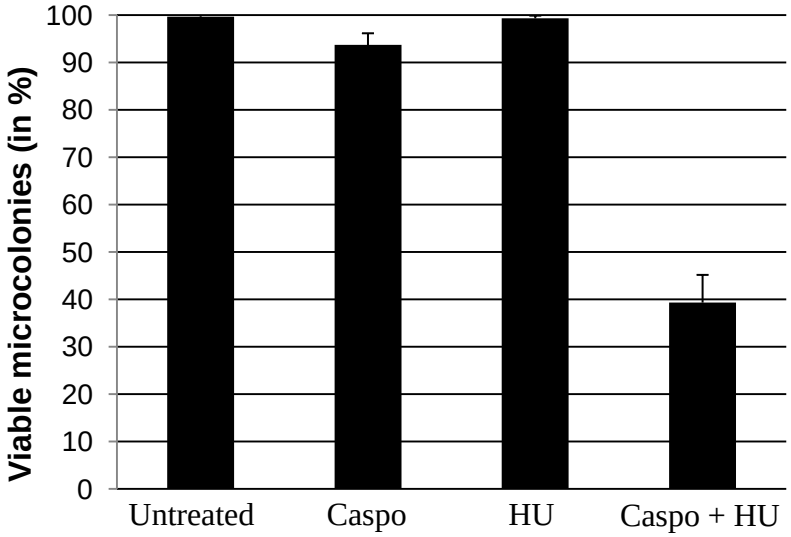

C.

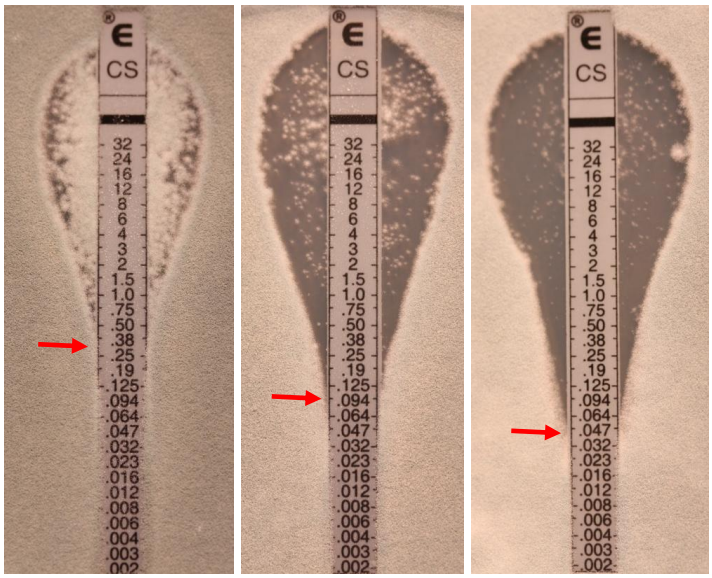

DEO (in %) 0 0.015 0.025

Figure 33. Synergistic activity of septum formation inhibitors with echinocandins. (A and B) Conidia of the sGFP-expressing wild type (wt_{sGFP}) were inoculated on cover slips in YG and incubated at 37°C. When indicated, AMM was supplemented with 0.025 % (v/v) DEO (A) or 9 mM HU (B). After 12 h incubation, 0.1 µg/ml caspofungin was added when indicated (Caspo). After additional 2 h incubation, cells were fixed and the number of viable microcolonies was quantified. For each condition 3 x 100 microcolonies were analyzed. (C) A total of 2.5 x 10^5 conidia of wild type were spread on YG agar plates and caspofungin Etest strips were applied. When indicated, YG was supplemented with 0.015 or 0.025 % (v/v) diepoxyoctane (DEO) and the agar plates were incubated at 37 °C. Representative photos were taken after 38 h (red arrows indicate respective MIC).

5. Discussion

5.1. Characterization of Rom2 in cell wall stress response signalling

The cell wall integrity signalling pathway is shown to be essential for cell wall biosynthesis and stress response, with the central signalling components conserved in several fungi, including *Aspergillus fumigatus*. This pathway is well characterized in *S. cerevisae*, whereby the CWI model consists of a family of cell surface sensors (Wsc1-3, MidA and Mtl1) that transduce the stress signal to guanine nucleotide exchange factors (GEFs) ScRom1/2 to activate downstream ScRho1 GTPase and its effector protein kinase C (ScPkc1). This ultimately leads to the activation of the linear tripartite MAPK module via ScBck1 (MAPKKK), ScMkk1/2 (MAPKK) and the end kinase, ScMpkA which triggers transcription of several genes regulating cell wall biogenesis (Levin, 2005). According to the CWI model derived from *S. cerevisae*, the Rho GEFs ScRom1/2 function as a connecting link between the upstream sensors and the downstream Rho GTPase (Figure 8). Recently, the sensors and Rho GTPases involved in CWI in *A. fumigatus* have been identified and characterized (Dichtl *et al*., 2012). Since *A. fumigatus* genome harbours a single homologue of the partially redundant GEFs ScRom1/2, it was intriguing to probe if AfRom2 acts as an upstream regulator in the CWI pathway and integrates combination of phenotypes of the CWI sensors as well as its interacting Rho GTPase. Therefore, an in-depth characterization of AfRom2 was attempted in order to understand its link to the CWI pathway as well as its significance in antifungal sress response in *A. fumigatus*. The findings of this work establish the fundamental role of Rom2 as a GEF, placing it between the cell surface sensors and Rho1 and its downstream effectors.

5.1.1. The apparent role of Rom2 in cell wall stress response and its correlation with CWI sensors.

According to previous reports, the CWI pathway in *A. fumigatus* is mainly mediated by the three sensors, namely Wsc1, Wsc2 and MidA (Dichtl et al., 2012). The $rom2_{tetOn}$ mutant under repressive conditions shares several phenotypes with the deletion mutants of these three CWI sensors (Dichtl *et al*., 2012). Downregulation of *rom2* resulted in significantly reduced radial growth and sporulation. This result is in agreement with the drastically impaired radial growth and sporulation observed in the Δ*wsc1*Δ*wsc3*Δ*midA* triple mutant as well as the downstream MAPK module mutant strains Δ*mkk2* and Δ*mpkA*, as previously reported (Dichtl *et al*., 2012; Dirr *et al.*, 2010). On the contrary, none of the single deletions of *wsc1*, *wsc3* and *midA* significantly reduced radial growth or sporulation, while the double deletion of

Δ*wsc1* and Δ*wsc3* only slightly reduced radial growth and sporulation as compared to wild type (Dichtl *et al*., 2012, Dirr *et al*., 2010). These results indicate that the partial growth redundancy of the three sensors is most likely incorporated in the single homologue of Rom2.

Repression of *rom2* resulted in an increasing susceptibility to β-1,3-D-glucan synthase inhibitor caspofungin. While Wsc3 and MidA are dispensable for caspofungin tolerance, deletion of *wsc1* exhibited a significant decrease in MIC with caspofungin (Dichtl *et al*., 2012). Similarly, the $rom2_{tetOn}$ mutant under repressive conditions exhibits increased sensitivity to cell wall perturbing agents such as Congo red, Calcofluor white and elevated temperature and the temperature-sensitive growth defect is partially osmoremediable. Additionally, the phosphorylation of MpkA was not further induced in presence of CFW in the repressed $rom2_{tetOn}$ mutant. Among the CWI sensors, MidA but not Wsc1 or Wsc3 showed a very similar sensitivity to CR, CFW and heat. In agreement with the role of MidA as a stress sensor for these agents, the CFW-induced MpkA phosphorylation was reduced in a mutant lacking *midA* activity (Dichtl *et al*., 2012). Remarkably, the $rom2_{tetOn}$ mutant did not show any altered sensitivity to farnesol which is in agreement with the previous data on CWI sensor mutants in *A. fumigatus*. In contrast, the Δ*mkk2* and Δ*mpkA* mutants showed increased susceptibility to this agent, which has been shown to inhibit prenylation of proteins such as Rho GTPases and interferes with their function (Dichtl *et al*., 2010, Dichtl *et al*., 2012). In agreement with the previous results, it is evident that the CWI signaling inhibition by farnesol is strictly restricted to the Rho GTPases and downstream components, and therefore, does not alter the sensitivity of upstream CWI sensors and GEF. Taken together, these data suggest that the function of the three sensors and Rom2 is congruent with the model whereby Rom2 acts as a downstream signaling molecule that relays and integrates the signals of these sensors (Figure 34).

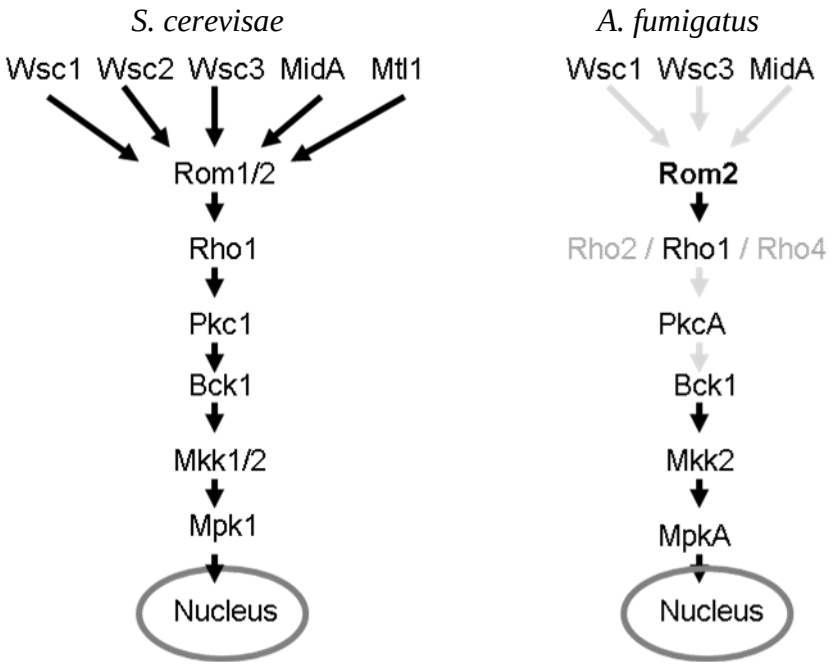

Figure 34. Schematic presentation of CWI models in *S. cerevisae* and *A. fumigatus*. In response to stress, the cell surface sensors activate the Rho1-GTPase by stimulating nucleotide exchange via GEF. Hypothetical signal transduction and components are indicated by gray arrows and proteins.

5.1.2. Growth inhibition of *rom2$_{tetOn}$* on complete media.

Remarkably, the *rom2$_{tetOn}$* mutant failed to grow on complete medium such as yeast glucose, saboraud dextrose and potato dextrose under repressive conditions. However, the growth is restored when overexpressed with doxycycline. Further, addition of sorbitol partially rescued growth which possibly suggests that this growth defect is partly due to lack of CWI and hence, partially compensated by osmotic stabilization. Since yeast extract composition is not completely defined, the exact nature of this growth inhibition on complete media aroused further interest. Interestingly, supplementing the minimal media with rich nitrogen sources phenocopies the growth inhibition effect. Apparently, the presence of reduced nitrogen sources delays germination of the mutant, potentially suggesting that Rom2 activity is essential for utilizing reduced nitrogen sources. These peculiar phenotypes point towards the role of Rom2 in nutrient or nitrogen sensing, but its underlying mechanism or possible link with other nutrient-sensing pathways is not clear. Notably, in *S. cerevisae*, the ScTOR1/2 (Target-of-Rapamycin) proteins, a pair of conserved Ser/Thr kinases are implicated in regulating cell cycle progression in response to nutrients (mainly nitrogen) in addition to actin

cytoskeleton regulation, a function unique to ScTOR2 which is mediated via the ScRom2 GEF (Barbet *et al*., 1996; Schmidt *et al*., 1997). Although, the TOR proteins are widely conserved among fungal species (Crespo and Hall, 2002), the exact role of *A. fumigatus* TOR homologs is not yet characterized. Nevertheless, this speculative role of Rom2 in nutrients sensing and TOR signaling in *A. fumigatus* requires further investigation, which is beyond the scope of this study.

5.1.3. Increased basal MpkA phosphorylation of the repressed *rom2$_{tetOn}$* mutant.

Importantly, the dual phosphorylation and activation of the MAPK ScMpkA in *S. cerevisae* is suggestive of an active CWI signaling. ScMpk1 is activated by phosphorylation of neighboring threonyl and tyrosyl residues within its activation loop, analogous to Thr202/Tyr204 of mammalian p44/p42 MAP kinase (Erk) which can be detected by commercially available antibodies against phospho-p42/p44. Activation of ScMpkA is induced by agents causing cell wall stress such as Calcofluor white, Congo red and other lytic enzymes. Alternatively, mutants with impaired cell wall are also known to result in ScMpkA activation (Martin *et al*., 2000; Levin, 2005). Therefore, activation of ScMpkA indicates impaired cell wall integrity irrespective of the nature of cell wall stress, which also holds true for other fungi.

The *rom2$_{tetOn}$* mutant cultured under repressed growth conditions shows significantly enhanced basal MpkA phosphorylation as compared to wild type. This obviously suggests that the repressed *rom2* conditional mutant has a weakened cell wall. However, this is indeed surprising, since Rom2 is an upstream activator of the CWI cascade. Therefore, one would expect reduced MpkA phosphorylation and activation upon abolishing Rom2 activity. However, similar observations have been made previously with Rom2 homologues in *S. cerevisae* and *N. crassa*. The deletion of *ScROM2* results in an increased basal phosphorylation of ScMpk1 (Lorberg *et al*., 2001). Likewise, a heterokaryon deletion of *Ncrgf-1* (encoding *N. crassa* Rom2 homologue) also results in increased basal phosphorylation of the MpkA homologue NcMak1 (Richthammer *et al*., 2012). One possible explanation to this can be that there exist alternative lateral signaling influxes similar to *S. cerevisae* which potentially activate CWI MAPK module either through ScMkk1/2 or ScMpk1 directly. Interestingly, as previously reported by Harrison and colleagues, a notable increase in the activation of ScMpk1 was observed upon heat shock in strains lacking *ScPKC1* (harboring a constitutively active *ScBCK1-20* allele) and *ScBCK1* (harboring a

constitutively active *ScMKK1*^{DD} allele) (Harrison *et al*., 2004). This may well explain the significant activation of AfMpkA in the absence of *rom2* function which results in cell lysis and generates chronic cell wall stress, possibly triggering such a lateral cross-talk event rather than acting in a linear, hypothetical manner via Rom2-Rho1-MAPK.

5.1.4. Rom2 specifically interacts with Rho1 GTPase.

Among the six Rho GTPases in *Aspergillus*, only Rho1, Rho2 and Rho4 homologues are relevant for maintaining cell wall integrity (Kwon *et al.*, 2011; Dichtl *et al*., 2012). In *A. fumigatus*, while deletion of *rho2* and *rho4* did not result in significant growth defects other than slightly reduced radial growth and sporulation, deletion of *rho1* was lethal and conditional downregulation of *rho1* resulted in cell lysis and cytoplasmic leakage (Dichtl *et al*., 2012). Interestingly, *Afrom2* is also essential for *A. fumigatus* and repression of *rom2* also results in dramatic growth defects such as absence of sporulation and radial growth on minimal media (AMM) and cell lysis on complete media. Secondly, in this study we have shown that Rom2-GFP localizes preferentially to hyphal tips. A similar localization pattern has been previously observed for GFP-Rho1 and GFP-Rho3 in *A. fumigatus* (Dichtl *et al*., 2012). However, the pull down assay result demonstrates that Rho1 and not Rho3 is co-immunoprecipitated with Rom2, thereby proving specific interaction module between Rom2 and Rho1 in *A. fumigatus*. This is in good agreement with the findings from *N. crassa* whereby, the GEF NcRgf1 specifically promotes nucleotide exchange *in vitro* on the ScRho1 homologue NcRho1 and not any other Rho GTPases (Richthammer *et al*., 2012). These results together suggest specificity of ScRom1/Rom2 homologues for the cognate Rho GTPase is well conserved from yeasts to filamentous fungi.

Interestingly, the localization pattern of GFP-tagged Rom2 to newly formed septa is similar to GFP-Rho4 (Dichtl *et al*., 2012). These findings suggest possible interaction of these proteins which could either point towards the involvement of Rom2 in septum formation or an additional role for Rho4 in regulating CWI. However, Rho4 is specifically involved in septum formation in *Aspergillus* and a Δ*rho4* mutant lacks septa (Si *et al*., 2010; Kwon *et al*., 2011; Dichtl *et al*., 2012). In contrast, the *rom2*$_{tetOn}$ mutant under repressive conditions shows several septa. Furthermore, it has been previously reported that in *A. nidulans*, AnBud3 acts a GEF for AnRho4 to regulate septum formation (Si *et al*., 2010). Likewise, in *N. crassa* GEFs NcBud3 and NcRgf3 have been identified as two non-redundant GEFs of NcRho4 (Justa-Schuch *et al*., 2010). Therefore, it is more likely that the GEF activity on AfRho4 in *A.*

fumigatus may also be regulated by the orthologues of Bud3 (AFUA_5G11890) or Rgf3 (AFUA_5G07430). Additionally, the role of Rho4 in mediating CWI is rather speculative, since the MpkA phosphorylation induced by Calcofluor white is not reduced in the Δ*rho4* mutant, even though the mutant is shown to be increasingly susceptible to the agent (Dichtl *et al*., 2012). Although the localization of AfRom2 to septa is puzzling, it possibly reflects a potential role for Rho1 in contractile actomyosin ring (CAR) assembly during septum formation or cytokinesis. The CAR is an actin band that acts as a landmark for deposition of septal wall material and the CAR assembly therefore, precedes the process of septation (Si *et al*., 2010; Harris 2001). Increasing evidences reveal that the CAR assembly requires a network of protein kinases that constitute the septum initiation network (SIN) and other regulatory proteins such as septins and formins (Harris 2001). This reportedly requires Rho1 activation and recruitment to the sites of newly forming septa, a process mediated via its GEF, as evident in *S. cerevisae* and *S. pombe* (Perez and Rincón, 2010; Yoshida *et al*., 2009; Mutoh *et al*., 2005). Without the recruitment of Rho1 GEF to the division site, the Rho1 GTPase is never activated and concentrated at the division site (Yoshida *et al*., 2009; García *et al*., 2006). Interestingly, the role of Rho1 in CAR assembly is further supported by its interaction with the actin regulator or formin, Bni1 in both *S. cerevisae* and *N. crassa* (Kohno *et al*., 1996; Richthammer *et al*., 2012). Based on the above observations and localization pattern of Rom2-GFP, it appears that AfRom2 is involved in Rho1 recruitment during CAR assembly. However, the presence of septa in the repressed $rom2_{tetOn}$ strain may contradict the GEF-dependent process. Surprisingly, a Δ*Scmyo1* mutant strain in *S. cerevisae* lacking the myosin heavy chain and a functional contractile ring is still able to complete cytokinesis and septum formation via GEF-independent localized cell wall chitin synthesis (Bi *et al*., 1998). In contrast, a strain lacking *ScCHS3* (mostly responsible for salvage septum synthesis) and *ScMYO1*, but not *ScCHS2* and *ScMYO1*, has severe growth defects suggesting secondary septum formation compensates cytokinesis in absence of CAR assembly (Schmidt *et al*., 2002).

5.1.5. Autoinhibitory effect of DEP domain of Rom2 in *A. fumigatus*

Comparison of AfRom2 to its homologues in yeasts and another filamentous fungus *N. crassa* revealed a conserved domain structure of the GEFs. They possess a catalytic DH domain flanked by an N-terminal DEP and a C-terminal CNH (Citron Homology) domain (Figure 12). The CNH domain is a regulatory motif implicated in binding exclusively to the GTP-

bound active forms of Rho and Rac GTPases (Madaule *et al*., 1995). The DEP domains, on the other hand, are mostly found in G-protein signaling proteins and regulate intramolecular interactions between proteins, as in case of G-protein-coupled receptor signalling in yeast (Ballon *et al*., 2006).

Interestingly, the N-terminal DEP domain of NcRGF1 was shown to exert a self-inhibitory effect on its GEF activity in *N. crassa.* It was observed that in vitro the GEF domain of NcRGF1 can induce nucleotide exchange on NcRHO1 only if the N-terminal part harbouring the DEP domain was not included in the construct. According to the proposed model (Figure 35), the N-terminal region of NcRGF1 interacts with the NcWsc1 sensor under cell wall stress conditions. This, in turn, relieves the auto-inhibitory effect of the DEP domain on the GEF domain possibly via conformational change and allows activation of NcRHO1 via the GEF domain (Richthammer *et al*., 2012). Similarly, in this study, it is demonstrated that in contrast to the overexpression of full-length AfRom2, the overexpression of a truncated Rom2 construct lacking the N-terminus region including the DEP domain, induces a strikingly stronger growth phenotype. Additionally, the overexpression of the truncated AfRom2, but not the full-length GEF results in significant hyphal growth inhibition that mimics the constitutive activation of AfRho1. Taken together, these findings suggest that the auto-inhibitory model of the DEP domain also applies to *A. fumigatus*.

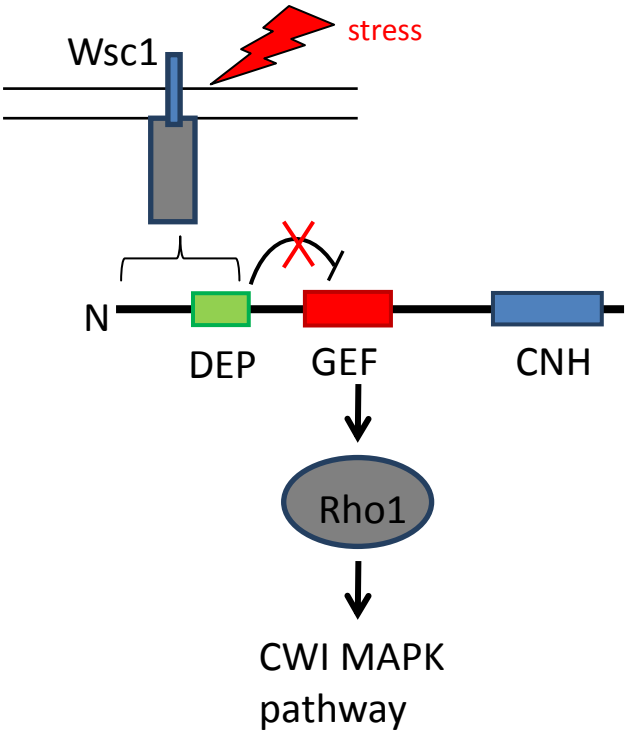

Figure 35. Model illustrating the self-inhibitory effect of DEP domain on GEF activity. The DEP domain of Rho1 GEF inhibits GEF activity possibly through intra-molecular interaction and prevents nucleotide exchange on Rho1 GTPase. However, in presence of cell wall stress, the N-terminal part of the GEF interacts with the sensor and this relieves the autoinhibiton on GEF domain, thereby, activating Rho1 and CWI pathway (adapted from Richthammer *et al*., 2012).

5.2. Characterizing the echinocandin tolerance of *A. fumigatus.*

Echinocandins are clinically significant antifungals and constitute a part of the current treatment module for invasive aspergillosis, besides azoles and polyenes. However, these drugs are generally fungistatic to *A. fumigatus* in contrast to the other two classes of antifungals. Therefore, the β-1,3-glucan synthase subunit and echinocandin drug target, Fks1 was characterized in greater detail in order to understand and redress the static effect of echinocandins against *Aspergillus*. Importantly, these drugs inhibit the enzyme β-1,3-glucan synthase, resulting in depletion of β-1,3-glucan which constitutes an important component of the fungal cell wall. This is clearly evident in *S. cerevisae*, whereby, the deletion of two *fks* homologues *ScFKS1* and *ScFKS2* is lethal. Similarly, the *CaFKS1* in *C. albicans* is shown to be essential (Douglas et al., 1997; Mio et al., 1997). Therefore, to elucidate the significance of the only *fks1* homologue for growth and antifungal resistance of *A. fumigatus*, a conditional $fks1_{tetOn}$ is employed.

5.2.1. The β-1,3-glucan synthase is not essential in *A. fumigatus.*

The echinocandin class of antifungals is known to be mostly fungistatic against *Aspergillus*. This limited activity of echinocandins can be explained by either of the two plausible arguments, the first being that β-1,3-glucan is not essential for *A. fumigatus* viability and the other may be due to incomplete inhibition of β-1,3-glucan synthesis. This point of conflict is well explained with the growth phenotype of a conditional $fks1_{tetOn}$ under repressive conditions. As expected, the growth of the $fks1_{tetOn}$ mutant in absence of doxycycline resembled that of *A. fumigatus* wild type treated with caspofungin, and was characterized by slow and stunted hyphal growth, frequent branching and cell lysis. Additionally, the co-immunostaining of wild type and conditional fks1 mutant cultured under repressive growth conditions with the β-1,3-glucan-specific mAb, 2G8 revealed a differential staining pattern. While the wild type hypha showed an even distribution of β-1,3-glucan on the cell surface,

the conditional *fks1* mutant remained unstained, suggesting the lack of cell wall β-1,3-glucan in the mutant. Further, the growth of the *fks1* mutant is not inhibited even at higher concentrations of echinocandin caspofungin as shown with the E-tests. These results confirm that the mutant lacked any residual β-1,3-glucan synthase activity and the viability of the mutant is not driven by basal *fks1* expression. In agreement, the generation of a viable *fks1* deletion mutant further justifies that the limited efficacy of echinocandins against *A. fumigatus* is not based on incomplete inhibiton of β-1,3-glucan synthesis, but instead reveals that β-1,3-glucan synthase is not essential, which is in contrast to previous report (Firon *et al*., 2002).

5.2.2. Implication of echinocandin treatment on Platelia-galactomannan index.

The β-1,3-glucan also acts as a scaffold matrix for other cell wall components such as galactomannan which remain covalently linked to the glucans (Fontaine *et al*., 2000). Galactomannan is a distinct polysaccharide component of the Aspergillus cell wall and its quantification serves as a surrogate marker for evaluating fungal burden (Musher *et al*., 2004). The detection of serum galactomannan with the PlateliaAspergillus EIA, the galactomannan index (GMI) has been adopted as a criterion in the diagnosis of IA and also considered significant for monitoring the response to treatment (De Pauw *et al*., 2008; Marr 2008). Decreasing levels of galactomannan have been observed in infection models as well as in patients successfully treated with amphotericin B or azoles (Maertens *et al*., 2001; Olson *et al*., 2010; Jeans *et al*., 2012). In contrast, a paradoxical increase in the serum galactomannan index was observed in a patient undergoing caspofungin monotherapy (Klont *et al*., 2006). In agreement, caspofungin treatment in animal models of invasive aspergillosis also revealed higher galactomannan indices as compared to untreated controls despite a significant reduction in fungal burden (Scotter *et al*., 2005; Calvo *et al*., 2011).

Immunostaining of the $fks1_{tetOn}$ mutant hypha cultured under repressive conditions with the galactomannan-specific mAb also revealed a diffused staining pattern in contrast to wild type hypha which showed a distinct cell surface distribution of galactomannan. This also suggests that galactomannan integration into the cell wall is decreased when β-1,3-glucan synthesis is compromised. Interestingly, in contrast to less cell wall galactomannan, higher galactomannan index was observed in cell culture supernatants of the mutant. These results altogether suggest that in absence of β-1,3-glucan, galactomannan is no longer covalently bound in the cell wall and consequently released into circulation, resulting in increased galactomannan index. The

findings of the present study, jointly in agreement with the results proposed by Klont *et al*., conclude that echinocandin treatment indeed results in increased circulating galactomannan levels. These observations also point towards the necessary optimization of galactomannan-based *Aspergillus* antigen tests for evaluating the progress of echinocandin therapy.

5.2.3. Mechanisms promoting echinocandin tolerance in *A. fumigatus*.

The results of this work demonstrate that *A. fumigatus* is viable even when lacking cell wall β-1,3-glucan. These results also reflect potential mechanisms driving the viability of the fungus when *fks1* expression is downregulated. This is indeed of fundamental interest, since compromising such mechanisms will alleviate echinocandin tolerance of the pathogen and significantly enhance the efficacy of echinocandins. First, the $fks1_{tetOn}$ mutant cultured under repressive growth conditions shows a significantly increased chitin content, suggesting a compensatory role for cell wall chitin. This is further supported by the increased susceptibility of the mutant to the chitin-binding agent Calcofluor white. These results are in good agreement with previously reported increase in expression of chitin synthase genes induced by high concentrations of caspofungin (Fortwendel *et al.*, 2010). On the other hand, the increased resistance of the $fks1_{tetOn}$ mutant to Congo red (CR), which has a similar mode of action as Calcofluor white (CFW) may argue against the compensatory chitin increase. A possible explanation to the differential phenotypes with CFW and CR may be rendered due to the different structures of these compounds, as well as their reportedly differential affinity for β-1,3-glucan (Hill *et al*., 2006). The CR is known for its strong affinity for β-1,3-glucan as the dye forms a complex with glucan chains, which is also evident in *S. cerevisae* (Wood, 1980; Kopecká and Gabriel, 1992). In such a situation, the $fks1_{tetOn}$ mutant with reduced β-1,3-glucan exhibits increased resistance to CR, which further confirms its glucan-binding affinity.

Second, echinocandin treatment results in frequent lysis at hyphal tips leading to cytoplasmic leakage. The ability of the fungus to survive such physical damage is facilitated by compartmentalisation of hyphae by septa that serve as a blockade to restrict cytoplasmic loss and damage to a few hyphal compartments. In *Aspergillus*, such efficient barrier function is exclusively mediated by the septa and septal plugs (Woronin bodies) that significantly contribute to echinocandin tolerance. It is shown that the respective mutants are further impaired in growth on additional loss of β-1,3-glucan, suggesting that septal sealing partially compensates loss of β-1,3-glucan. Congruently, inhibition of septum formation by hydroxyurea and diepoxyoctane strikingly enhances the fungicidal potency of caspofungin.

However, these compounds are toxic and therefore not suitable for clinical applications. Since the process of septum formation and the septum itself is lacking in mammalian host and unique to the fungus, the development of specific septum formation inhibitors could be a promising strategy for improving efficacy of current echinocandin therapy.

5.3. Future perspectives

Invasive aspergillosis is a lethal infection manifested with discernible mortality. Despite drastic improvements in diagnosis and drug formulations, the mortality rate remains high, thereby, compelling the need for novel and effective antifungals (Lin *et al*., 2001). In such a scenario, the fungistatic effect of echinocandins appears to be a major concern for treating invasive aspergillosis. Although the present study brings into light several relevant findings that explain the nature of echinocandin tolerance in *Aspergillus*, several aspects deserve further intensive research for the purpose of new antifungal drug screening. For instance, the increased echinocandin sensitivity of the GEF Rom2 and the CWI sensor Wsc1 emphasizes the substantial role of CWI pathway for echinocandin tolerance in the pathogen. A comprehensive approach of genome-wide expression profiling of the fungus challenged with echinoandin would provide a unique opportunity to unravel the repertoire of effector genes and other antifungal resistance pathways. Next, the phenomenon of reduced susceptibility of the fungal cell with elevated chitin upon exposure to sub-MIC echinocandin doses, observed in vitro, requires further investigation to validate it clinically in infected patients treated with similar doses of echinocandin. Finally, it appears that functional septa largely attribute to the static effect of echinocandins on *A. fumigatus*. Although CAR is a key constituent of the cytokinetic machinery in fungi, the precise mechanism of CAR formation in filamentous fungi and role of regulatory proteins remain to be characterized (Berepiki *et al*., 2011). In *N. crassa* and *A. nidulans*, the Rho4-Bud3 module is highly implicated in regulating CAR assembly (Justa-Schuch *et al*., 2010; Si *et al*., 2010). Similarly, the formin genes, *sepA* and *bni-1* are essential for viability of *A. nidulans* and *N. crassa* respectively (Sharpless *et al*., 2002; Justa-Schuch *et al.*, 2010). In *C. albicans*, a Δ*Cabni1* mutant shows morphological defects and attenuated virulence in a murine systemic candidiasis infection model (Li *et al*., 2005). A more complete understanding of the CAR dynamics in filamentous fungi and the elucidation of regulatory proteins will be crucial to bridge the connecting links between antifungal tolerance and cytokinetic dynamics. Research advances in these areas could

potentially strengthen the effectiveness of clinically relevant drugs and help optimize the future antifungal design.

6. References

- Abad A., Fernández-Molina J.V., Bikandi J., Ramírez A., Margareto J., Sendino J., Hernando F.L., Pontón J., Garaizar J. & Rementeria A. (2010) What makes *Aspergillus fumigatus* a successful pathogen? Genes and molecules involved in invasive aspergillosis. Rev. Iberoam. Micol. 27(4):155-182.

- Anderson J.B. (2005) Evolution of antifungal-drug resistance: mechanisms and pathogen fitness. Nat. Rev. Microbiol. 3(7):547-556.

- Arnaud M.B., Chibucos M.C., Costanzo M.C., Crabtree J. Inglis D.O., Lotia A., Orvis J., et al. (2010) The Aspergillus Genome Database, a curated comparative genomics resource for gene, protein and sequence information for the *Aspergillus* research community. Nucleic Acids Res. 38 (Suppl. 1):D420–D427.

- Ashley E. S. D., Lewis R., Lewis J. S., Martin C. and Andes D. (2006) Pharmacology of systemic antifungal agents. Clin. Infect. Dis. 43(Suppl.1):S28-S39.

- Ballon D.R., Flanary P.L., Gladue D.P., Konopka J.B., Dohlman H.G. & Thorner J. (2006) DEP-domain-mediated regulation of GPCR signaling responses. Cell 126(6): 1079-1093.

- Barbet N.C., Schneider U., Helliwell S.B., Stansfield I., Tuite M.F. & Hall M.N. (1996). TOR controls translation initiation and early G1 progression in yeast. Mol Biol Cell 7(1):25-42.

- Barnes P.D. & Marr K.A. (2006) Aspergillosis: spectrum of disease, diagnosis, and treatment. Infect. Dis. Clin. North Am. 20(3):545–561.

- Bennett J.W. & Klich M.A. (1992) *Aspergillus*: biology and industrial applications. Reed Publishing: Stoneham, Massachusetts, USA.

- Beauvais A., Maubon D., Park S., Morelle W., Tanguy M., Huerre M., Perlin D.S. & Latgé JP. (2005) Two alpha(1-3) glucan synthases with different functions in *Aspergillus fumigatus*. Appl. Environ. Microbiol. 71(3):1531-1538.

- Beauvais A., Bruneau J.M., Mol P.C., Buitrago M.J., Legrand R. & Latgé J.P. (2001) Glucan synthase complex of *Aspergillus fumigatus*. J. Bacteriol. 183(7):2273-2279.

- Beck J., Echtenacher B. & Ebel F. (2013) Woronin bodies, their impact on stress resistance and virulence of the pathogenic mould *Aspergillus fumigatus* and their anchoring at the septal pore of filamentous Ascomycota. Mol. Microbiol. 89(5):857-871.

- Beck J. & Ebel F. (2013) Characterization of the major Woronin body protein HexA of the human pathogenic mold *Aspergillus fumigatus*. Int. J. Med. Microbiol. 303(2):90-97.

- Berepiki A., Lichius A. & Read N.D. (2011) Actin organization and dynamics in filamentous fungi. Nat. Rev. Microbiol. 9(12):876-887.

- Bertani G. (1951) Studies on lysogenesis. I. The mode of phage liberation by lysogenic *Escherichia coli*. J. Bacteriol. 62(3):293-300.

- Bi E., Maddox P., Lew D.J., Salmon E.D., McMillan J.N., Yeh E. & Pringle J.R. (1998) Involvement of an actomyosin contractile ring in *Saccharomyces cerevisiae* cytokinesis. J. Cell. Biol. 142(5):1301-1312.

- Brown G.D., Taylor P.R., Reid D.M., Willment J.A., Williams D.L., Martinez-Pomares L., Wong S.Y. & Gordon S. (2002) Dectin-1 is a major beta-glucan receptor on macrophages. J. Exp. Med. 196(3):407-412.

- Bowman J.C., Hicks P.S., Kurtz M.B., Rosen H., Schmatz D.M., Liberator P.A. & Douglas C.M. (2002) The antifungal echinocandin caspofungin acetate kills growing cells of *Aspergillus fumigatus* in vitro. Antimicrob. Agents Chemother. 46(9):3001-3012.

- Bowman S.M. & Free S.J. (2006) The structure and synthesis of the fungal cell wall. Bioessays. 28(8):799-808.

- Cabib E. and Duran A. (1975) Simple and sensitive procedure for screening yeast mutants that lyse at nonpermissive temperatures. J. Bacteriol. 124(3):1604-1606.

- Calvo E., Pastor F.J., Mayayo E., Salas V. & Guarro J. (2011) In vitro activity and in vivo efficacy of anidulafungin in murine infections by *Aspergillus flavus*. Antimicrob. Agents Chemother. 55(3):1290-1292.

- Cao W., Maruyama J., Kitamoto K., Sumikoshi K., Terada T., Nakamura S. & Shimizu K. (2009) Using a new GPI- anchored-protein identification system to mine the protein databases of *Aspergillus fumigatus*, *Aspergillus nidulans* and *Aspergillus oryzae*. J. Gen. Appl. Microbiol. 55(5):381-393.

- Chai L.Y., Vonk A.G., Kullberg B.J. & Netea M.G. (2011) Immune Response to *Aspergillus fumigatus* in Compromised Hosts: From Bedside to Bench. Future Microbiol. 6(1):73-83.

- Crespo J.L. and Hall M.N. (2002) Elucidating TOR signaling and rapamycin action:

lessons from *Saccharomyces cerevisiae*. Microbiol. Mol. Biol. Rev. 66(4):579-591.

- Dagenais T.R.T. and Keller N.P. (2009) Pathogenesis of *Aspergillus fumigatus* in Invasive Aspergillosis. Clin. Microbiol. Rev. 22(3):447-465.

- de Groot P.W., Ruiz C., Vázquez de Aldana C.R., Duenas E., Cid V.J., Del Rey F., Rodríquez-Peña J.M , Pérez P., Andel A., *et al*. (2001) A genomic approach for the identification and classification of genes involved in cell wall formation and its regulation in *Saccharomyces cerevisiae*. Comp. Funct. Genomics. 2(3):124-142.

- de Groot P.W.J, Ram A.F. & Klis F.M. (2005) Features and functions of covalently linked proteins in fungal cell walls. Fungal Genet. Biol. 42(8): 657–675.

- Denning D.W. (2003) Echinocandin antifungal drugs. Lancet 362(9390):1142–1151.

- De Pauw B., Walsh T.J., Donnelly J.P., Stevens D.A., Edwards J.E., et al. (2008) Revised definitions of invasive fungal disease from the European Organization for Research and Treatment of Cancer/Invasive Fungal Infections Cooperative Group and the National Institute of Allergy and Infectious Diseases Mycoses Study Group (EORTC/MSG) Consensus Group. Clin. Infect. Dis. 46(12):1813–1821.

- De Sampaïo G., Bourdineaud J.P. & Lauquin G.J. (1999) A constitutive role for GPI anchors in *Saccharomyces cerevisiae*: cell wall targeting. Mol. Microbiol. 34(2):247–256.

- Dichtl K., Ebel F., Dirr F., Routier F.H., Heesemann J. & Wagener J. (2010) Farnesol misplaces tip-localized Rho proteins and inhibits cell wall integrity signalling in *Aspergillus fumigatus*. Mol. Microbiol. 76(5):1191-204.

- Dichtl K., Helmschrott C., Dirr F. & Wagener J. (2012) Deciphering cell wall integrity signalling in *Aspergillus fumigatus*: identification and functional characterization of cell wall stress sensors and relevant Rho GTPases. Mol. Microbiol. 83(3):506-519.

- Dirr, F., Echtenacher B., Heesemann J., Hoffmann P., Ebel F. & Wagener J. (2010) AfMkk2 is required for cell wall integrity signaling, adhesion, and full virulence of the human pathogen *Aspergillus fumigatus*. Int. J. Med. Microbiol. 300(7):496-502.

- Douglas C.M., Foor F., Marrinan J.A., Morin N., Nielsen J.B., Dahl A.M., Mazur P., Baginsky W., Li W., el-Sherbeini M., et al. (1994) The *Saccharomyces cerevisiae* FKS1 (ETG1) gene encodes an integral membrane protein which is a subunit of 1,3-beta-D-glucan synthase. Proc. Natl. Acad. Sci. U.S.A. 91(26):12907-12911.

- Douglas C.M., D'Ippolito J.A., Shei G.J., Meinz M., Onishi J., Marrinan J.A., Li W., Abruzzo G.K., Flattery A., Bartizal K., Mitchell A. & Kurtz M.B. (1997) Identification of the FKS1 gene of *Candida albicans* as the essential target of 1,3-beta-D-glucan synthase inhibitors. Antimicrob. Agents Chemother. 41(11):2471-2479.

- Dransart E., Olofsson B. & Cherfils J. (2005), RhoGDIs revisited: novel roles in Rho regulation. Traffic. 6(11):957–966.

- Ellis D. (2002) Amphotericin B: spectrum and resistance. J. Antimicrob. Chemother. 49 Suppl 1:7-10.

- Espinel-Ingroff A. (1998) Comparison of in vitro activities of the new triazole SCH56592 and the echinocandins MK-0991 (L-743,872) and LY303366 against opportunistic filamentous and dimorphic fungi and yeasts. J. Clin. Microbiol. 36(10): 2950-2956.

- Filler S.G. & Sheppard D.C. (2006) Fungal invasion of normally non-phagocytic host cells. PLoS Pathog. 2(12): e129.

- Firon A., Beauvais A., Latgé J.P., Couvé E., Grosjean-Cournoyer M.C. & D'Enfert C. (2002) Characterization of essential genes by parasexual genetics in the human fungal pathogen *Aspergillus fumigatus*: impact of genomic rearrangements associated with electroporation of DNA. Genetics. 161(3):1077-1087.

- Fontaine T., Simenel C., Dubreucq G., Adam O., Delepierre M., Lemoine J., Vorgias C.E., Diaquin M., Latgé J.P. (2000) Molecular organization of the alkali-insoluble fraction of *Aspergillus fumigatus* cell wall. J. Biol. Chem. 275(36):27594-27607.

- Fortwendel J.R., Juvvadi P.R., Perfect B.Z., Rogg L.E., Perfect J.R. & Steinbach W.J. (2010) Transcriptional regulation of chitin synthases by calcineurin controls paradoxical growth of *Aspergillus fumigatus* in response to caspofungin. Antimicrob. Agents. Chemother. 54(4):1555-1563.

- Fuchs B.B., Tang R.J. & Mylonakis E. (2007) The temperature-sensitive role of *Cryptococcus neoformans* ROM2 in cell morphogenesis. PLoS One.2(4):e368.

- Futagami T. and Goto M. (2011) Putative stress sensors WscA and WscB are involved in hypo-osmotic and acidic pH stress tolerance in *Aspergillus nidulans*. Eukaryot. Cell. 10(11):1504-15.

- Free S.J. (2013) Fungal cell wall organization and biosynthesis. Adv. Genet. 81:33-82.

- Galagan, J.E., Calvo S.E., Cuomo C., Ma L.J., Wortman J.R., Batzoglou S., Lee S.I. *et*

al. (2005) Sequencing of *Aspergillus nidulans* and comparative analysis with *A. fumigatus* and *A. oryzae*. Nature 438(7071):1105-1115.

- García P., Tajadura V., García I. & Sánchez Y. (2006) Rgf1p is a specific Rho1-GEF that coordinates cell polarization with cell wall biogenesis in fission yeast. Mol. Biol. Cell. 17(4):1620-1631.

- García P., García I., Marcos F., de Garibay G.R. & Sánchez Y. (2009) Fission yeast rgf2p is a rho1p guanine nucleotide exchange factor required for spore wall maturation and for the maintenance of cell integrity in the absence of rgf1p.Genetics. 181(4): 1321-1334.

- Gardiner R.E., Souteropoulos P., Park S. & Perlin D.S. (2005) Characterization of *Aspergillus fumigatus* mutants with reduced susceptibility to caspofungin. Med. Mycol. 43 Suppl 1:S299-305.

- Gastebois A., Mouyna I., Simenel C., Clavaud C., Coddeville B., Delepierre M., Latgé J.P. & Fontaine T. (2010) Characterization of a new beta(1-3)-glucan branching activity of *Aspergillus fumigatus*. J. Biol. Chem. 285(4):2386-2396.

- Gibbons, J.G. & Rokas, A. (2013) The function and evolution of the *Aspergillus* genome. Trends Microbiol. 21(1):14-22.

- Gieser D.M., Klich M.A., Frisvad J.C., Peterson S.W., Varga J. & Samson R.A. (2007) The current status of species recognition and identification in *Aspergillus*. Stud Mycol. 59:1–10.

- Goto M., Harada Y., Oka T., Matsumoto S., Takegawa K. & Furukawa K. (2009) Protein O-mannosyltransferases B and C support hyphal development and differentiation in *Aspergillus nidulans*. Eukaryot. Cell. 8(10):1465-1474.

- Guest G.M., Lin X. & Momany M. (2004) *Aspergillus nidulans* RhoA is involved in polar growth, branching, and cell wall synthesis. Fungal. Genet. Biol. 41(1):13-22.

- Hanahan D. (1983) Studies on transformation of *Escherichia coli* with plasmids. J. Mol. Biol. 166(4):557-580.

- Harris S.D. & Kraus P.R. (1998) Regulation of septum formation in *Aspergillus nidulans* by a DNA damage checkpoint pathway. Genetics. 148(3):1055-1067.

- Harrison J.C., Zyla T.R., Bardes E.S. & Lew D.J. (2004) Stress-specific activation mechanisms for the "cell integrity" MAPK pathway. J Biol Chem. 279(4):2616-22.

- Heesemann L., Kotz A., Echtenacher B., Broniszewska M., Routier F., Hoffmann P. &

  Ebel F. (2011) Studies on galactofuranose-containing glycostructures of the pathogenic mold *Aspergillus fumigatus*. Int. J. Med. Microbiol. 301(6):523-530.

- Heinisch J.J., Dupres V., Alsteens D. & Dufrêne Y.F. (2010) Measurement of the mechanical behavior of yeast membrane sensors using single-molecule atomic force microscopy Nat. Protoc. 5:670–677.

- Helmschrott C., Sasse A., Samantaray S., Krappmann S. & Wagener J. (2013) Upgrading fungal gene expression on demand: improved systems for doxycycline-dependent silencing in *Aspergillus fumigatus*. Appl. Environ. Microbiol. 79(5):1751-1754.

- Henry C., Latgé J.P. & Beauvais A. (2012) α1,3 glucans are dispensable in *Aspergillus fumigatus*. Eukaryot. Cell. 11(1):26-29.

- Herth W. (1980) Calcofluor white and congo red inhibit chitin microfibril assembly of Poterioochromonas: evidence for a gap between polymerization and microfibril formation. J. Cell Biol. 87(2 Pt 1): 442-450.

- Hill T.W. & Käfer E. (2001) Improved protocols for *Aspergillus* minimal medium: trace element and minimal medium salt stock solutions. Fungal Genet. Newsl. 48, 20-21.

- Hill T.W., Loprete D.M., Momany M., Ha Y., Harsch L.M., Livesay J.A., Mirchandani A., Murdock J.J., Vaughan M.J. & Watt M.B. (2006) Isolation of cell wall mutants in *Aspergillus nidulans* by screening for hypersensitivity to calcofluor white. Mycologia. 98(3):399-409.

- Hohl T.M. & Feldmesser M. (2007) *Aspergillus fumigatus*: principles of pathogenesis and host defense. Eukaryot. Cell 6(11):1953-1963.

- Horn B.W., Moore G.G. & Carbone I. (2009) Sexual reproduction in *Aspergillus flavus*. Mycologia 101(3):423-429.

- Ingham C.J. & Schneeberger P.M. (2012) Microcolony imaging of *Aspergillus fumigatus* treated with echinocandins reveals both fungistatic and fungicidal activities. PLoS ONE 7(4):e35478.

- Inoue H., Nojima H. & Okayama H. (1990) High efficiency transformation of *Escherichia coli* with plasmids. Gene. 96(1): 23-28.

- Ishihara S., Hirata A., Nogami S., Beauvais A., Latge J.P. & Ohya Y. (2007)

Homologous subunits of 1,3-beta-glucan synthase are important for spore wall assembly in *Saccharomyces cerevisiae*. Eukaryot. Cell. 6(2):143-56.

- Jain R., Valiante V., Remme N., Docimo T., Heinekamp T., Hertweck C., Gershenzon J., Haas H. & Brakhage A.A. (2011) The MAP kinase MpkA controls cell wall integrity, oxidative stress response, gliotoxin production and iron adaptation in *Aspergillus fumigatus*. Mol. Microbiol. 82(1):39-53.

- Jiménez-Ortigosa C., Aimanianda V., Muszkieta L., Mouyna I., Alsteens D., Pire S., Beau R., Krappmann S., Beauvais A., Dufrêne Y.F., Roncero C., Latgé J.P. (2012) Chitin synthases with a myosin motor-like domain control the resistance of *Aspergillus fumigatus* to echinocandins. Antimicrob. Agents Chemother. 56(12): 6121-6131.

- Joly V., Saint-Pierre-Chazalet M., Saint-Julien L., Bolard J., Carbon C. & Yeni P. (1992) Inhibiting cholesterol synthesis reduces the binding and toxicity of amphotericin B against rabbit renal tubular cells in primary culture. J. Infect. Dis. 165(2):337-343.

- Jungmann J. & Munro S. (1998) Multi-protein complexes in the *cis* Golgi of *Saccharomyces cerevisiae* with α-1,6-mannosyltransferase activity. EMBO J. 17(2):423–434.

- Justa-Schuch D., Heilig Y., Richthammer C. & Seiler S. (2010) Septum formation is regulated by the RHO4-specific exchange factors BUD3 and RGF3 and by the landmark protein BUD4 in *Neurospora crassa*. Mol. Microbiol. 76(1):220–235.

- Kelly R., Register E., Hsu M.J., Kurtz M. & Nielsen J. (1996) Isolation of a gene involved in 1,3-beta-glucan synthesis in *Aspergillus nidulans* and purification of the corresponding protein. J. Bacteriol. 178(15):4381-4391.

- Ketela T., Green R. & Bussey H. (1999) *Saccharomyces cerevisiae* mid2p is a potential cell wall stress sensor and upstream activator of the PKC1-MPK1 cell integrity pathway. J. Bacteriol. 181(11):3330-40.

- Klich M.A. (2007) *Aspergillus flavus*: the major producer of aflatoxin. Mol Plant Pathol. 8(6):713-722.

- Klis F.M., Mol P., Hellingwerf K. & Brul S. (2002) Dynamics of cell wall structure in *Saccharomyces cerevisiae*. FEMS Microbiol. Rev. 26(3):239-256.

- Klont R.R., Mennink-Kersten M.A., Ruegebrink D., Rijs A.J., Blijlevens N.M., Donnelly J.P. & Verweij P.E. (2006) Paradoxical increase in circulating *Aspergillus* antigen during treatment with caspofungin in a patient with pulmonary aspergillosis. Clin. Infect. Dis. 43(3):e23-e25.

- Kohno H., Tanaka K., Mino A., Umikawa M., Imamura H., Fujiwara T., Fujita Y., Hotta K., Qadota H., Watanabe T., Ohya Y. & Takai Y. (1996) Bni1p implicated in cytoskeletal control is a putative target of Rho1p small GTP binding protein in *Saccharomyces cerevisiae*. EMBO J. 15(22):6060-6068.

- Kopecká M. & Gabriel M. (1992) The influence of congo red on the cell wall and (1----3)-beta-D-glucan microfibril biogenesis in *Saccharomyces cerevisiae*. Arch. Microbiol. 158(2):115-26.

- Kousha M., Tadi R. & Soubani A.O. (2011) Pulmonary aspergillosis: a clinical review. Eur Respir Rev. 20(121):156-174.

- Krappmann S., Sasse C. & Braus G.H. (2006) Gene targeting in *Aspergillus fumigatus* by homologous recombination is facilitated in a nonhomologous end-joining-deficient genetic background. Eukaryot. Cell. 5(1):212–215.

- Krijgsheld P.,Bleichrodt R., van Veluw G.J., Wang F., Müller W.H., Dijksterhuis J. & Wösten H.A.B. (2012) Development in *Aspergillus*. Stud Mycol. 74(1):1–29.

- Kwon M.J., Arentshorst M., Roos E.D., van den Hondel C.A., Meyer V. & Ram A.F. (2011) Functional characterization of Rho GTPases in *Aspergillus niger* uncovers conserved and diverged roles of Rho proteins within filamentous fungi. Mol. Microbiol. 79(5):1151-1167.

- Lambou K., Perkhofer S., Fontaine T. & Latge J.P. (2010) Comparative functional analysis of the OCH1 mannosyltransferase families in *Aspergillus fumigatus* and *Saccharomyces cerevisiae*. Yeast. 27(8):625-636.

- Latgé J.P. (1999) *Aspergillus fumigatus* and aspergillosis. Clin. Microbiol. Rev. 12(2): 310-350.

- Latgé J.P., Mouyna I., Tekaia F., Beauvais A., Debeaupuis J.P. & Nierman W. (2005) Specific molecular features in the organization and biosynthesis of the cell wall of *Aspergillus fumigatus*. Med. Mycol. 43 Suppl.1:S15-S22.

- Latgé J.P. (2010) Tasting the fungal cell wall. Cell Microbiol. 12(7):863-872.

- Lee K.S., Irie K., Gotoh Y., Watanabe Y., Araki H., Nishida E., Matsumoto K., Levin D.E. (1993) A yeast mitogen-activated protein kinase homolog (Mpk1p) mediates signalling by protein kinase C. Mol. Cell Biol.13(5):3067-3075.

- Levin D.E. (2005) Cell wall integrity signaling in *Saccharomyces cerevisiae* Microbiol. Mol. Biol. Rev. 69(2):262–291.

- Levin D.E. (2011) Regulation of cell wall biogenesis in *Saccharomyces cerevisiae*: the cell wall integrity signaling pathway. Genetics 189(4):1145-1175.

- Li C.R., Wang Y.M., De Zheng X., Liang H.Y., Tang J.C. & Wang Y. (2005) The formin family protein CaBni1p has a role in cell polarity control during both yeast and hyphal growth in *Candida albicans*. J. Cell. Sci. 118(12):2637-2648.

- Li H., Zhou H., Luo Y., Ouyang H., Hu H. & Jin C. (2007) Glycosylphosphatidylinositol (GPI) anchor is required in *Aspergillus fumigatus* for morphogenesis and virulence. Mol. Microbiol. 64(4):1014–1027.

- Lin S.J., Schranz J. & Teutsch S.M. (2001) Aspergillosis case-fatality rate: systematic review of the literature. Clin. Infect. Dis. 32(3):358-366.

- Logan P.M. & Müller N.L. (1996) High-resolution computed tomography and pathologic findings in pulmonary aspergillosis: a pictorial essay. Can. Assoc. Radiol. J. 47(6):444-452.

- Machida, M. Yamada O. & Gomi K. (2008) Genomics of *Aspergillus oryzae*: Learning from the history of koji mold and exploration of its future. DNA Res.15 (4): 173-183.

- Madaule P., Axel R. & Myers A.M. (1987) Characterization of two members of the rho gene family from the yeast *Saccharomyces cerevisiae*. Proc. Natl. Acad. Sci. USA. 84(3):779-783.

- Madaule P., Furuyashiki T., Reid T., Ishizaki T., Watanabe G., Morii N. & Narumiya S. (1995) A novel partner for the GTP-bound forms of rho and rac. FEBS Lett. 377(2):243-248.

- Maertens J., Verhaegen J, Lagrou K, Van Eldere J & Boogaerts M. (2001) Screening for circulating galactomannan as a noninvasive diagnostic tool for invasive aspergillosis in prolonged neutropenic patients and stem cell transplantation recipients: a prospective validation. Blood 97(6):1604-1610.

- Maertens J.A. (2004) History of the development of azole derivatives. Clin. Microbiol. Infect. 10 Suppl 1: 1-10.

- Marchetti O., Entenza J.M., Sanglard D., Bille J., Glauser M.P. & Moreillon P. (2000) Fluconazole plus cyclosporine: a fungicidal combination effective against experimental endocarditis due to *Candida albicans*. Antimicrob. Agents Chemother. 44(11): 2932-2938.

- Marchetti O., Moreillon P., Entenza J.M., Vouillamoz J., Glauser M.P., Bille J. &

Sanglard D. (2003) Fungicidal synergism of fluconazole and cyclosporine in *Candida albicans* is not dependent on multidrug efflux transporters encoded by the CDR1, CDR2, CaMDR1, and FLU1 genes. Antimicrob. Agents Chemother. 47(5):1565–1570.

- Marr K.A. (2008) *Aspergillus* galactomannan index: a surrogate end point to assess outcome of therapy? Clin. Infect. Dis. 46(9):1423-1425.

- Martín H., Rodríguez-Pachón J.M., Ruiz C., Nombela C. & Molina M. (2000) Regulatory mechanisms for modulation of signaling through the cell integrity Slt2-mediated pathway in *Saccharomyces cerevisiae*. J. Biol. Chem. 275(2):1511-1519.

- Maubon D., Park S., Tanguy M., Huerre M., Schmitt C., Prévost M.C., Perlin D.S., Latgé J.P. & Beauvais A. (2006) AGS3, an alpha(1-3)glucan synthase gene family member of *Aspergillus fumigatus*, modulates mycelium growth in the lung of experimentally infected mice. Fungal Genet. Biol. 43(5):366-375.

- Mazur P., Morin N., Baginsky W., El-Sherbeini M., Clemas J. A., Nielsen J. B. & Foor, F. (1995) Differential expression and function of two homologous subunits of yeast 1,3-beta-D-glucan synthase. Mol. Cell Biol. 15(10):5671–5681.

- Mellado E., Aufauvre-Brown A., Specht C.A., Robbins P.W. & Holden D.W. (1995) A multigene family related to chitin synthase genes of yeast in the opportunistic pathogen *Aspergillus fumigatus*. Mol. Gen. Genet. 246(3):353-359.

- Mellado E., Aufauvre-Brown A., Gow N. A. R. & Holden, D. W. (1996) The *Aspergillus fumigatus* chsC and chsG genes encode class III chitin synthases with different functions. Mol. Microbiol. 20(3):667–679.

- Meyer V., Wanka F., van Gent J., Arentshorst M., van den Hondel C.A. & Ram A.F. (2011) Fungal Gene Expression on Demand: an Inducible, Tunable, and Metabolism-Independent Expression System for *Aspergillus niger*. Appl. Environ. Microbiol. 77(9):2975–2983.

- Mio T., Adachi-Shimizu M., Tachibana Y., Tabuchi H., Inoue S.B., Yabe T. , Yamada-Okabe T., Arisawa M., Watanabe T. & Yamada-Okabe H. (1997) Cloning of the *Candida albicans* homolog of *Saccharomyces cerevisiae* GSC1/FKS1 and its involvement in beta-1,3-glucan synthesis. 179(13):4096-4105.

- Musher B., Fredricks D., Leisenring W., Balajee S.A., Smith C. & Marr K.A. (2004) *Aspergillus* galactomannan enzyme immunoassay and quantitative PCR for diagnosis of invasive aspergillosis with bronchoalveolar lavage fluid. J. Clin. Microbiol. 42(12): 5517–5522.

- Mutoh T., Nakano K. & Mabuchi I. (2005) Rho1-GEFs Rgf1 and Rgf2 are involved in formation of cell wall and septum, while Rgf3 is involved in cytokinesis in fission yeast. Genes Cells. 10(12):1189-1202.

- Nakajima T. & Ichishima E. (1994) Chemical Structure of the galactomannan moiety in the cell wall glycoproteins of *Aspergillus oryzae*. Journal of Fermentation and Bioengineering. 78(6):472–475.

- Nierman W.C., Pain A., Anderson M.J., Wortman J.R., Kim H.S., Arroyo J., Berriman M., Abe K., Archer D.B., Bermejo C., Bennett J. et al. (2005) Genomic sequence of the pathogenic and allergenic filamentous fungus *Aspergillus fumigatus*. Nature 438(7071):1151-1156.

- O' Gorman C.M., Fuller H. & Dyer P.S. (2009) Discovery of a sexual cycle in the opportunistic fungal pathogen *Aspergillus fumigatus*. Nature 457(7228):471-474.

- Olson J.A., George A., Constable D., Smith P., Proffitt R.T. & Adler-Moore J.P. (2010) Liposomal amphotericin B and echinocandins as monotherapy or sequential or concomitant therapy in murine disseminated and pulmonary *Aspergillus fumigatus* infections. Antimicrob. Agents Chemother. 54(9):3884-3894.

- Ozaki K., Tanaka K., Imamura H., Hihara T., Kameyama T., Nonaka H., Hirano H., Matsuura Y. & Takai Y. (1996) Rom1p and Rom2p are GDP/GTP exchange proteins (GEPs) for the Rho1p small GTP binding protein in *Saccharomyces cerevisiae*. EMBO J. 15(9):2196-2207.

- Palacios D., Dailey I., Siebert D.M., Wilcock B.C. & Burke M.D. (2011) Synthesis-enabled functional group deletions reveal key underpinnings of amphotericin B ion channel and antifungal activities. Proc. Natl. Acad. Sci. U.S.A. 108(17):6733-6738.

- Paravicini G., Cooper M., Friedli L., Smith D.J., Carpentier J.L., Klig L.S. & Payton M.A. (1992) The osmotic integrity of the yeast cell requires a functional PKC1 gene product. Mol. Cell Biol. 12(11):4896-905.

- Pel H.J., de Winde J.H., Archer D.B., Dyer P.S., Hofmann G., Schaap P.J., Turner G., de Vries R.P. et al. (2007) Genome sequencing and analysis of the versatile cell factory *Aspergillus niger* CBS 513.88. Nat. Biotechnol. 25(2):221-231.

- Perez P. & Rincón S.A. (2010) Rho GTPases: regulation of cell polarity and growth in yeasts. Biochem. J. 426(3):243-253.

- Petraitiene R., Petraitis V., Groll A.H., Sein T., Schaufele R.L., Francesconi A. , Bacher J., Avila N.A. & Walsh T.J. (2002) Antifungal efficacy of caspofungin (MK-

0991) in experimental pulmonary aspergillosis in persistently neutropenic rabbits: pharmacokinetics, drug disposition, and relationship to galactomannan antigenemia. Antimicrob. Agents Chemother. 46(1):12-23.

- Philip B. & Levin D.E. (2001) Wsc1 and Mid2 are cell surface sensors for cell wall integrity signaling that act through Rom2, a guanine nucleotide exchange factor for Rho1. Mol. Cell. Biol. 21(1):271–280.

- Pinto P.S. (2004) The CT Halo Sign1. Radiology, 230(1):109-110.

- Ram A.F. & Klis F.M. (2006) Identification of fungal cell wall mutants using susceptibility assays based on calcofluor white and congo red. Nat. Protoc.1(5):2253-2256.

- Richthammer C., Enseleit M., Sanchez-Leon E., März S., Heilig Y., Riquelme M. & Seiler S. (2012) RHO1 and RHO2 share partially overlapping functions in the regulation of cell wall integrity and hyphal polarity in *Neurospora crassa*. Mol. Microbiol. 85(4):716-733.

- Rocha E.M., Garcia-Effron G., Park S. & Perlin D.S. (2007) A Ser678Pro substitution in Fks1p confers resistance to echinocandin drugs in *Aspergillus fumigatus*. Antimicrob. Agents Chemother. 51(11):4174-4176.

- Roncero C. & Durán A. (1985) Effect of calcofluor white and congo red on fungal cell wall morphogenesis: in vivo activation of chitin polymerization. J Bacteriol. 163(3): 1180-1185.

- Ronen R., Sharon H., Levdansky E., Romano J., Shadkchan Y. & Osherov N. (2007) The *Aspergillus nidulans* pkcA gene is involved in polarized growth, morphogenesis and maintenance of cell wall integrity. Curr Genet. 51(5): 321-329.

- Rossman K.L., Der C.J. & Sondek J. (2005) GEF means go: turning on RHO GTPases with guanine nucleotide-exchange factors. Nat Rev Mol Cell Biol. 6(2): 167-180.

- Rypien, K.L., Andras J.P. & Harvell C.D. (2008) Globally panmictic population structure in the opportunistic fungal pathogen *Aspergillus sydowii*. Mol. Ecol. 17(18): 4068-4078.

- Samson R.A. & Varga J. (2009) What is a species in *Aspergillus*? Med. Mycol. 47 Suppl 1:S13-20.

- Sanglard D. (2003) Resistance and tolerance mechanisms to antifungal drugs in fungal pathogens. Mycologist. 7(2):74-78.

- Scotter J.M. & Chambers S.T. (2005) Comparison of galactomannan detection, PCR-enzyme-linked immunosorbent assay, and real-time PCR for diagnosis of invasive aspergillosis in a neutropenic rat model and effect of caspofungin acetate. Clin. Diagn. Lab Immunol. 12(11):1322-1327.

- Schmalhorst P.S., Krappmann S., Vervecken W., Rohde M., Müller M., Braus G.H., Contreras R., Braun A., Bakker H. & Routier F.H. (2008) Contribution of galactofuranose to the virulence of the opportunistic pathogen *Aspergillus fumigatus*. Eukaryot. Cell. 7(8):1268-1277.

- Schmelzle T., Helliwell S.B. & Hall M.N. (2002) Yeast protein kinases and the RHO1 exchange factor TUS1 are novel components of the cell integrity pathway in yeast. Mol. Cell. Biol. 22(5):1329-1339.

- Schmidt A., Bickle M., Beck T. & Hall M.N. (1997) The yeast phosphatidylinositol kinase homolog TOR2 activates RHO1 and RHO2 via the exchange factor ROM2. Cell. 88(4):531–542.

- Schmidt A. & Hall A. (2002) Guanine nucleotide exchange factors for Rho GTPases: turning on the switch. Genes Dev. 16(13):1587-1609.

- Schmidt M., Bowers B., Varma A., Roh D.H. & Cabib E. (2002) In budding yeast, contraction of the actomyosin ring and formation of the primary septum at cytokinesis depend on each other. J. Cell Sci. 115(2):293-302.

- Sharpless K.E. & Harris S.D. (2002) Functional characterization and localization of the *Aspergillus nidulans* formin *SEPA*. Mol. Biol. Cell. 13(2):469-479.

- Sheehan D.J., Hitchcock C.A. & Sibley C.M. (1999) Current and emerging azole antifungal agents. Clin Microbiol Rev. 12(1):40-79.

- Si H., Justa-Schuch D., Seiler S. & Harris S.D. (2010) Regulation of septum formation by the Bud3-Rho4 GTPase module in *Aspergillus nidulans*. Genetics 185(1):165–176.

- Spreadbury C., Holden D., Aufauvre-Brown A., Bainbridge B. & Cohen J. (1993) Detection of *Aspergillus fumigatus* by polymerase chain reaction. J. Clin. Microbiol. 31(3):615-621.

- Tajadura V., García B., García I., García P. & Sánchez Y. (2004) *Schizosaccharomyces pombe* Rgf3p is a specific Rho1 GEF that regulates cell wall beta-glucan biosynthesis through the GTPase Rho1p. J. Cell Sci. 117(25):6163–6174.

- Teepe A.G., Loprete D.M., He Z., Hoggard T.A. & Hill T.W. (2007) The protein kinase

C orthologue PkcA plays a role in cell wall integrity and polarized growth in *Aspergillus nidulans.* Fungal Genet. Biol. 44(6):554-562.

- Torosantucci A., Bromuro C., Chiani P., De Bernardis F., Berti F., Galli C., Norelli F., Bellucci C., Polonelli L., Costantino P., Rappuoli R. & Cassone A. (2005) A novel glyco-conjugate vaccine against fungal pathogens. J. Exp. Med. 202(5):597-606.

- Valiante V., Heinekamp T., Jain R., Härtl A. & Brakhage A.A. (2008) The mitogen-activated protein kinase MpkA of *Aspergillus fumigatus* regulates cell wall signaling and oxidative stress response. Fungal Genet Biol. 45(5):618-627.

- Valiante, V., Jain R., Heinekamp T. & Brakhage A.A. (2009) The MpkA MAP kinase module regulates cell wall integrity signaling and pyomelanin formation in *Aspergillus fumigatus.* Fungal Genet. Biol. 46(12):909-918.

- Verweij P.E., Brinkman K., Kremer H.P., Kullberg B.J. & Meis J.F. (1999) *Aspergillus meningitis*: diagnosis by non-culture-based microbiological methods and management. J. Clin. Microbiol. 37(4):1186-1189.

- Walker L.A., Munro C.A., de Bruijn I., Lenardon M.D., McKinnon A. & Gow N.A. (2008) Stimulation of chitin synthesis rescues *Candida albicans* from echinocandins. PLoS Pathog. 4(4):e1000040.

- Walker L.A., Gow N.A. & Munro C.A. (2010) Fungal echinocandin resistance. Fungal Genet. Biol. 47(2):117–126.

- Walsh T.J., Anaissie E.J., Denning D.W., Herbrecht R., Kontoyiannis D.P. & Marr K.A. *et al.* (2008) Clin Infect Dis. 46(3):327–360.

- Watt K., Manzoni P., Cohen-Wolkowiez M., Rizzollo S., Boano E., Jacqz-Aigrain E. & Benjamin D.K. (2013) Triazole use in the nursery: fluconazole, voriconazole, posaconazole, and ravuconazole. Curr. Drug Metab. 14(2):193-202.

- Wood P.J. (1980) Specificity in the interaction of direct dyes with polysaccharides. Carbohydr. Res. 85(2):271–287.

- Yamochi W., Tanaka K., Nonaka H., Maeda A., Musha T. & Takai Y. (1994) Growth site localization of Rho1 small GTP-binding protein and its involvement in bud formation in *Saccharomyces cerevisiae*. J. Cell Biol. 125(5):1077-1093.

- Yoshida S., Bartolini S. & Pellman D. (2009) Mechanisms for concentrating Rho1 during cytokinesis. Genes Dev. 23(7):810-823.

- Zdobnov E.M. & Apweiler R. (2001) InterProScan–an integration platform for the signature-recognition methods in InterPro. Bioinformatics 17(9):847–848.

7. Abbreviations

α	Anti
Ab	Antibody
AIDS	Acquired immunodeficiency syndrome
AMM	Aspergillus minimal medium
Amp	Ampicillin
AP	Alkaline phosphatise
APS	Ammonium persulphate
ATP	Adenosine triphosphate
BCIP	5-bromo-4-chloro-3-indolyl-phosphate
BLAST-P	Basic Local Alignment Search Tool for protein sequences
β-ME	Beta Mercaptoethanol
BSA	Bovine serum albumin
C-terminus	Carboxy terminus
CFW	Calcofluor white
CNH	Citron Homology
CR	Congo Red
CS	Caspofungin
ddH_2O	Double-distilled water
DEO	1,2:7,8-Diepoxyoctane
DEP	Dishevelled, Egl-10 and Pleckstrin
DH	Dbl Homology
DMSO	Dimethyl Sulfoxide
DNA	Deoxyribonucleic acid
dNTP	Deoxynucleotide triphosphate
EDTA	Ethylene diamine tetra-acetate
EtOH	Ethanol
et al.	*el alteri*
g	Gravitational force
GEF	Guanine-nucleotide exchange factor
GDP	Guanosine diphosphate
GTP	Guanosine triphosphate
GFP	Green fluorescence protein
GPI	Glycophophatidyl inositol
h	Hour
HIV	Human immuno-deficiency virus
HU	Hydroxyurea
Hyg	Hygromycin
kb	Kilobase
kDa	Kilodalton
LB	Lysogeny Broth
mAb	Monoclonal antibody

MIC	Minimal inhibitory concentration
Mb	Megabase
MEC	Minimum effective concentration
PAGE	Polyacrylamide gel electrophoresis
PCR	Polymerase chain reaction
pH	*potential Hygrogenii*
PI	Protease inhibitor
PMSF	Phenyl methyl sulfonyl fluoride
PBS/T	Phosphate buffer saline/Tween
ptrA	Pyrithiamine
rpm	revolutions per minute
RT	Room temperature
s	Second
SDS	Sodium dodecyl sulphate
SOD	Superoxide dismutase
TBS	Tris-buffered saline
TEMED	N,N,N',N' tetramethyl-ethylenediamine
Tris	Tris (hydroxymethyl) amino methane
w/v	weight per volume
U	units
VO	Voriconazole
v/v	volume per volume

Units:

µg	microgram
mg	milligram
µl	microliter
ml	milliliter
µM	micromolar
mM	millimolar
m/s	meter per second
ng	nanogram

8. Appendix

8.1. PCR verification of additional mutants

Verification of *HA-rom2(733-1199)$_{tetOn}$* :

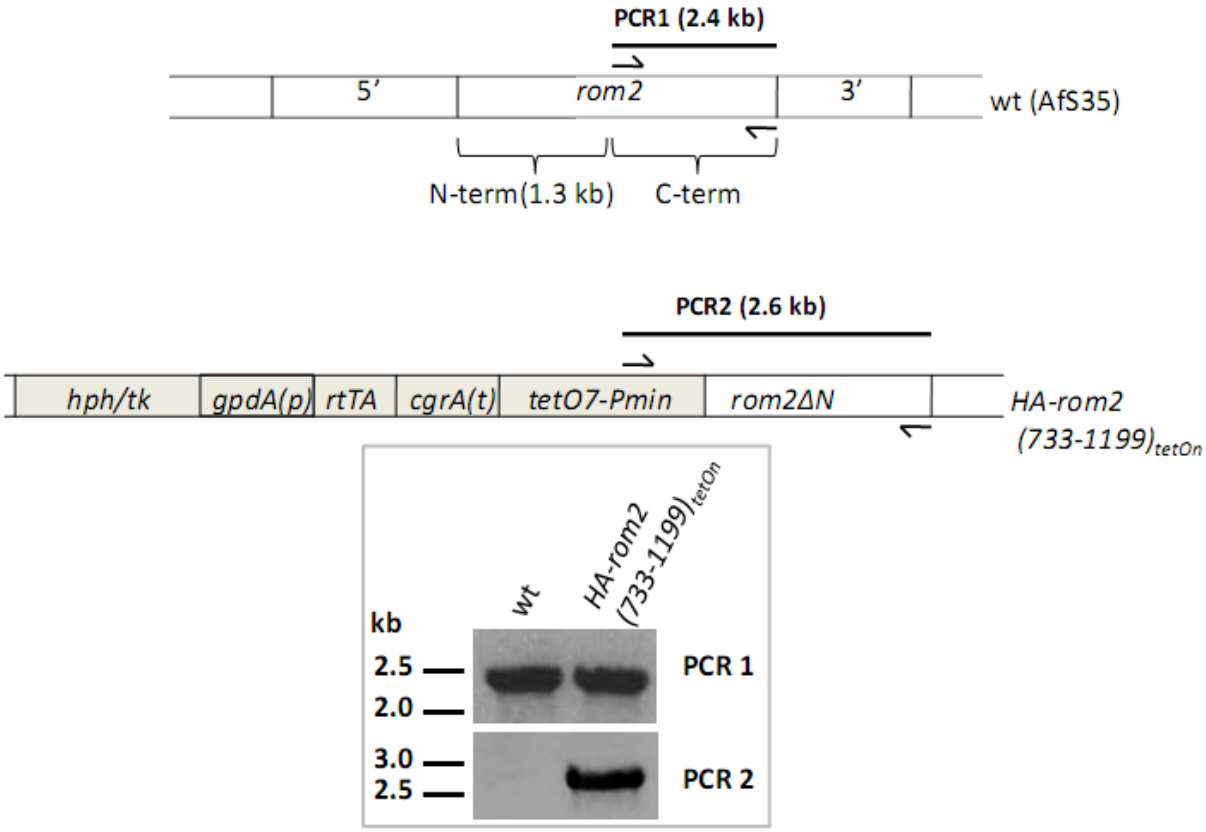

Verification of *rho1$^{G14V}_{tetOn}$*:

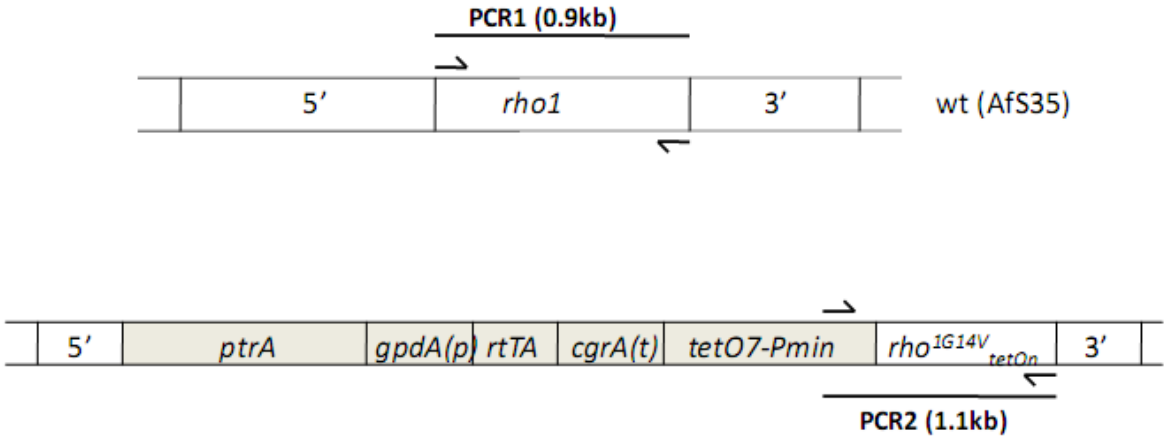

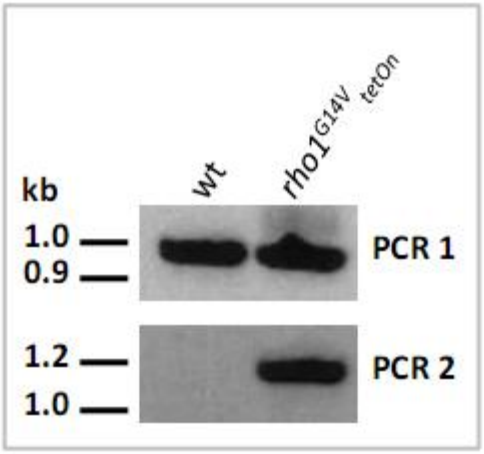

Verification of *rom2-His*$_{tetOn}$:

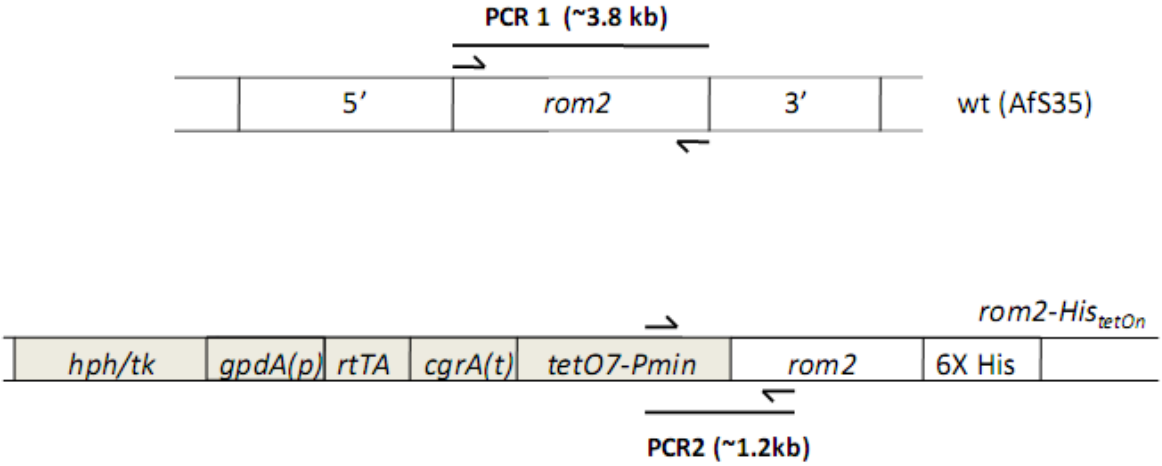

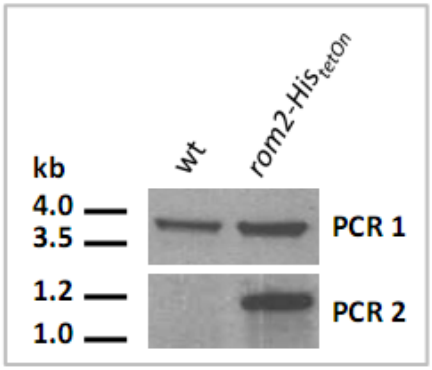

Verification of *rom2-GFP*$_{tetOn}$ and *rom2-GFP*:

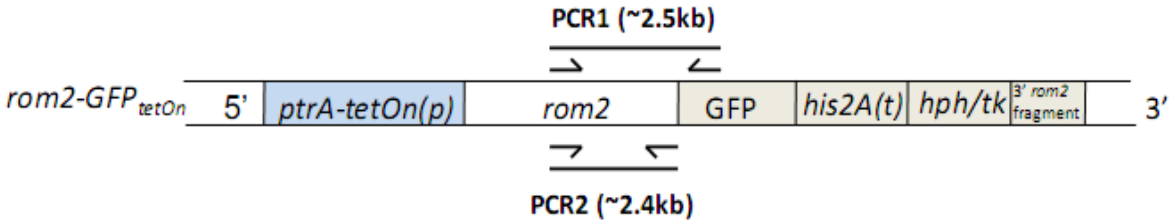

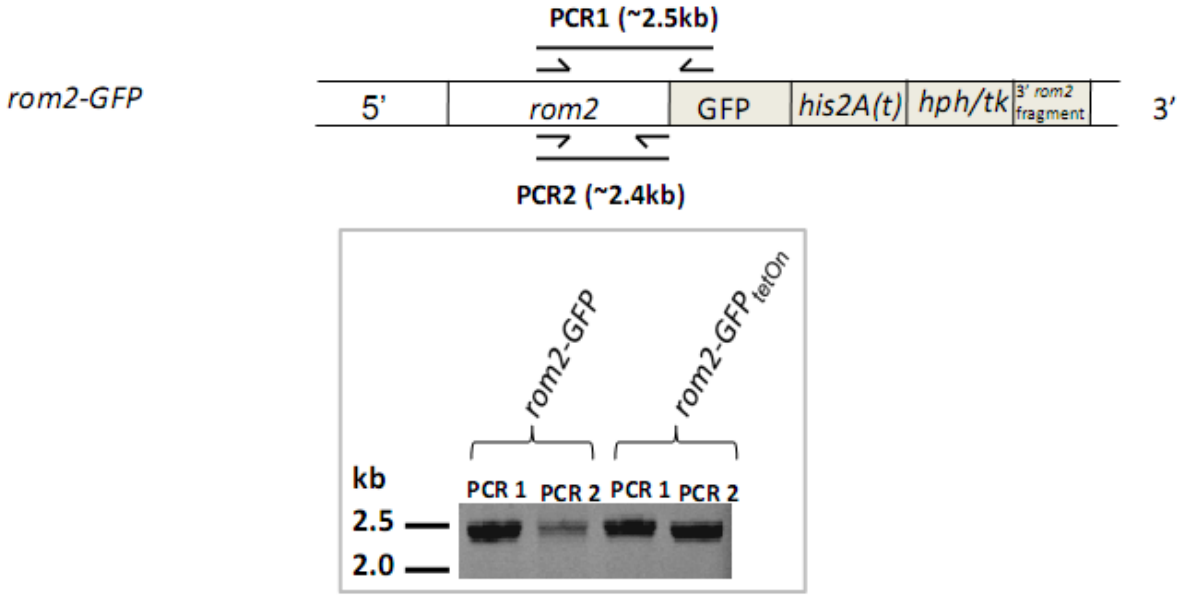

8.2. Composition of buffers used:

<u>20X Salt Mix:</u>

For 1000 ml,

$NaNO_3$	120 g
KCl	10.4 g
KH_2PO_4	16.3 g
K_2HPO_4	20.9 g

Dissolve in 800 ml ddH_2O and make up volume to 1000 ml.

<u>200X $MgSO_4.7H_2O$:</u>

0.4 M $MgSO_4.7H_2O$ 52 g

Dissolve in 500 ml ddH_2O and autoclave.

<u>1000X Trace elements:</u>

$ZnSO_47H_2O$ (Zinc sulphate)	2.2 g
H_3BO_3 (Boric acid)	1.1 g
$MnCl_2 \cdot 4H_2O$ (Manganous chloride)	0.5 g
$FeSO_4 \cdot 7H_2O$ (Ferrous sulphate)	0.5g
$CoCl_2 \cdot 6H_2O$ (Cobaltous chloride)	0.16 g
$CuSO_4 \cdot 5H_2O$ (Cupric sulphate)	0.16 g
$(NH_4)_6Mo_7O_{24} \cdot 4H_2O$ (Ammonium molybdate)	0.11g
$Na_4EDTA \cdot 4H_2O$ (EDTA, tetrasodium salt)	6.0g

Dissolve these salts in 80 ml ddH_20 and make up final volume to 100 ml. The unadjusted pH will be about 6.5.

Citrate Buffer:

For 2000 ml,

KCl	22.36 g
NaCl	67.78 g
Sodium citrate dihydrate	29.4 g

Adjust pH to 5.5 with HCl.

STC 1700:

1.2 M Sorbitol
10mM Tris pH 5.5
50mM $CaCl_2$
35mM NaCl

PEG 4000 Mix:

10mM Tris pH 7.5
50Mm CaCl2
60 % (w/v) PEG 4000

Top agar:

1% D- Glucose
0.7% Agar
1.2M Sorbitol

Dissolve in half volume ddH_2O and autoclave. Then add 1X Salt mix, $MgSO_4.7H_2O$ and trace elements and mix well before use.

25X TBS:

For 2000 ml,

Tris	121 g
NaCl	399.5 g

Adjust pH to 7.6.

1X TBS-T:

For 1000 ml,

TBS (1X)	1000 ml
Tween-20	1 ml

50X TAE:

For 1000 ml,

Tris	242 g
Acetic acid	57.1 g
EDTA	18.6 g

10X PBS:

NaCl	80 g
KCl	2 g
Na2HPO4	14.4 g

Adjust pH to 7.4. and make up volume to 1000 ml.

2X Lämmli buffer:

4 % SDS
10% (w/v) β- Mercaptoethanol
0.125 M Tris-HCl (pH 6.8)
20% (v/v) Glycerol
0.004% (w/v) Bromophenolblue

10X SDS Electrophoresis buffer:

1% SDS
0.025 M Tris
0.192 M Glycine

Coomassie staining solution:

Methanol	500ml
Acetic acid	100ml
Water	400ml

0.25%Coomasie Brilliant blue R

Destaining solution:

For 500 ml,

Acetic acid	50 ml
Methanol	200 ml
Water	250 ml

1X Blotting buffer:

For 2000 ml,

Tris	11.6 g
Glycine	5.8 g
SDS	0.37 %
Methanol	600 ml

1X Tank blot buffer:

25mM Tris
192mM Glycine
KH2PO4 2.4 g
20% Methanol

Ponceau-S solution:

0.25 % Ponceau-S
40 % Methanol
15% Acetic acid

9. Acknowledgement

It is indeed a great pleasure for me to accolade all those who have helped me throughout my journey of doctoral study. It is an honour to thank them all in my humble acknowledgement.

First of all, I would extend my humble prayers and gratitude to the Almighty for his blessings and strength that he has bestowed upon me so far in my life. I thank him for giving me this wonderful opportunity and memories to cherish.

I would like to express my deep sense of gratitude to my supervisor Dr. med. Johannes Wagener for giving me the opportunity to work at the Max von Pettenkofer Institute for Hygiene and Medical Microbiology, LMU. Thanks to you for your guidance, constructive suggestions and support during my research tenure. I am also very thankful to you for helping me to settle down in Munich, when I first arrived in Germany.

I am equally thankful to Prof. Frank Ebel for his fruitful advices and guidance. His humility, knowledge and experience have indeed been a great source of inspiration.

I am grateful to our collaborator Prof. Dr. Sven Krappmann at the University Hospital of Erlangen for his valuable and timely support and experimental cooperation in our research endeavours.

I thank all my lab friends and colleagues for their exteremely warm support and love for the good cherished times we spent in the lab. With you all, it was always fun and exciting to work with. I owe a special word of thanks to my good friend and colleague, Dr. Med. Karl Dichtl for his unwavering help and excellent suggestions in experimental work. It was indeed a pleasure working with you. I would also like to thank Emilia Sieger for excellent technical assistance to carry out the research successfully, Christoph Helmschrott and Michael Neubauer for helping me with experiments. I am deeply indebted to Allison and Julia for their professional and emotional support during my stay in Munich. You both have been really wonderful friends and will always be cherished. My heartfelt regards for others including Marzena, Anne, Yaya, Tamara and Axel for always making me smile. You all have given me many treasured moments that will remain with me forever. I would also extend my gratitude and regards to my other Indian friends outside lab: Shrikant, Onkar, Supriya, Santhosh, Jyaysi, Sneha, Dhawal, Rupa and Hari for your wonderful company and making me feel at home. You were like my ‘Munich family’. I wish you all the very best in your future endeavours.

My basket of thanks would be incomplete without acknowledging my beloved family, my mother, my sisters and my caring brother-in-laws for their endless love, emotional support and constant encouragement. Thank you all for always being for me and with me, even when I am miles away!

Curriculum Vitae

Address of correspondence:
Max von Pettenkofer Institute for Hygiene and Medical Microbiology
AG Wagener
Pettenkofer strasse 9a
Munich 80336, Germany
E-mail: **sweta.sam@gmail.com**
Phone: +49-17698301321, +49-89-218072868

CAREER PROFILE:

- Ambitious and enthusiastic Ph.D. scholar with 2 first-author and 1 co-author publications in peer-reviewed journals.
- Productive independent researcher as well as cooperative team player.
- Strong academic credentials.

EDUCATION:

Doctoral student, Medical Microbiology April 2011- April 2014
Max von Pettenkofer Institute for Hygiene and Medical Microbiology
Ludwig-Maximilians-Universität, Germany

Master of Science (M.Sc.), Biotechnology 2008- 2010
School of Biotechnology
KIIT University, India

Bachelor of Science (B.Sc.) 2005-2008
Ravenshaw University, India

10+2 (Higher Secondary 2003-2005
S.B. Women's College, C.H.S.E. Board, Odisha, India

10th/Matriculation 1991-2003
S.C.B. Medical Public School, I.C.S.E. Board, India

RESEARCH EXPERIENCE:

- February 2010- June 2010
  M.Sc. Research Trainee, Institute of Genomics and Integrative Biology, Delhi, India
- April 2011- April 2014
  Ph.D. candidate, Max von Pettenkofer Institute, LMU

TECHNICAL EXPERTISE:

Cell Biology:

- Immunocytochemistry and live cell imaging
- Microscopy- Fluorescence, light and confocal microscopy

Microbiology:

- Liquid and solid culture of bacteria and fungi

- Isolation and transformation
- Antifungal susceptibility assays

Molecular Biology:

- Vector design- primer design, restriction analysis, ligation, PCR cloning and transformation (chemical method)
- Isolation and quantification of DNA, RNA and protein
- Genetic screening and manipulations in *Aspergillus fumigatus*
- Application of tet-On (doxycycline regulated) conditional promoter system
- Site-directed mutagenesis & Epitope tagging

Biochemistry:

- Electrophoresis
- Western blot (Semi-dry, Tank blot), Protein purification (column chromatography), Co-immunoprecipitation
- ELISA, enzymatic and in-vitro cell based diagnostic assays

Analytical methods:

- Titrations, Chromatography (thin layer, affinity column, gel filtration)
- UV/Visible and fluorescence spectrophotometry

Bioinformatics/Computing skills:

- Proficient in use of MS-Office (Word and Excel)
- Sequence Alignment and Phylogenetic Analysis
- Homology modeling by Modweb

PUBLICATIONS:

- **Samantaray S**, Neubauer M, Helmschrott C, Wagener J. (2013).
  Role of the guanine nucleotide exchange factor Rom2 in cell wall integrity maintenance of Aspergillus fumigatus.
  Eukaryot. Cell 12(2):288-98.

- Helmschrott C, Sasse A, **Samantaray S**, Krappmann S, Wagener J. (2013).
  Upgrading fungal gene expression on demand: improved systems for doxycycline-dependent silencing in Aspergillus fumigatus.
  Appl.Environ. Microbiol. 79(5):1751-4.

- Dichtl Karl*, **Samantaray Sweta***, Frank Ebel, Johannes Wagener (2014).
  Aspergillus fumigatus devoid of cell wall β-1,3-glucan is viable, massively sheds galactomannan and is killed by septum formation inhibitors.
  Mol. Microbiol. **(Submitted) *Equal contribution.**

PRESENTATIONS:

- Characterization of the putative Rho1 guanine nucleotide exchange factor Rom2 of *Aspergillus fumigatus*. International Journal of Medical Microbiology Abstracts. 302S1:114. Oral presentation delivered at the **64th Annual Meeting of the German Society for Hygiene and Microbiology (DGHM)**, October 2012.

- J. Wagener, C. Helmschrott, **S. Samantaray** (2012) Rapid generation of conditional doxycycline-regulated mutants in *Aspergillus fumigatus*. International Journal of Medical Microbiology Abstracts. 302S1:17. Poster presented by Dr. med. Johannes Wagener at the **64th Annual Meeting of the German Society for Hygiene and Microbiology (DGHM)**, October 2012.
- Molecular characterization of the cell wall integrity pathway in *Aspergillus fumigatus*. Mycoses Abstracts. 55S4:188. Poster presented by Dr. med. Johannes Wagener at the **18th Congress of the International Society for Human and Animal Mycology (ISHAM)**, June 2012.

PERSONAL SKILLS:

- Ability to work in multicultural milieu and collaborate effectively.
- Hard-working and capable of working under pressure, successfully delivering timely and precise results.
- Excellent oral communication and writing skills demonstrated by presentations to international audience.
- Highly self motivated and result-oriented.

CERTIFICATES:

- Qualified **GATE 2010 (Biotechnology)** with **97.02 percentile** (a national level entrance test organized jointly by IISc and IITs in India).
- Awarded **Certificate of Merit** in the annual Scholarship examinations organized by the **Association of Orissa I.C.S.E. Schools.**

ACADEMIC MEMBERSHIPS:

2011-present Deutschen Gesellschaft für Hygiene und Mikrobiologie (DGHM)

PERSONAL PROFILE:

Date of Birth : March 12, 1987

Nationality : Indian

Languages : English (fluent), Hindi (fluent), Oriya (native), German (basic)